

SUPPORTING INFORMATION

Self-sorting of two imine-based metal complexes: balancing kinetics and thermodynamics in constitutional dynamic networks

Jean-François Ayme^{1,2}, Jean-Marie Lehn^{1,2*}

¹Institute of Nanotechnology, Karlsruhe Institute of Technology, 76344 Eggenstein-Leopoldshafen, Germany.

²Laboratoire de Chimie Supramoléculaire, Institut de Science et d'Ingénierie Supramoléculaires, Université de Strasbourg, 8 allée Gaspard Monge, 67000 Strasbourg, France.

Email : lehn@unistra.fr

Table des matières

1.	General experimental section	4
1.1	General material	4
1.2	Characterization and analysis methods	4
2.	Synthesis	4
2.1	Synthesis of the ligands	4
2.1.1	Synthesis of aldehyde 7	4
2.1.2	Synthesis of imine constituent (1,4)	5
2.2	Synthesis of mononuclear metal complexes	5
2.2.1	General synthetic procedure	5
2.2.2	Synthesis of Cu ^I complex [Cu(1,4) ₂](BF ₄)	5
2.2.3	Synthesis of Fe ^{II} complex [Fe(2,3) ₂](BF ₄) ₂	6
2.2.4	Synthesis of Fe ^{II} complex [Fe(2,4) ₂](BF ₄) ₂	7
2.2.5	Synthesis of Fe ^{II} complex [Fe(2,3)(2,4)](BF ₄) ₂	8
2.2.6	Synthesis of Fe ^{II} complex [Fe(2,7) ₂](BF ₄) ₂	10
2.2.7	Synthesis of Fe ^{II} complex [Fe(2,3)(2,7)](BF ₄) ₂	11
2.2.8	Synthesis of Cu ^I complex [Cu(4,5) ₂](BF ₄)	14
2.2.9	Synthesis of Cu ^I complex [Cu(1,6) ₂](BF ₄)	14
2.2.10	Synthesis of Cu ^I complex [Cu(1,7) ₂](BF ₄)	15
2.2.11	Synthesis of Cu ^I complex [Cu(5,7) ₂](BF ₄)	16
2.2.12	Synthesis of Cu ^I complex [Cu(7,8) ₂](BF ₄)	17
2.2.13	Synthesis of Cu ^I complex [Cu(4,8) ₂](BF ₄)	18
2.2.14	Synthesis of Fe ^{II} complex [Fe(3,9) ₂](BF ₄) ₂	18
2.2.15	Synthesis of Ag ^I complex [Ag(7,8) ₂](BF ₄)	20
2.2.16	Synthesis of Zn ^{II} complex [Zn(2,3) ₂](BF ₄) ₂	21
2.2.17	Synthesis of Zn ^{II} complex [Zn(2,7) ₂](BF ₄) ₂	21
2.2.18	Synthesis of Zn ^{II} complex [Zn(2,3)(2,7)](BF ₄) ₂	22
2.2.19	Synthesis of Zn ^{II} complex [Zn(3,9) ₂](BF ₄) ₂	25
2.2.20	Synthesis of Zn ^{II} complex [Zn(7,9) ₂](BF ₄) ₂	26
2.2.21	Synthesis of Zn ^{II} complex [Zn(3,9)(7,9)](BF ₄) ₂	27
3.	Self-sorting reactions	30
3.1	General synthetic procedure	30
3.2	Self-sorting of complexes [Cu(1,4) ₂] ⁺ and [Fe(2,3) ₂] ²⁺	30

3.2.1	Simultaneous generation of complexes $[\text{Cu}(\mathbf{1},\mathbf{4})_2]^+$ and $[\text{Fe}(\mathbf{2},\mathbf{3})_2]^{2+}$ at 2.7 mM	30
3.2.2	Effect of concentration on the self-sorting of complexes $[\text{Cu}(\mathbf{1},\mathbf{4})_2]^+$ and $[\text{Fe}(\mathbf{2},\mathbf{3})_2]^{2+}$	31
3.3	Self-sorting of complexes $[\text{Cu}(\mathbf{4},\mathbf{5})_2]^+$ and $[\text{Fe}(\mathbf{2},\mathbf{3})_2]^{2+}$	37
3.3.1	Simultaneous generation of complexes $[\text{Cu}(\mathbf{4},\mathbf{5})_2]^+$ and $[\text{Fe}(\mathbf{2},\mathbf{3})_2]^{2+}$	37
3.3.2	Monitoring of the formation of complexes $[\text{Cu}(\mathbf{4},\mathbf{5})_2]^+$ and $[\text{Fe}(\mathbf{2},\mathbf{3})_2]^{2+}$	38
3.4	Self-sorting of complexes $[\text{Cu}(\mathbf{1},\mathbf{6})_2]^+$ and $[\text{Fe}(\mathbf{2},\mathbf{3})_2]^{2+}$	40
3.5	Self-sorting of complexes $[\text{Cu}(\mathbf{1},\mathbf{7})_2]^+$ and $[\text{Fe}(\mathbf{2},\mathbf{3})_2]^{2+}$	40
3.5.1	Simultaneous generation of complexes $[\text{Cu}(\mathbf{1},\mathbf{7})_2]^+$ and $[\text{Fe}(\mathbf{2},\mathbf{3})_2]^{2+}$	40
3.5.2	Monitoring of the formation of complexes $[\text{Cu}(\mathbf{1},\mathbf{7})_2]^+$ and $[\text{Fe}(\mathbf{2},\mathbf{3})_2]^{2+}$	41
3.6	Self-sorting of complexes $[\text{Cu}(\mathbf{5},\mathbf{7})_2]^+$ and $[\text{Fe}(\mathbf{2},\mathbf{3})_2]^{2+}$	42
3.6.1	Simultaneous generation of complexes $[\text{Cu}(\mathbf{5},\mathbf{7})_2]^+$ and $[\text{Fe}(\mathbf{2},\mathbf{3})_2]^{2+}$	42
3.6.2	Monitoring of the formation of complexes $[\text{Cu}(\mathbf{5},\mathbf{7})_2]^+$ and $[\text{Fe}(\mathbf{2},\mathbf{3})_2]^{2+}$	43
3.6.3	Probing of the selectivity of the self-assembly of $[\text{Cu}(\mathbf{5},\mathbf{7})_2]^+$ and $[\text{Fe}(\mathbf{2},\mathbf{3})_2]^{2+}$ from a mixture of components 1 , 2 , 3 and 7	44
3.7	Self-sorting of complexes $[\text{Cu}(\mathbf{7},\mathbf{8})_2]^+$ and $[\text{Fe}(\mathbf{2},\mathbf{3})_2]^{2+}$	45
3.7.1	Simultaneous generation of complexes $[\text{Cu}(\mathbf{7},\mathbf{8})_2]^+$ and $[\text{Fe}(\mathbf{2},\mathbf{3})_2]^{2+}$	45
3.7.2	Monitoring of the formation of complexes $[\text{Cu}(\mathbf{7},\mathbf{8})_2]^+$ and $[\text{Fe}(\mathbf{2},\mathbf{3})_2]^{2+}$	46
3.8	Self-sorting of complexes $[\text{Cu}(\mathbf{4},\mathbf{8})_2]^+$ and $[\text{Fe}(\mathbf{3},\mathbf{9})_2]^{2+}$	47
3.9	Self-sorting of complexes $[\text{Cu}(\mathbf{7},\mathbf{8})_2]^+$ and $[\text{Fe}(\mathbf{3},\mathbf{9})_2]^{2+}$	48
3.9.1	Simultaneous generation of complexes $[\text{Cu}(\mathbf{7},\mathbf{8})_2]^+$ and $[\text{Fe}(\mathbf{3},\mathbf{9})_2]^{2+}$	48
3.9.2	Monitoring of the formation of complexes $[\text{Cu}(\mathbf{7},\mathbf{8})_2]^+$ and $[\text{Fe}(\mathbf{3},\mathbf{9})_2]^{2+}$	49
3.10	Comparison of the rate of formation of bis-2,2':6'2''-terpyridine-like Fe ^{II} complexes	50
3.11	Self-sorting of complexes $[\text{Ag}(\mathbf{7},\mathbf{8})_2]^+$ and $[\text{Fe}(\mathbf{2},\mathbf{3})_2]^{2+}$	51
3.12	Self-sorting of complexes $[\text{Cu}(\mathbf{7},\mathbf{8})_2]^+$ and $[\text{Zn}(\mathbf{2},\mathbf{3})_2]^{2+}$	51
3.12.1	Simultaneous generation of complexes $[\text{Cu}(\mathbf{7},\mathbf{8})_2]^+$ and $[\text{Zn}(\mathbf{2},\mathbf{3})_2]^{2+}$	51
3.12.2	Monitoring of the formation of complexes $[\text{Cu}(\mathbf{7},\mathbf{8})_2]^+$ and $[\text{Zn}(\mathbf{2},\mathbf{3})_2]^{2+}$	52
3.13	Self-sorting of complexes $[\text{Cu}(\mathbf{7},\mathbf{8})_2]^+$ and $[\text{Zn}(\mathbf{3},\mathbf{9})_2]^{2+}$	54
3.13.1	Simultaneous generation of complexes $[\text{Cu}(\mathbf{7},\mathbf{8})_2]^+$ and $[\text{Zn}(\mathbf{3},\mathbf{9})_2]^{2+}$	54
3.13.2	Probing the selectivity of Zn ^{II} cations for aldehyde 3 over aldehyde 7 in the presence of aminoquinoline 9	54
4.	References	55

1. General experimental section

1.1 General material

Unless stated otherwise, solvents and commercial reagents were used as received. Dry toluene was obtained by passing the solvent through an activated alumina on a Pure Solv solvent purification system. All reactions requiring anhydrous conditions were carried-out in oven-dried glassware and all reactions requiring inert gas atmosphere were performed under nitrogen using standard Schlenk techniques. All reactions not performed in a NMR tubes were agitated using magnetic stirrer bars. Room temperature is taken as 293 K. Flash column chromatography was carried out using silica gel (Geduran Si60, 40-63 μm , Merck) using eluents as specified. TLC was performed on precoated silica gel plates (Merck TLC silica gel 60 F254 aluminium plates) and product spots were visualized under UV light ($\lambda_{\text{max}} = 280 \text{ nm}$ or 365 nm) or by staining with KMnO_4 . Celite[®] was obtained from Sigma-Aldrich and refers to diatomaceous earth. Brine refers to a saturated aqueous solution of NaCl. Ammonia in methanol was prepared by bubbling gaseous ammonia in methanol.

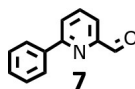
1.2 Characterization and analysis methods

NMR spectra were recorded on a Bruker Avance III 400 MHz, Bruker Avance III HD 400 MHz spectrometer or Bruker Avance Neo 500 MHz spectrometer. NMR spectra were digitally processed (phase and baseline corrections, integration, peak analysis) using MestReNova 10.0. Deuterated acetonitrile (CD_3CN) was obtained from Sigma-Aldrich and used without further purification. Deuterated chloroform (CDCl_3) was obtained from Sigma-Aldrich and was passed through a plug of sodium bicarbonate immediately before use to remove any acidic impurities. Chemical shifts are reported in parts per million (ppm) from low to high frequency using residual protonated solvent signals as reference (for ^1H NMR spectra $\text{CDCl}_3 = 7.26 \text{ ppm}$, $\text{CD}_3\text{CN} = 1.94 \text{ ppm}$; for ^{13}C NMR spectra $\text{CDCl}_3 = 77.16 \text{ ppm}$, $\text{CD}_3\text{CN} = 1.32 \text{ ppm}$). Coupling constants (J) are reported in hertz (Hz). The multiplicity of the ^1H signals are indicated using the following standard abbreviations: s = singlet, d = doublet, t = triplet, dd = double doublet, q = quartet, m = multiplet, br = broad, ddd = doublet of double doublets. NMR signals are reported in terms of chemical shift (δ), multiplicity, coupling constants (J), relative integral, and assignment, in that order. All resonances are reported to the nearest 0.01 ppm. ^1H and ^{13}C NMR assignments were made using 2D-NMR methods (COSY, ROESY, TOCSY, HSQC, HMBC) and are unambiguous unless stated otherwise. High resolution ESI mass spectra were obtained in-house at the Institute of Science and Supramolecular Engineering (ISIS) by direct injection into a ThermoFisher Exactive Plus EMR Orbitrap mass spectrometer.

2. Synthesis

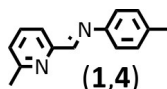
2.1 Synthesis of the ligands

2.1.1 Synthesis of aldehyde 7



7 was synthesized as described in the literature. NMR and mass data were consistent with those previously reported.^[S1]

2.1.2 Synthesis of imine constituent (1,4)

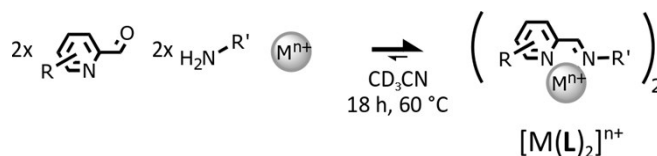


(1,4) was synthesized as described in the literature. NMR and mass data were consistent with those previously reported.^[S2]

2.2 Synthesis of mononuclear metal complexes

2.2.1 General synthetic procedure

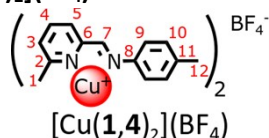
The general synthetic procedure for forming the mononuclear complexes metal complexes is shown in Scheme S1.



Scheme S1. Synthesis of mononuclear complexes $[M(L)_2]^{n+}$.

General synthetic procedure: CD_3CN solutions of the 2-formylpyridine containing component (100 μ L of 320 mM, 32 μ mol, 2 eq.) and of the amine containing component (100 μ L of 320 mM, 32 μ mol, 2 eq.) were combined. The resulting mixture was either treated with a CD_3CN solution of $Fe(BF_4)_2 \cdot 6H_2O$ (100 μ L of 160 mM, 16 μ mol, 1 eq.) or a CD_3CN solution of $[Cu(CH_3CN)_4](BF_4)$ (100 μ L of 160 mM, 16 μ mol, 1 eq.) or a CD_3CN solution of $[Zn(C_2H_6OS)_6](BF_4)_2$ (100 μ L of 160 mM, 16 μ mol, 1 eq.) and heated at 60 $^\circ$ C for 18 h. After cooling to room temperature, diisopropyl ether (\sim 1 mL) was added. A fine suspension of material formed which was collected on Celite, washed with water, EtOH, diethylether. The resulting solid was dissolved in acetonitrile and concentrated under reduced pressure to give the desired complex. In all cases, the desired complex appeared pure by NMR spectroscopy.

2.2.2 Synthesis of Cu^I complex $[Cu(1,4)_2](BF_4)$



$[Cu(1,4)_2](BF_4)$ was synthesized using the general procedure described in section 2.2.1.

¹H-NMR (500 MHz, CD_3CN): δ (ppm) 9.11 (s, 2H, H⁷), 8.06 (t, $J = 7.7$ Hz, 2H, H⁴), 7.89 (d, $J = 7.6$ Hz, 2H, H⁵), 7.61 (d, $J = 7.8$ Hz, 2H, H³), 7.38 (d, $J = 8.0$ Hz, 2H, H⁹), 7.17 (d, $J = 8.0$ Hz, 2H, H¹⁰), 2.31 (s, 6H, H¹), 2.30 (s, 6H, H¹²).

¹³C-NMR (125.8 MHz, CD_3CN): δ (ppm) 159.19 (C²), 158.44 (C⁷), 151.50 (C⁶), 145.35 (C⁸), 140.61 (C¹¹), 139.47 (C⁴), 131.07 (C¹⁰), 129.16 (C³), 126.48 (C⁵), 123.18 (C⁹), 25.11 (C¹), 20.99 (C¹²).

HRMS (ESI+): m/z calcd. for $[Cu(1,4)_2]^+$ 483.1604 found 483.1599.

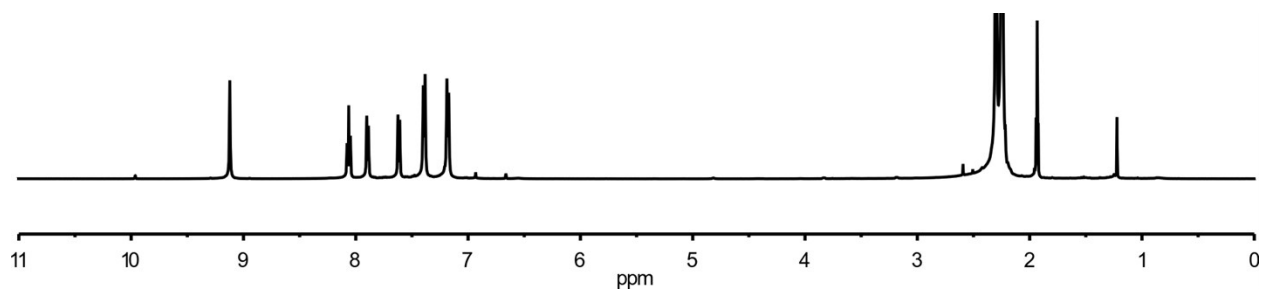


Figure S1. ^1H NMR (500 MHz, 297 K, CD_3CN) of Cu^{I} complex $[\text{Cu}(\mathbf{1},\mathbf{4})_2](\text{BF}_4)$.

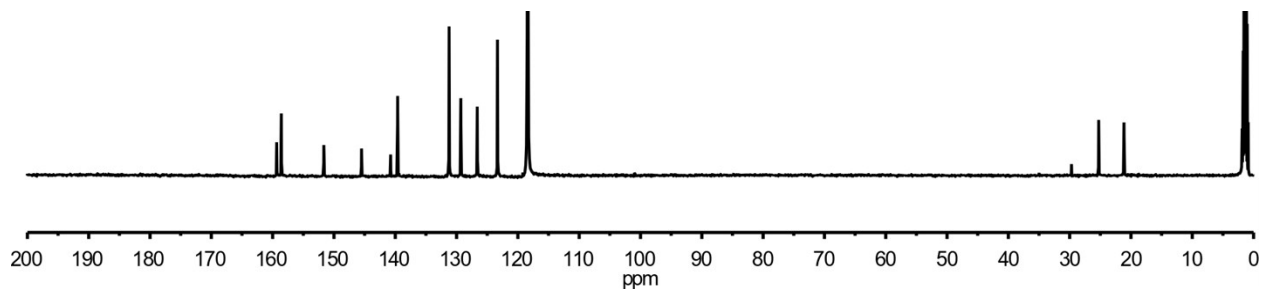


Figure S2. ^{13}C NMR (125 MHz, 297 K, CD_3CN) of Cu^{I} complex $[\text{Cu}(\mathbf{1},\mathbf{4})_2](\text{BF}_4)$.

2.2.3 Synthesis of Fe^{II} complex $[\text{Fe}(\mathbf{2},\mathbf{3})_2](\text{BF}_4)_2$



The complex $[\text{Fe}(\mathbf{2},\mathbf{3})_2](\text{BF}_4)_2$ was synthesized as described in the literature. NMR and mass data were consistent with those previously reported.^[S3]

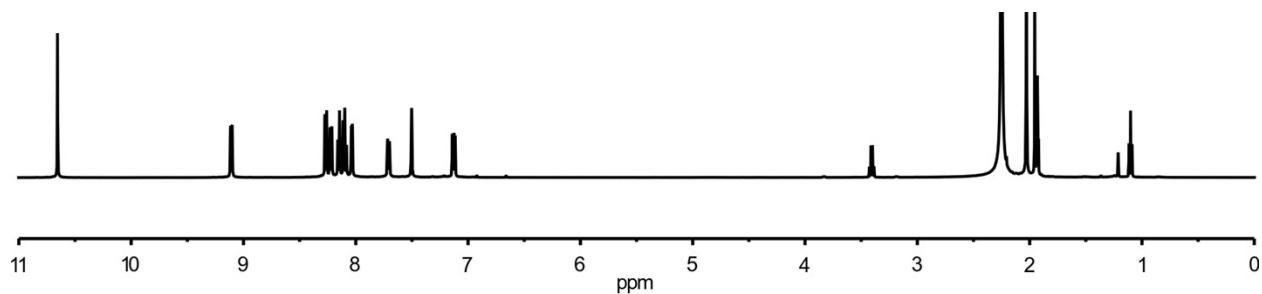


Figure S3. ^1H NMR (500 MHz, 297 K, CD_3CN) of Fe^{II} complex $[\text{Fe}(\mathbf{2},\mathbf{3})_2](\text{BF}_4)_2$.

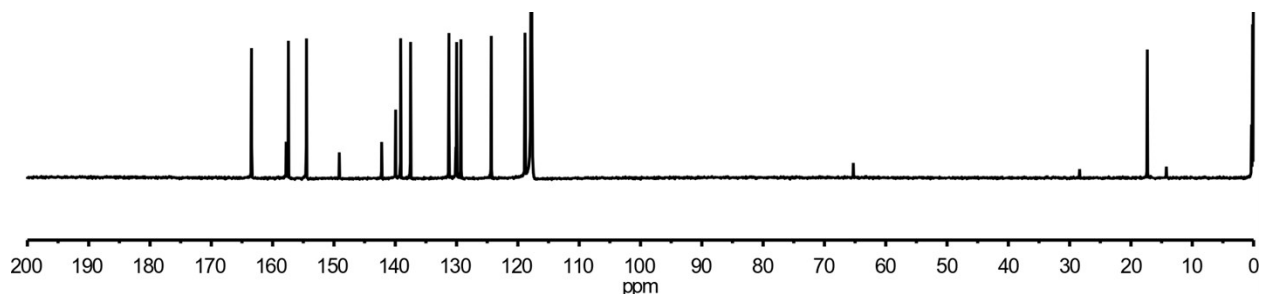
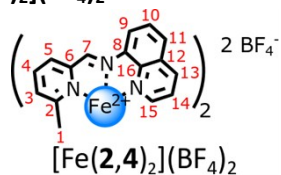


Figure S4. ^{13}C NMR (125 MHz, 297 K, CD_3CN) of Fe^{II} complex $[\text{Fe}(\mathbf{2},\mathbf{3})_2](\text{BF}_4)_2$.

2.2.4 Synthesis of Fe^{II} complex $[\text{Fe}(\mathbf{2},\mathbf{4})_2](\text{BF}_4)_2$



$[\text{Fe}(\mathbf{2},\mathbf{4})_2](\text{BF}_4)_2$ was synthesized using the general procedure described in section 2.2.1.

^1H -NMR (500 MHz, CD_3CN): δ (ppm) 12.33 (br s, 2H, H^7), 9.26 (d, $J = 7.7$ Hz, 2H, H^9), 8.70 (br s, 2H, H^{15}), 8.55 (d, $J = 7.6$ Hz, 2H, H^5), 8.29 (d, $J = 8.2$ Hz, 2H, H^{11}), 8.20 (t, $J = 8.0$ Hz, 2H, H^{10}), 8.14 (d, $J = 8.3$ Hz, 2H, H^{13}), 7.91 (t, $J = 7.7$ Hz, 2H, H^4), 7.49 (dd, $J = 8.2, 4.9$ Hz, 2H, H^{14}), 7.43 (d, $J = 7.8$ Hz, 2H, H^3), 2.06 (s, 6H).

^{13}C -NMR (125.8 MHz, CD_3CN): δ (ppm) 171.12 (C^2), 164.32 (C^7), 157.72 (C^6), 157.33 (C^{15}), 147.03 (C^{16}), 140.67 (C^8), 139.71 (C^4), 138.51 (C^{13}), 134.31 (C^3), 132.50 (C^{11}), 131.65 (C^{5+12}), 130.27 (C^{10}), 128.53 (C^{14}), 120.98 (C^9), 25.88 (C^1).

HRMS (ESI+): m/z calcd. for $[[\text{Fe}(\mathbf{2},\mathbf{4})_2](\text{BF}_4)]^+$ 637.1598 found 637.1580.

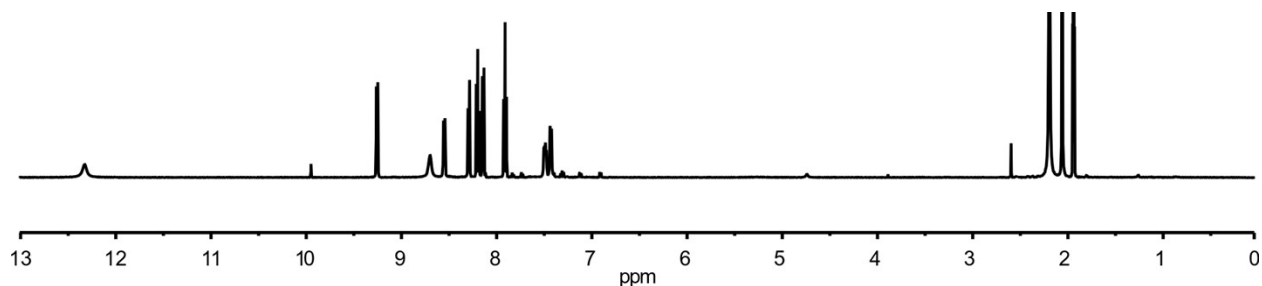


Figure S5. ^1H NMR (500 MHz, 297 K, CD_3CN) of Fe^{II} complex $[\text{Fe}(\mathbf{2},\mathbf{4})_2](\text{BF}_4)_2$.

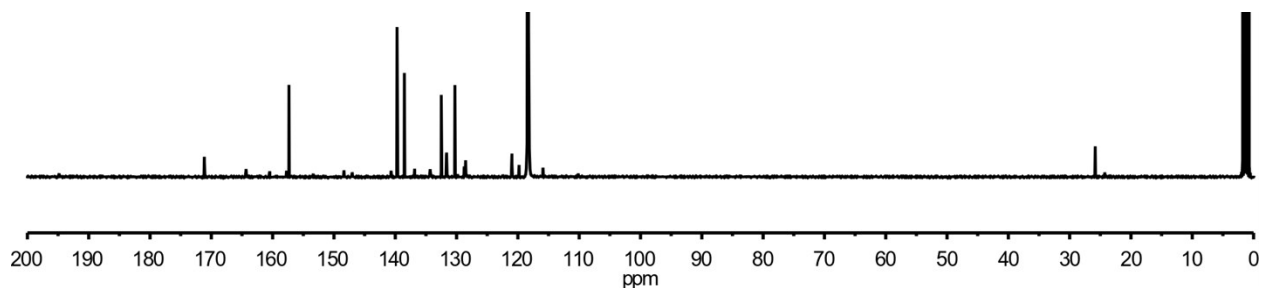
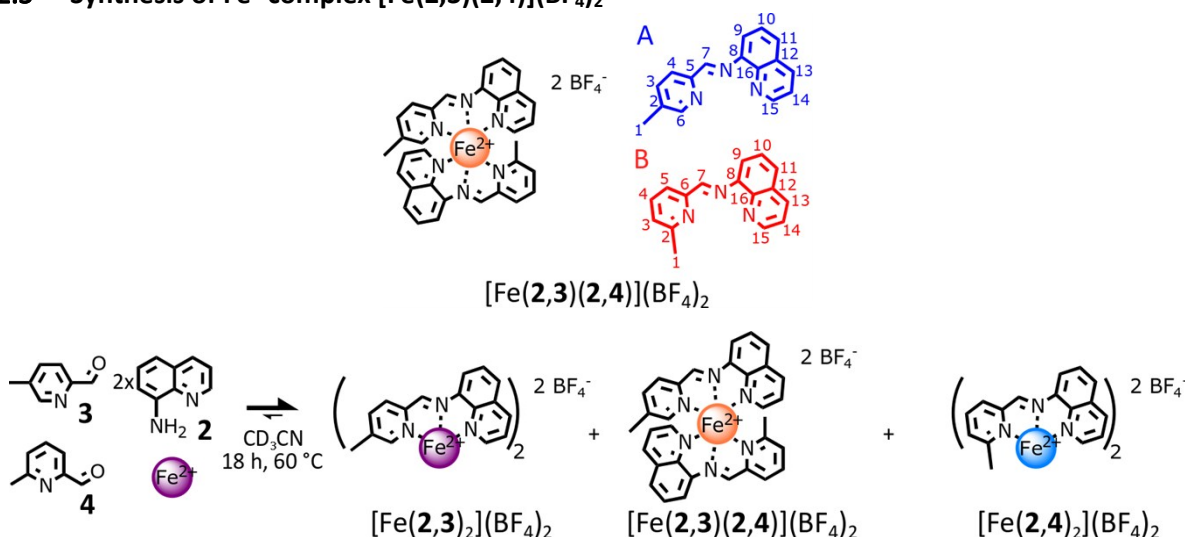


Figure S6. ^{13}C NMR (125 MHz, 297 K, CD_3CN) of Fe^{II} complex $[\text{Fe}(\mathbf{2},\mathbf{4})_2](\text{BF}_4)_2$.

2.2.5 Synthesis of Fe^{II} complex [Fe(2,3)(2,4)](BF₄)₂



Scheme S2. Synthesis of the heteroleptic complex [Fe(2,3)(2,4)]²⁺.

CD₃CN solutions of the 2-formylpyridines **3** (50 μL of 320 mM, 16 μmol, 1 eq.) and **4** (50 μL of 320 mM, 16 μmol, 1 eq.) and a CD₃CN solution of amine **2** (100 μL of 320 mM, 32 μmol, 2 eq.) were combined. The resulting mixture was treated with a CD₃CN solution of Fe(BF₄)₂ (100 μL of 160 mM, 16 μmol, 1 eq.) and was heated at 60 °C for 18 h. The complexes were not isolated, all the following analysis were done on the crude reaction mixture.

The heteroleptic complex [Fe(2,3)(2,4)]²⁺ could not be isolated. However, its ¹H and ¹³C NMR data could be determined by comparing the HMBC, HSQC, ROESY and COSY spectra of complexes [Fe(2,3)₂](BF₄)₂ and [Fe(2,4)₂](BF₄)₂ prepared in isolation with the spectra of the reaction mixture described above. Due to overlapping signals in the ¹H NMR spectrum, the multiplicity of some of the peaks could not be determined with precision.

¹H-NMR (500 MHz, CD₃CN): δ (ppm) 10.89 (s, 1H, H^{7B}), 10.70 (s, 1H, H^{7A}), 9.20-9.15 (m, 2H, H^{9A+9B}), 8.29 (d, *J* = 7.8 Hz, 1H, H^{4A+5B}), 8.27 (1H, H¹⁵), 8.26 (1H, H^{13A+11A or 11B}), 8.18 (1H, H^{11A or 11B}), 8.13 (1H, H^{10A+13B}), 8.09 (1H, H^{10B}), 7.84 (t, *J* = 7.7 Hz, 1H, H^{4B}), 7.74 (d, *J* = 7.8 Hz, 1H, H^{3A}), 7.76 (s, 1H, H^{6A}), 7.58 (dd, *J* = 5.2, 1.3 Hz, 1H, H^{15B}), 7.20 (dd, *J* = 8.3, 5.1 Hz, 1H, H^{14A}), 7.06 (dd, *J* = 8.3, 5.2 Hz, 1H, H^{14B}), 7.00 (d, *J* = 7.8, 1.1 Hz, 1H, H^{3B}), 2.09 (s, 3H, H^{1A}), 1.94 (s, 3H, H^{1B}).

¹³C-NMR (125.8 MHz, CD₃CN): δ (ppm) 168.40 (C^{2B}), 166.62 (C^{7B}), 164.89 (C^{7A}), 159.78 (C^{6B}), 158.90 (C^{15A}), 158.86 (C^{5A}), 156.92 (C^{15B}), 155.55 (C^{6A}), 150.18 (C^{16A}), 149.30 (C^{16B}), 143.09 (C^{8A}), 142.61 (C^{8B}), 140.53 (C^{2A}), 139.68 (C^{3A}), 139.63 (C^{4B}), 138.15 (C^{13A}), 138.08 (C^{13B}), 131.93 (C^{11A or 11B}), 131.81 (C^{10B}), 130.82 (C^{4A}), 130.72 (C^{12A or 12B}), 130.07 (C^{12A or 12B}), 130.49 (C^{11A or 11B}), 129.92 (C^{5B}), 129.91 (C^{10A}), 129.88 (C^{3B}), 125.14 (C¹⁴), 124.89 (C^{14B}), 119.71 (C^{9A or 9B}), 119.29 (C^{9A or 9B}), 24.31 (C^{1B}), 18.77 (C^{1A}).

As [Fe(2,3)(2,4)](BF₄)₂, [Fe(2,3)₂](BF₄)₂ and [Fe(2,4)₂](BF₄)₂ have the same mass, the formation of [Fe(2,3)(2,4)](BF₄)₂ could not be confirmed by mass spectrometry.

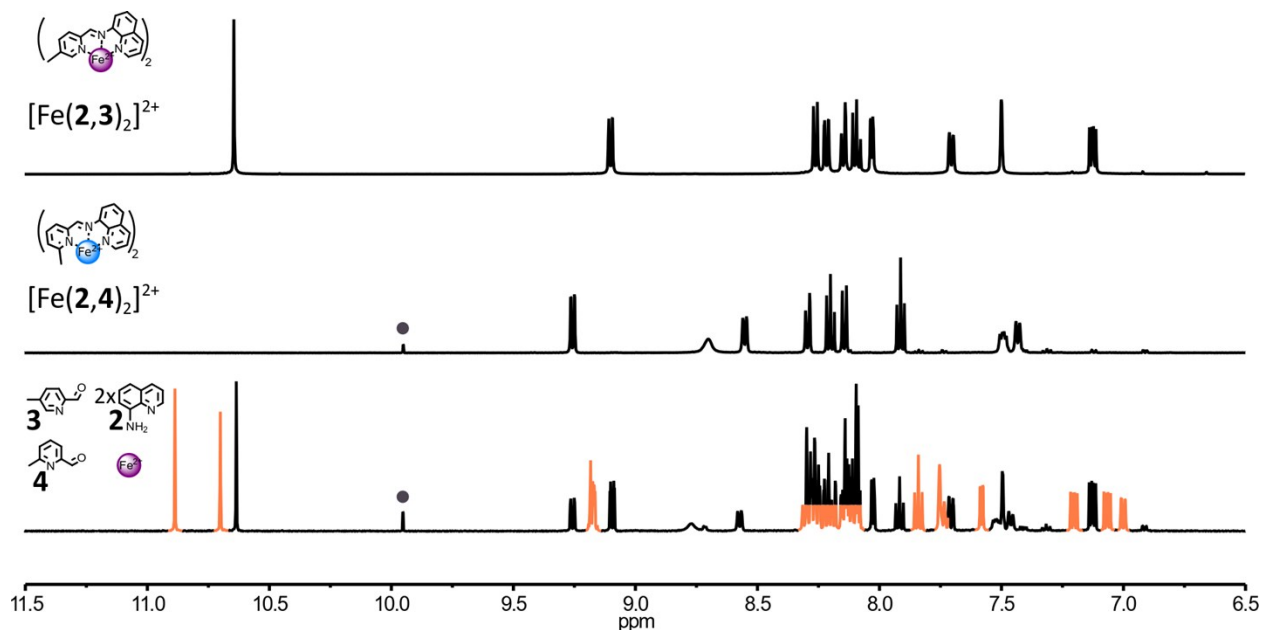


Figure S7. Partial ^1H NMR spectra (500 MHz, CD_3CN , 297 K) of: (top) complex $[\text{Fe}(\mathbf{2},\mathbf{3})_2]^{2+}$, (middle) complex $[\text{Fe}(\mathbf{2},\mathbf{4})_2]^{2+}$, (bottom) the crude reaction mixture obtained by mixing $\mathbf{2}$, $\mathbf{3}$, $\mathbf{4}$ and $\text{Fe}(\text{BF}_4)_2$ in the molar ratio 2:1:1:1 at 60 °C for 18 h. The diagnostic signals of the heteroleptic complex $[\text{Fe}(\mathbf{2},\mathbf{3})(\mathbf{2},\mathbf{4})]^{2+}$ are colored in orange and one of the diagnostic signals of the free aldehyde $\mathbf{4}$ is highlighted by a grey circle.

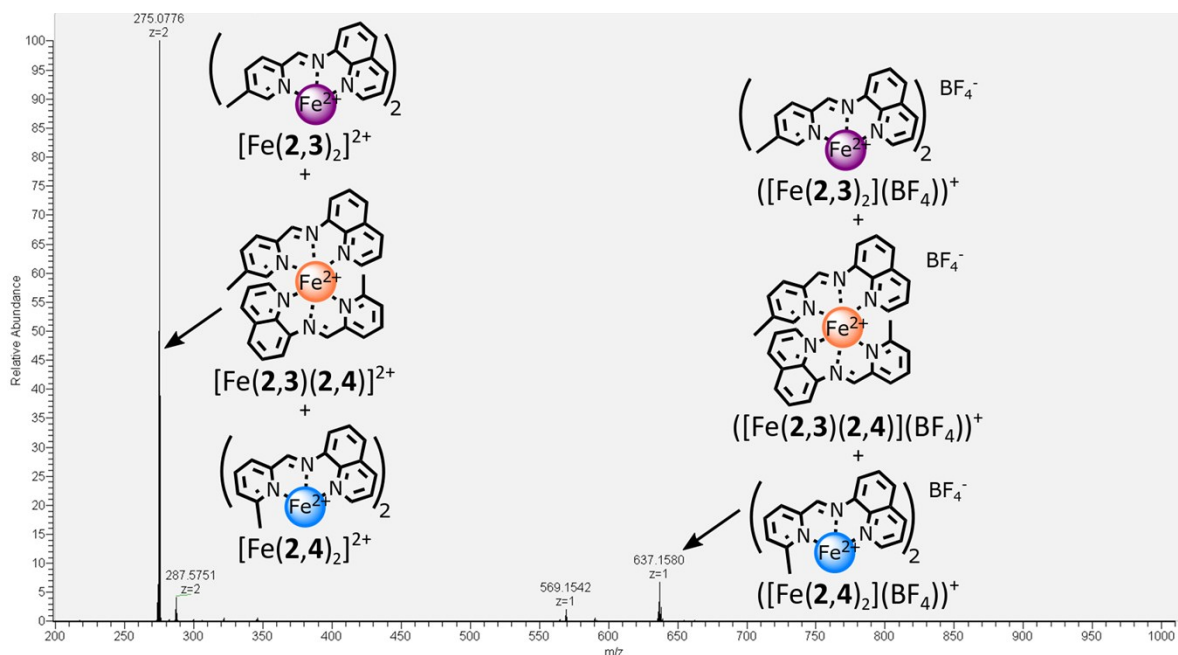


Figure S8. Partial HRESI-MS spectra of the reaction mixture obtained by mixing $\mathbf{2}$, $\mathbf{3}$, $\mathbf{4}$ and $\text{Fe}(\text{BF}_4)_2$ in the molar ratio 2:1:1:1 at 60 °C for 18 h.

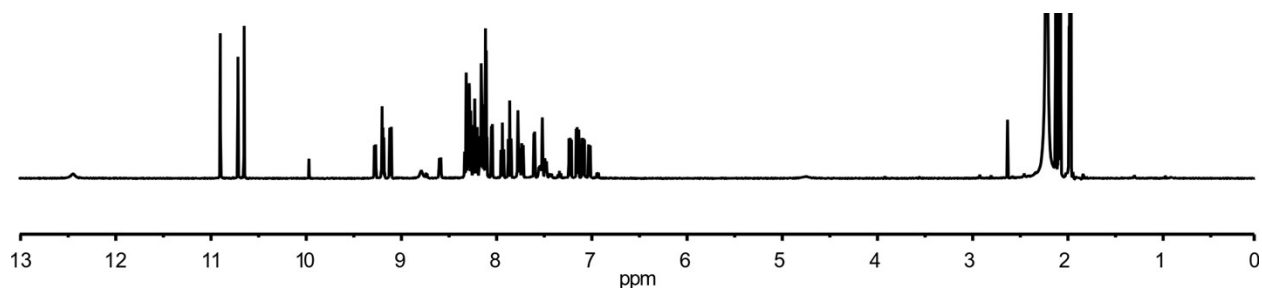


Figure S9. ^1H NMR (500 MHz, 297 K, CD_3CN) of the reaction mixture obtained by mixing **2**, **3**, **4** and $\text{Fe}(\text{BF}_4)_2$ in the molar ratio 2:1:1:1 at 60 °C for 18 h.

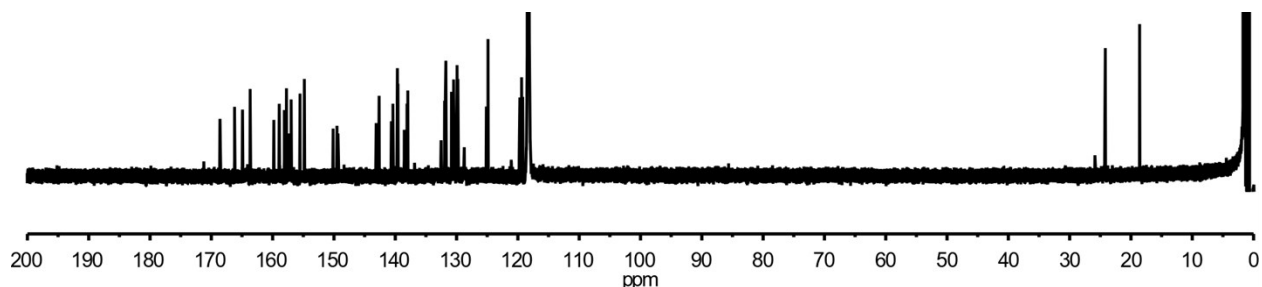
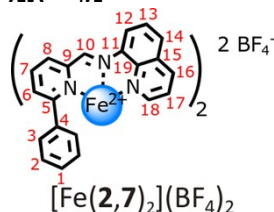


Figure S10. ^{13}C NMR (125 MHz, 297 K, CD_3CN) of the reaction mixture obtained by mixing **2**, **3**, **4** and $\text{Fe}(\text{BF}_4)_2$ in the molar ratio 2:1:1:1 at 60 °C for 18 h.

2.2.6 Synthesis of Fe^{II} complex $[\text{Fe}(\mathbf{2},\mathbf{7})_2](\text{BF}_4)_2$



$[\text{Fe}(\mathbf{2},\mathbf{7})_2](\text{BF}_4)_2$ was synthesized using the general procedure described in section 2.2.1.

Due to the broadness of most peaks of $[\text{Fe}(\mathbf{2},\mathbf{7})_2](\text{BF}_4)_2$ (at 297 K or 243 K in CD_3CN) the ^1H NMR and ^{13}C NMR spectra of the complex could not be assigned with precision.

^1H -NMR (500 MHz, CD_3CN): δ (ppm) 14.96 (br s, 2H), 11.04 (br s, 2H), 10.62 (br s, 2H), 10.31 (br s, 2H), 9.84 (br s, 2H), 8.93 (br s, 2H), 8.84 (br s, 2H), 8.51 (d, $J = 7.6$ Hz, 2H), 8.04 (d, $J = 7.9$ Hz, 2H), 7.42 (t, $J = 7.4$ Hz, 2H), 7.05 (br s, 4H), 6.54 (br s, 4H).

The chemical shift of two of the protons of $[\text{Fe}(\mathbf{2},\mathbf{7})_2](\text{BF}_4)_2$ could not be found.

^{13}C -NMR (125.8 MHz, 243 K, CD_3CN): δ (ppm) 194.79, 170.16, 161.83, 156.22, 140.78, 138.62, 138.09, 132.14, 131.68, 130.51, 129.68, 129.33, 128.82, 128.68, 127.65, 127.50, 125.50, 121.33, 120.64.

HRMS (ESI+): m/z calcd. for $[[\text{Fe}(\mathbf{2},\mathbf{7})_2](\text{BF}_4)]^+$ 761.1913 found 761.1895.

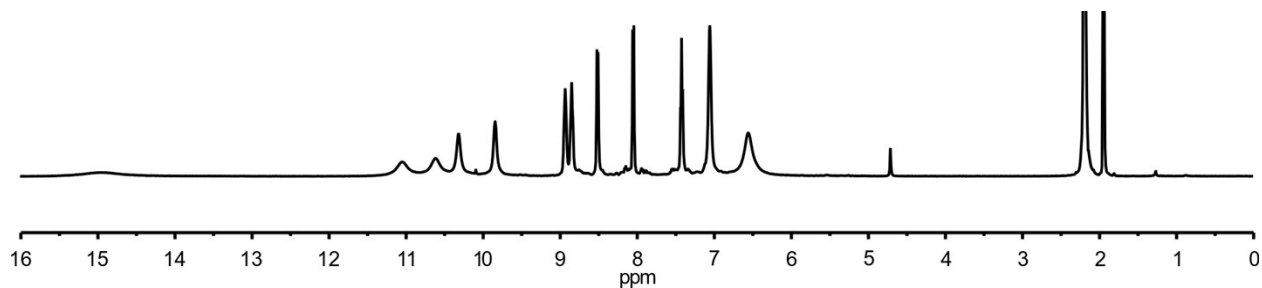


Figure S11. ^1H NMR (500 MHz, 297 K, CD_3CN) of Fe^{II} complex $[\text{Fe}(\mathbf{2},\mathbf{7})_2](\text{BF}_4)_2$.

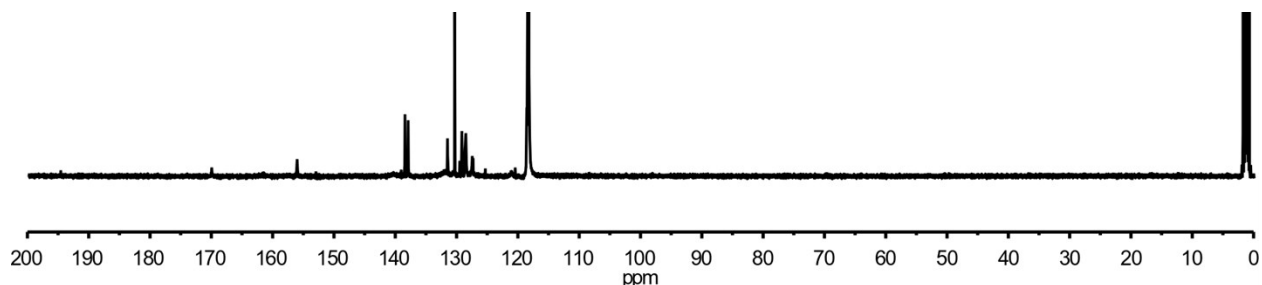
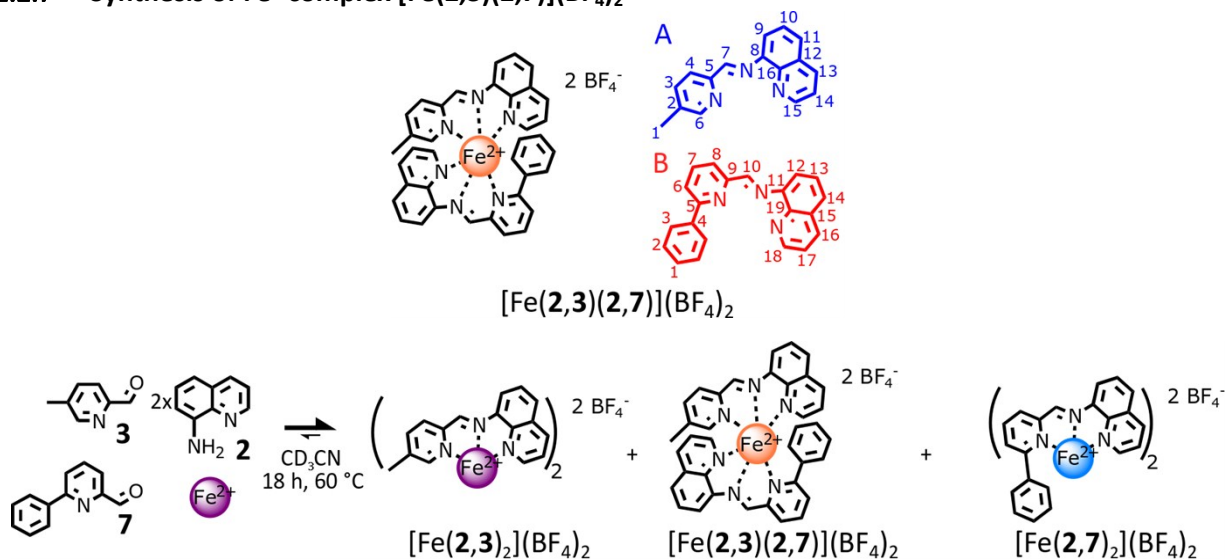


Figure S12. ^{13}C NMR (125 MHz, 243 K, CD_3CN) of Fe^{II} complex $[\text{Fe}(\mathbf{2},\mathbf{7})_2](\text{BF}_4)_2$.

2.2.7 Synthesis of Fe^{II} complex $[\text{Fe}(\mathbf{2},\mathbf{3})(\mathbf{2},\mathbf{7})](\text{BF}_4)_2$



Scheme S3. Synthesis of the heteroleptic complex $[\text{Fe}(\mathbf{2},\mathbf{3})(\mathbf{2},\mathbf{7})]^{2+}$.

CD_3CN solutions of the 2-formylpyridines **3** (50 μL of 320 mM, 16 μmol , 1 eq.) and **7** (50 μL of 320 mM, 16 μmol , 1 eq.) and a CD_3CN solution of amine **2** (100 μL of 320 mM, 32 μmol , 2 eq.) were combined. The resulting mixture was treated with a CD_3CN solution of $\text{Fe}(\text{BF}_4)_2$ (100 μL of 160 mM, 16 μmol , 1 eq.) and was heated at 60 $^\circ\text{C}$ for 18 h. The complexes were not isolated, all the following analysis were done on the crude reaction mixture.

The heteroleptic complex $[\text{Fe}(\mathbf{2},\mathbf{3})(\mathbf{2},\mathbf{7})]^{2+}$ could not be isolated. However, its ^1H and ^{13}C NMR data could be determined by comparing the HMBC, HSQC, ROESY and COSY spectra of complexes $[\text{Fe}(\mathbf{2},\mathbf{3})_2](\text{BF}_4)_2$ and $[\text{Fe}(\mathbf{2},\mathbf{7})_2](\text{BF}_4)_2$ prepared in isolation with the spectra of the reaction mixture described above.

¹H-NMR (500 MHz, CD₃CN): δ (ppm) 11.04 (s, 1H, H^{10B}), 9.77 (s, 1H, H^{7B}), 9.20 (dd, $J = 6.8, 2.1$ Hz, 1H, H^{12B}), 8.49 (dd, $J = 7.8, 1.5$ Hz, 1H, H^{8B}), 8.39 (dd, $J = 7.8, 1.0$ Hz, 1H, H^{9A}), 8.27 (dd, $J = 5.2, 1.4$ Hz, 1H, H^{15A}), 8.23 (dd, $J = 8.3, 1.3$ Hz, 1H, H^{16B}), 8.14 (d, $J = 8.0$ Hz, 1H, H^{4A}), 8.10 (d, $J = 8.1$ Hz, 1H, H^{11A}), 8.09 (t, $J = 8.1$, 1H, H^{13B}), 8.07 (dd, $J = 8.3, 1.3$, 1H, H^{14B+13A}), 7.96 (t, $J = 7.7$ Hz, 1H, H^{7B}), 7.90 (t, $J = 8.0$ Hz, 1H, H^{10A}), 7.78 (d, $J = 1.6$ Hz, 1H, H^{6A}), 7.76 (ddd, $J = 8.0, 1.9, 1.0$ Hz, 1H, H^{3A}), 7.52 (tt, $J = 7.6, 1.3$ Hz, 1H, H^{1B}), 7.37 (dd, $J = 5.2, 1.3$ Hz, 1H, H^{18B}), 7.34 (br s, 2H, H^{2B or 3B}), 7.21 (dd, $J = 8.3, 5.1$ Hz, 1H, H^{14A}), 6.98 (dd, $J = 7.6, 1.5$ Hz, 1H, H^{6B}), 6.97 (dd, $J = 8.2, 5.7$ Hz, 1H, H^{17B}), 6.71 (br s, 2H, H^{2B or 3B}), 2.13 (s, 3H, H^{1A})

¹³C-NMR (125.8 MHz, CD₃CN): δ (ppm) 169.26 (C^{5B}), 166.12 (C^{10B}), 163.07 (C^{7A}), 159.65 (C^{9B}), 158.84 (C^{5A}), 158.25 (C^{15A}), 157.13 (C^{18B}), 155.57 (C^{6A}), 149.83 (C^{16A}), 149.33 (C^{19B}), 142.84 (C^{8A}), 142.76 (C^{11B}), 140.20 (C^{2A}), 139.76 (C^{3A}), 139.05 (C^{7B}), 138.39 (C^{4B}), 138.12 (C^{16B}), 137.99 (C^{13A}), 131.85 (C^{14B}), 131.75 (C^{13B}), 131.54 (C^{11A}), 130.60 (C^{1B}), 130.53 (C^{8B}), 130.48 (C^{6B}), 130.44 (C^{4A}), 130.20 (C^{12A}), 129.82 (C^{15B}), 129.34 (C^{10A}), 128.69 (C^{2B+3B}), 124.86 (C^{14A}), 124.82 (C^{17B}), 119.72 (C^{9A}), 119.25 (C^{12B}), 18.74 (C^{1A}).

HRMS (ESI+): m/z calcd. for [[Fe(2,3)(2,7)](BF₄)⁺ 699.1750 found 699.1737.

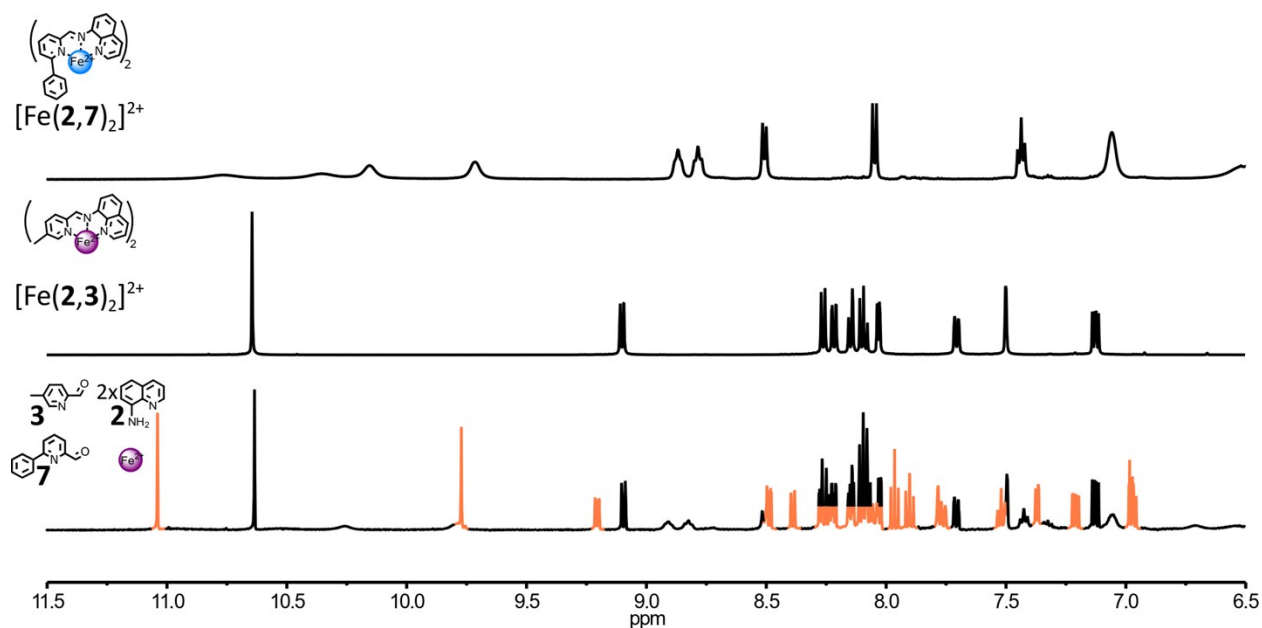


Figure S13. Partial ¹H NMR spectra (500 MHz, CD₃CN, 297 K) of: (top) complex [Fe(2,7)₂]²⁺, (middle) complex [Fe(2,3)₂]²⁺, (bottom) the crude reaction mixture obtained by mixing **2**, **3**, **7** and Fe(BF₄)₂ in the molar ratio 2:1:1:1 at 60 °C for 18 h. The diagnostic signals of the heteroleptic complex [Fe(2,3)(2,7)]²⁺ are colored in orange.

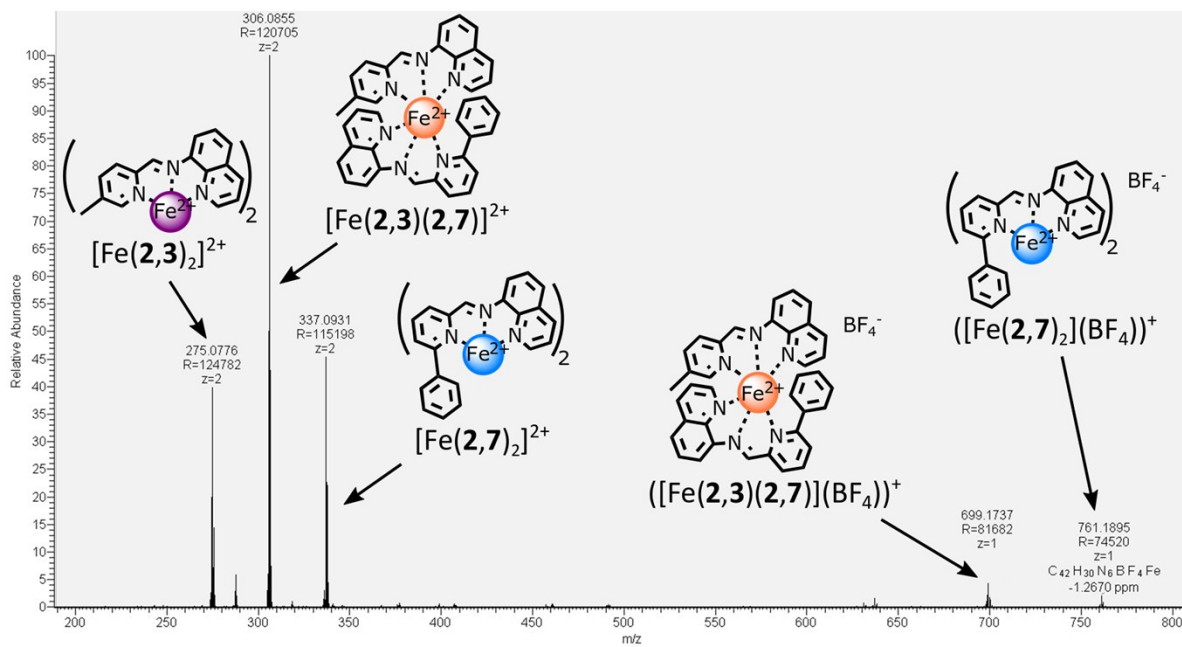


Figure S14. Partial HRESI-MS spectra of the reaction mixture obtained by mixing **2**, **3**, **7** and $\text{Fe}(\text{BF}_4)_2$ in the molar ratio 2:1:1:1 at 60 °C for 18 h.

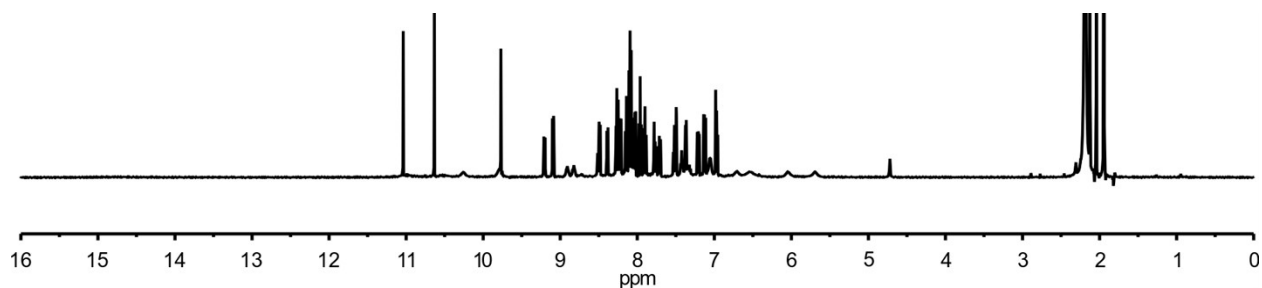


Figure S15. ^1H NMR (500 MHz, 297 K, CD_3CN) of the reaction mixture obtained by mixing **2**, **3**, **7** and $\text{Fe}(\text{BF}_4)_2$ in the molar ratio 2:1:1:1 at 60 °C for 18 h.

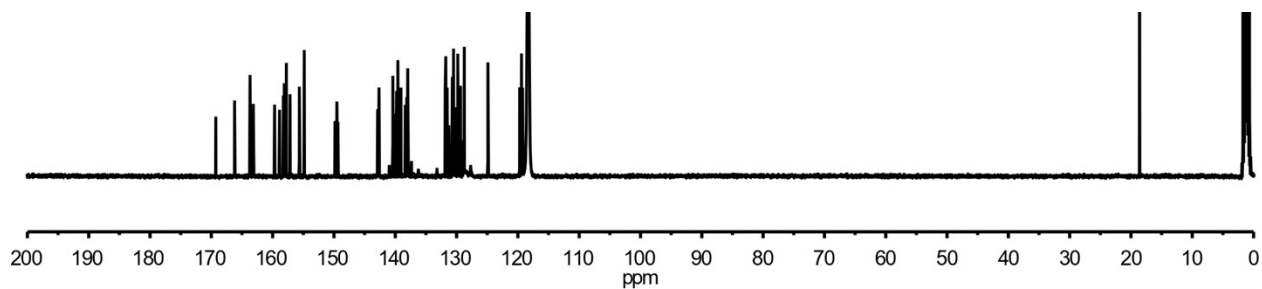


Figure S16. ^{13}C NMR (125 MHz, 297 K, CD_3CN) of the reaction mixture obtained by mixing **2**, **3**, **7** and $\text{Fe}(\text{BF}_4)_2$ in the molar ratio 2:1:1:1 at 60 °C for 18 h.

2.2.8 Synthesis of Cu^I complex [Cu(4,5)₂](BF₄)



[Cu(4,5)₂](BF₄) was synthesized using the general procedure described in section 2.2.1.

¹H-NMR (500 MHz, CD₃CN): δ (ppm) 9.02 (br s, 2H, H⁷), 7.99 (t, $J = 7.7$ Hz, 2H, H⁴), 7.76 (br s, 2H, H⁵), 7.52 (d, $J = 7.7$ Hz, 2H, H³), 7.46 (br s, 4H, H⁹), 6.65 (d, $J = 8.2$ Hz, 4H, H¹⁰), 2.93 (br s, 12H, H¹²), 2.25 (s, 6H, H¹).

¹³C-NMR (125.8 MHz, CD₃CN): δ (ppm) 158.92 (C²), 152.41 (C⁶), 152.14 (C⁷⁺¹¹), 139.32 (C⁴), 136.08 (C⁸), 127.99 (C³), 125.42 (C⁵), 125.06 (C⁹), 113.06 (C¹⁰), 40.47 (C¹²), 25.10 (C¹).

HRMS (ESI+): m/z calcd. for [Cu(4,5)₂]⁺ 541.2135 found 541.2125.

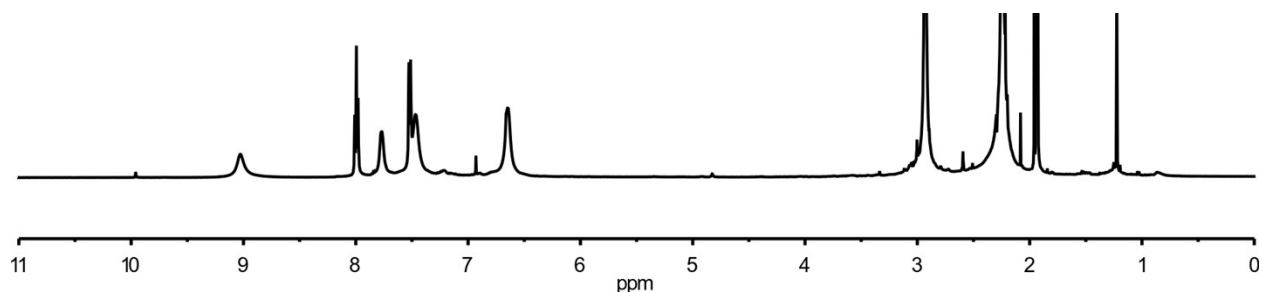


Figure S17. ¹H NMR (500 MHz, 297 K, CD₃CN) of Cu^I complex [Cu(4,5)₂](BF₄).

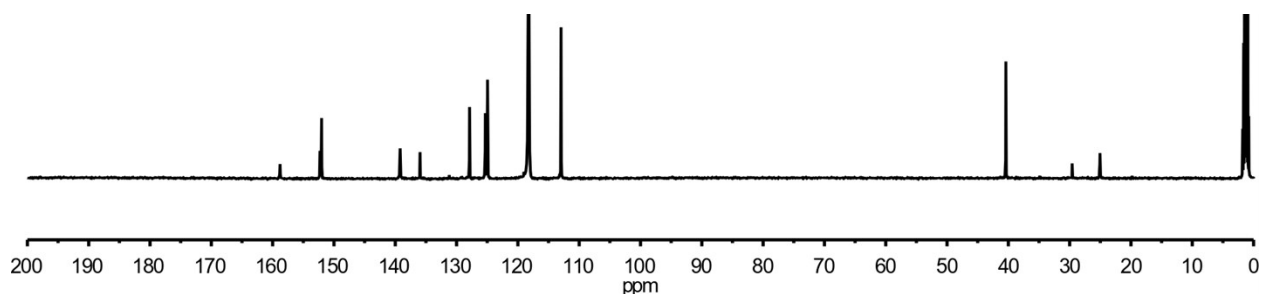


Figure S18. ¹³C NMR (125 MHz, 297 K, CD₃CN) of Cu^I complex [Cu(4,5)₂](BF₄).

2.2.9 Synthesis of Cu^I complex [Cu(1,6)₂](BF₄)



CD₃CN solutions of **1** (100 μ L of 320 mM, 32 μ mol, 2 eq.) and of **6** (100 μ L of 320 mM, 32 μ mol, 2 eq.) were combined. The resulting mixture was treated with a CD₃CN solution of [Cu(CH₃CN)₄](BF₄) (100 μ L of 160 mM, 16 μ mol, 1 eq.) and heated at 60 °C for 18 h. [Cu(1,6)₂](BF₄) was not stable enough to be isolated by precipitation, all the present experiments and analysis were done on the crude reaction mixture.

¹H-NMR (500 MHz, CD₃CN): δ (ppm) 8.95 (s, 2H, H⁷), 8.32 – 8.28 (m, 4H, H⁴⁺⁵), 8.07 – 8.01 (m, 2H, H³), 7.46 (d, *J* = 8.3 Hz, 4H, H⁹), 7.28 (d, *J* = 8.1 Hz, 4H, H¹⁰), 2.36 (s, 6H, H¹²).

¹³C-NMR (125.8 MHz, CD₃CN): δ (ppm) 157.86 (C⁷), 154.25 (C⁶), 147.42 (q, *J* = 34.7 Hz, C²), 146.24 (C⁸), 141.37 (C⁴), 140.47 (C¹¹), 131.15 (C¹⁰), 129.57 (C⁵), 124.88 (C³), 123.23 (C⁹), 121.89 (C¹), 21.14 (C¹²).

HRMS (ESI+): *m/z* calcd. for [Cu(1,6)₂]⁺ 591.1039 found 591.1031.

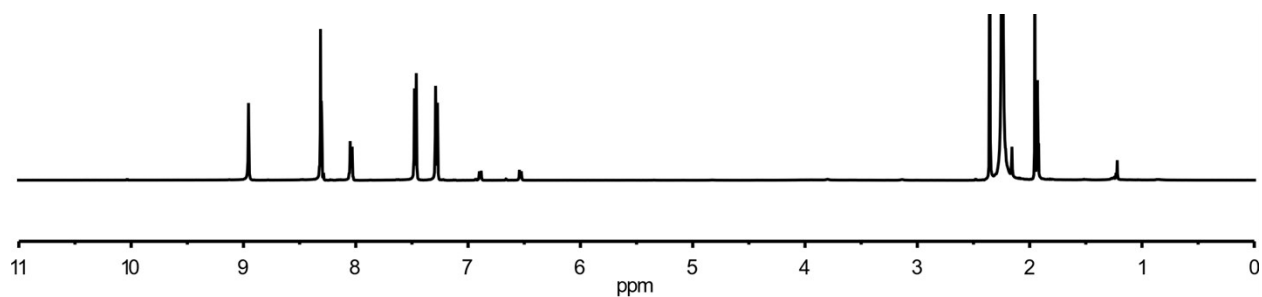


Figure S19. ¹H NMR (500 MHz, 297 K, CD₃CN) of Cu^I complex [Cu(1,6)₂](BF₄).

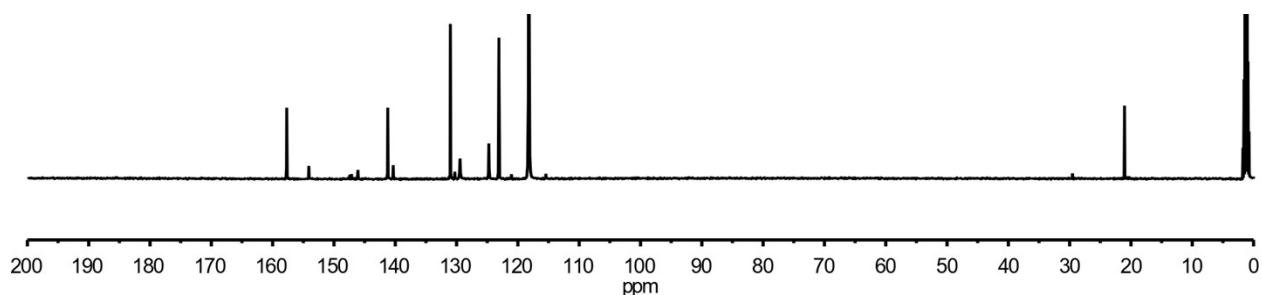


Figure S20. ¹³C NMR (125 MHz, 297 K, CD₃CN) of Cu^I complex [Cu(1,6)₂](BF₄).

2.2.10 Synthesis of Cu^I complex [Cu(1,7)₂](BF₄)



[Cu(1,7)₂](BF₄) was synthesized using the general procedure described in section 2.2.1.

¹H-NMR (500 MHz, CD₃CN): δ (ppm) 8.98 (s, 2H, H¹⁰), 8.03 (t, *J* = 7.8 Hz, 2H, H⁷), 7.80 (dd, *J* = 7.7, 1.0 Hz, 2H, H⁸), 7.70 (dd, *J* = 7.9, 1.0 Hz, 2H, H⁶), 7.41 (d, *J* = 8.4 Hz, 4H, H¹²), 7.36 (d, *J* = 7.3 Hz, 4H, H³), 7.19 (d, *J* = 8.2 Hz, 4H, H¹³), 7.15 (d, *J* = 7.4 Hz, 2H, H¹), 7.06 (t, *J* = 7.6 Hz, 4H, H²), 2.32 (s, 6H, H¹⁵).

¹³C-NMR (125.8 MHz, CD₃CN): δ (ppm) 158.85 (C⁵), 158.27 (C¹⁰), 152.17 (C⁹), 145.15 (C¹¹), 140.75 (C¹⁴), 139.70 (C⁴), 139.60 (C⁷), 131.14 (C¹³), 130.22 (C¹), 128.71 (C²), 128.40 (C³), 128.03 (C⁶), 127.35 (C⁸), 123.49 (C¹²), 21.11 (C¹⁵).

HRMS (ESI+): *m/z* calcd. for [Cu(1,7)₂]⁺ 607.1917 found 607.1902.

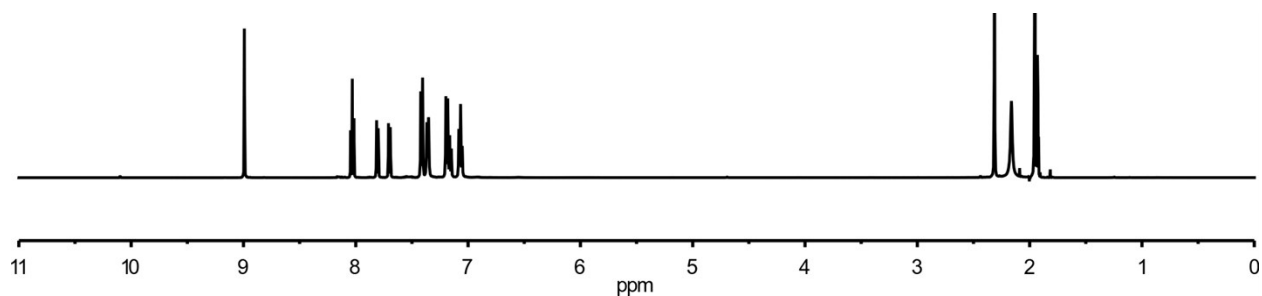


Figure S21. ^1H NMR (500 MHz, 297 K, CD_3CN) of Cu^{I} complex $[\text{Cu}(\mathbf{1},\mathbf{7})_2](\text{BF}_4)$.

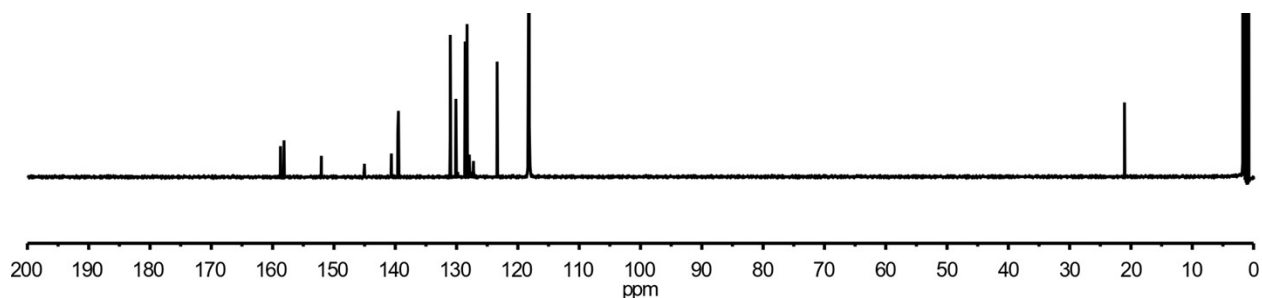
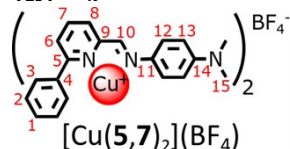


Figure S22. ^{13}C NMR (125 MHz, 297 K, CD_3CN) of Cu^{I} complex $[\text{Cu}(\mathbf{1},\mathbf{7})_2](\text{BF}_4)$.

2.2.11 Synthesis of Cu^{I} complex $[\text{Cu}(\mathbf{5},\mathbf{7})_2](\text{BF}_4)$



$[\text{Cu}(\mathbf{5},\mathbf{7})_2](\text{BF}_4)$ was synthesized using the general procedure described in section 2.2.1.

^1H -NMR (500 MHz, CD_3CN): δ (ppm) 8.91 (s, 2H, H^{10}), 7.95 (t, $J = 7.8$ Hz, 2H, H^7), 7.68 (d, $J = 7.4$ Hz, 2H, H^8), 7.58 (d, $J = 7.7$ Hz, 2H, H^6), 7.51 (d, $J = 9.1$ Hz, 4H, H^{12}), 7.31 (d, $J = 7.2$ Hz, 4H, H^3), 7.12 (t, $J = 7.3$ Hz, 2H, H^1), 7.02 (t, $J = 7.4$ Hz, 4H, H^2), 6.65 (d, $J = 9.1$ Hz, 4H, H^{13}), 2.95 (s, 12H, H^{15}).

^{13}C -NMR (125.8 MHz, CD_3CN): δ (ppm) 158.57 (C^5), 152.96 (C^9), 152.42 (C^{14}), 151.88 (C^{10}), 139.90 (C^4), 139.20 (C^7), 135.73 (C^{11}), 129.94 (C^1), 128.53 (C^2), 128.33 (C^3), 126.82 (C^6), 126.32 (C^8), 125.27 (C^{12}), 113.01 (C^{13}), 40.46 (C^{15}).

HRMS (ESI+): m/z calcd. for $[\text{Cu}(\mathbf{5},\mathbf{7})_2]^+$ 665.2448 found 665.2437.

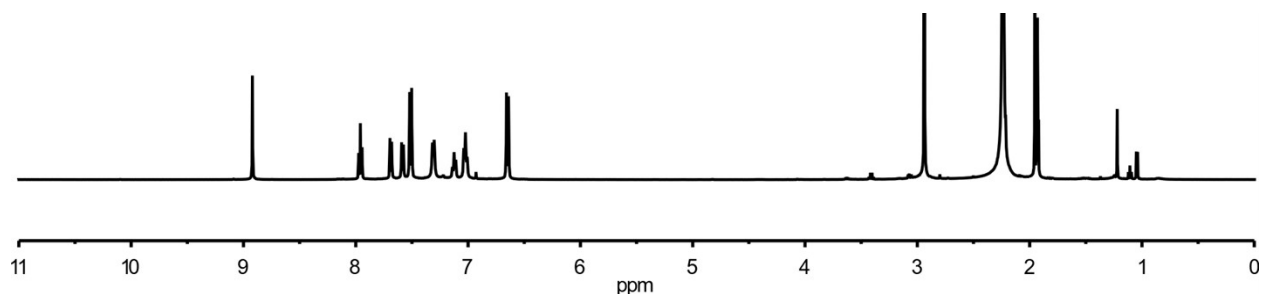


Figure S23. ^1H NMR (500 MHz, 297 K, CD_3CN) of Cu^{I} complex $[\text{Cu}(\mathbf{5},\mathbf{7})_2](\text{BF}_4)$.

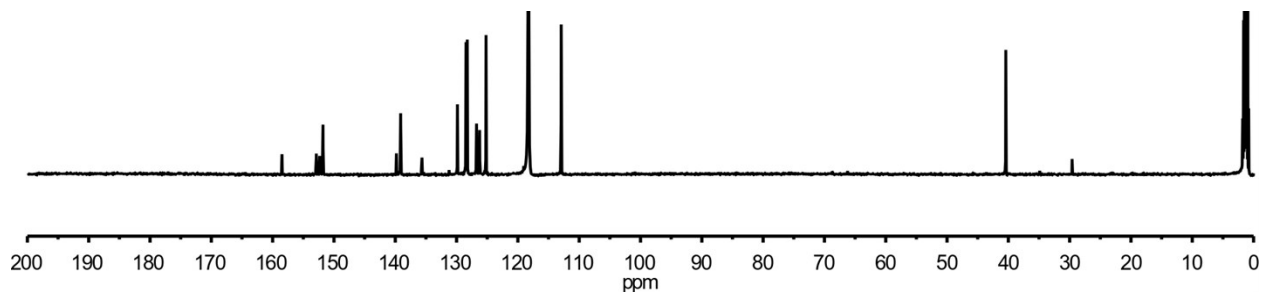


Figure S24. ^{13}C NMR (125 MHz, 297 K, CD_3CN) of Cu^{I} complex $[\text{Cu}(\mathbf{5},\mathbf{7})_2](\text{BF}_4)$.

2.2.12 Synthesis of Cu^{I} complex $[\text{Cu}(\mathbf{7},\mathbf{8})_2](\text{BF}_4)$



$[\text{Cu}(\mathbf{7},\mathbf{8})_2](\text{BF}_4)$ was synthesized using the general procedure described in section 2.2.1.

$^1\text{H-NMR}$ (500 MHz, CD_3CN): δ (ppm) 8.94 (s, 2H, H^{10}), 8.03 (t, $J = 7.7$ Hz, 2H, H^7), 7.79 (d, $J = 7.6$ Hz, 2H, H^8), 7.70 (d, $J = 7.8$ Hz, 2H, H^6), 7.50 (d, $J = 9.0$ Hz, 4H, H^{12}), 7.42 – 7.33 (m, 4H, H^3), 7.20 – 7.13 (m, 1H, H^1), 7.09 (t, $J = 6.7$ Hz, 4H, H^2), 6.90 (d, $J = 9.0$ Hz, 4H, H^{13}), 3.78 (s, 6H, H^{15}).

$^{13}\text{C-NMR}$ (125.8 MHz, CD_3CN): δ (ppm) 161.54 (C^{14}), 158.83 (C^5), 156.49 (C^{10}), 152.38 (C^9), 140.49 (C^4), 139.78 (C^{11}), 139.57 (C^7), 130.20 (C^1), 128.73 (C^2), 128.43 (C^3), 127.74 (C^6), 127.04 (C^8), 125.20 (C^{12}), 115.63 (C^{13}), 56.32 (C^{15}).

HRMS (ESI+): m/z calcd. for $[\text{Cu}(\mathbf{7},\mathbf{8})_2]^+$ 639.1816 found 639.1813.

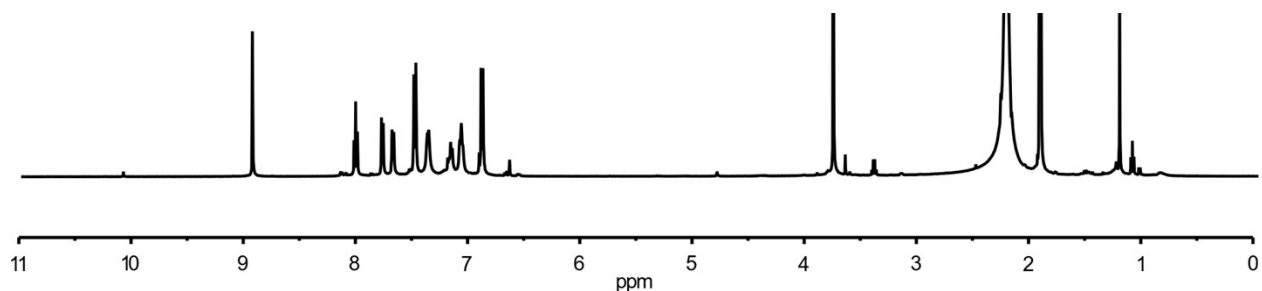


Figure S25. ^1H NMR (500 MHz, 297 K, CD_3CN) of Cu^{I} complex $[\text{Cu}(\mathbf{7},\mathbf{8})_2](\text{BF}_4)$.

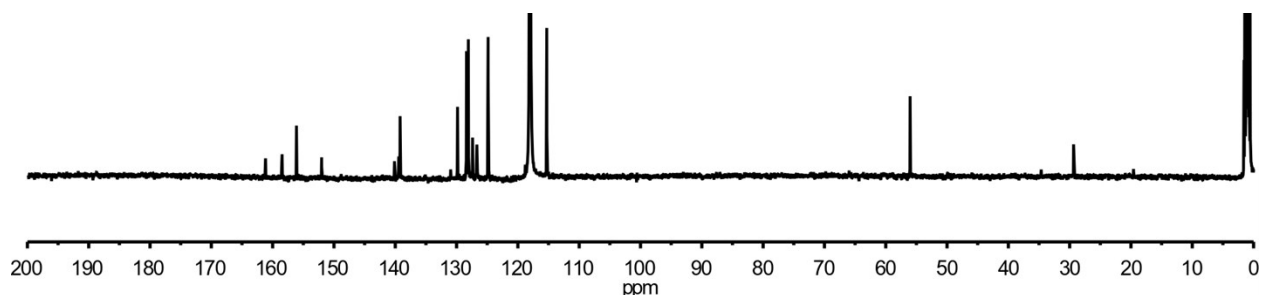


Figure S26. ^{13}C NMR (125 MHz, 297 K, CD_3CN) of Cu^{I} complex $[\text{Cu}(\mathbf{7},\mathbf{8})_2](\text{BF}_4)$.

2.2.13 Synthesis of Cu^I complex [Cu(4,8)₂](BF₄)



[Cu(4,8)₂](BF₄) was synthesized using the general procedure described in section 2.2.1.

¹H-NMR (500 MHz, CD₃CN): δ (ppm) 9.09 (s, 2H, H⁷), 8.05 (t, *J* = 7.7 Hz, 2H, H⁴), 7.87 (d, *J* = 7.6 Hz, 2H, H⁵), 7.59 (d, *J* = 7.8 Hz, 2H, H³), 7.48 (d, *J* = 8.9 Hz, 4H, H⁹), 6.89 (d, *J* = 9.0 Hz, 4H, H¹⁰), 3.76 (s, 6H, H¹²), 2.29 (s, 6H, H¹).

¹³C-NMR (125.8 MHz, CD₃CN): δ (ppm) 161.52 (C¹¹), 159.20 (C²), 156.74 (C⁷), 151.82 (C⁶), 140.74 (C⁸), 139.52 (C⁴), 128.95 (C³), 126.30 (C⁵), 125.00 (C⁹), 115.69 (C¹⁰), 56.29 (C¹²), 25.17 (C¹).

HRMS (ESI+): *m/z* calcd. for [Cu(4,8)₂]⁺ 515.1503 found 515.1496.

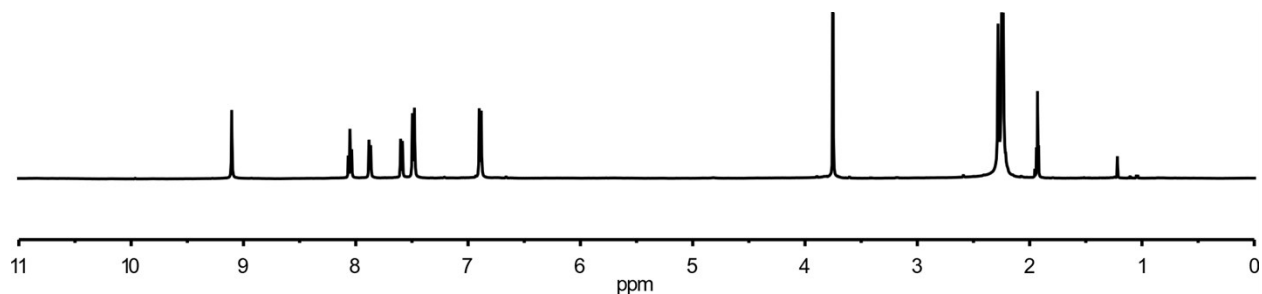


Figure S27. ¹H NMR (500 MHz, 297 K, CD₃CN) of Cu^I complex [Cu(4,8)₂](BF₄).

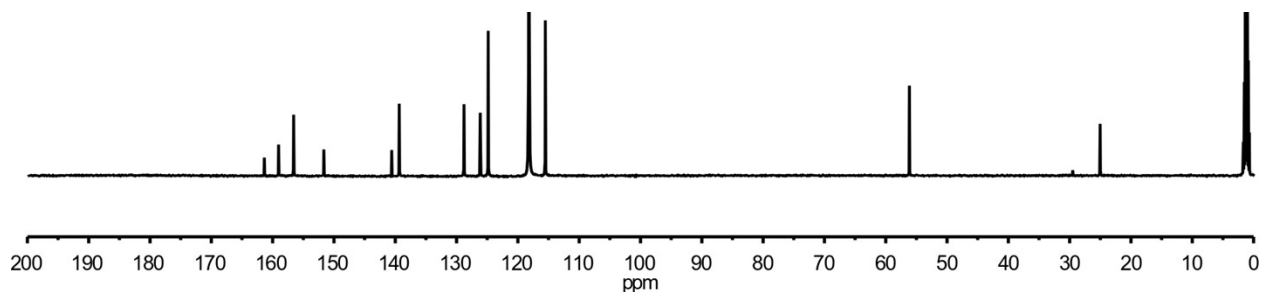
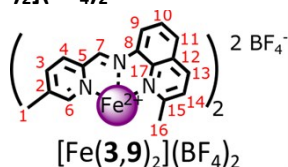


Figure S28. ¹³C NMR (125 MHz, 297 K, CD₃CN) of Cu^I complex [Cu(4,8)₂](BF₄).

2.2.14 Synthesis of Fe^{II} complex [Fe(3,9)₂](BF₄)₂



[Fe(3,9)₂](BF₄)₂ was synthesized using the general procedure described in section 2.2.1.

¹H-NMR (500 MHz, 275 K, CD₃CN): δ (ppm) 12.55 (br s, 2H, H⁷), 9.38 (d, *J* = 7.7 Hz, 2H, H⁹), 8.76 (br s, 2H, H⁶), 8.44 (d, *J* = 7.2 Hz, 2H, H¹¹), 8.43 (d, *J* = 6.6 Hz, 2H, H⁴), 8.29 (t, *J* = 7.8 Hz, 2H, H¹⁰), 8.19 (d, *J* = 8.3 Hz, 2H, H¹³), 7.76 (d, *J* = 7.8 Hz, 2H, H³), 7.50 (d, *J* = 8.1 Hz, 2H, H¹⁴), 2.12 (s, 6H, H¹), 1.99 (s, 6H, H¹⁶).

¹³C-NMR (125.8 MHz, 275 K, CD₃CN): δ (ppm) 175.67 (C¹⁵), 160.04 (C⁷), 154.16 (C⁶), 152.89 (C⁵), 148.23 (C¹⁷), 145.65 (C²), 142.41 (C⁸), 139.24 (C¹³), 138.40 (C³), 133.18 (C⁴), 132.72 (C¹¹), 131.72 (C¹⁴), 130.67 (C¹²), 129.35 (C¹⁰), 121.85 (C⁹), 27.33 (C¹⁶), 19.36 (C¹).

HRMS (ESI+): *m/z* calcd. for [Fe(3,9)₂]²⁺ 289.0935 found 289.0933.

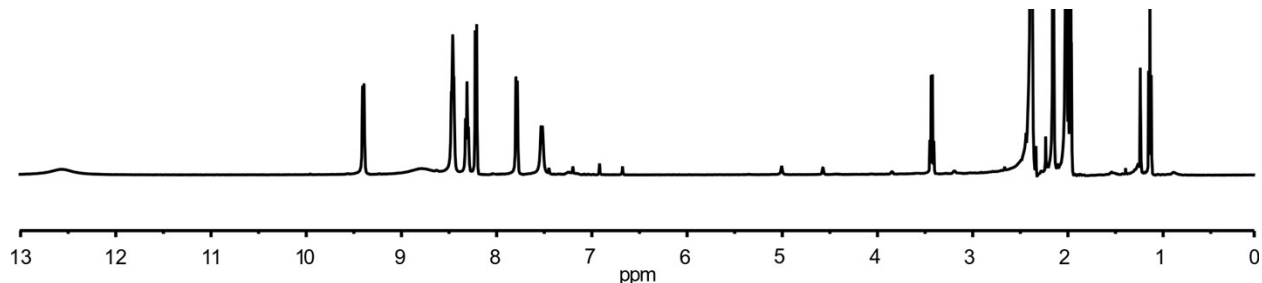


Figure S29. ¹H NMR (500 MHz, 275 K, CD₃CN) of Fe^{II} complex [Fe(3,9)₂](BF₄)₂.

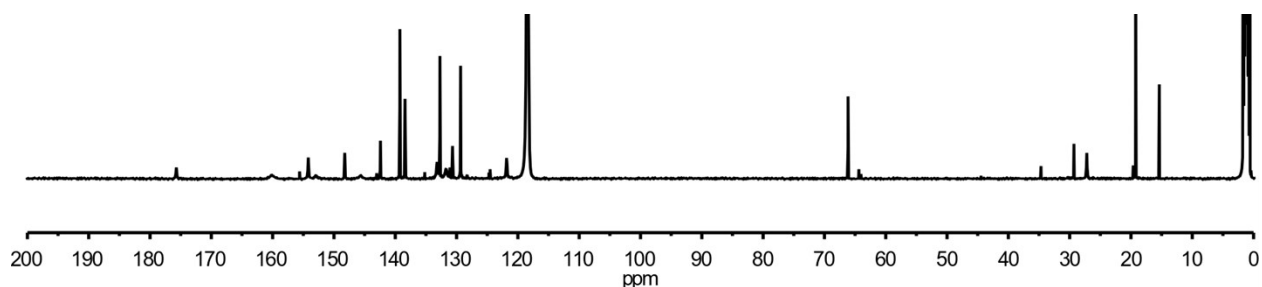


Figure S30. ¹³C NMR (125 MHz, 275 K, CD₃CN) of Cu^I complex [Fe(3,9)₂](BF₄)₂.

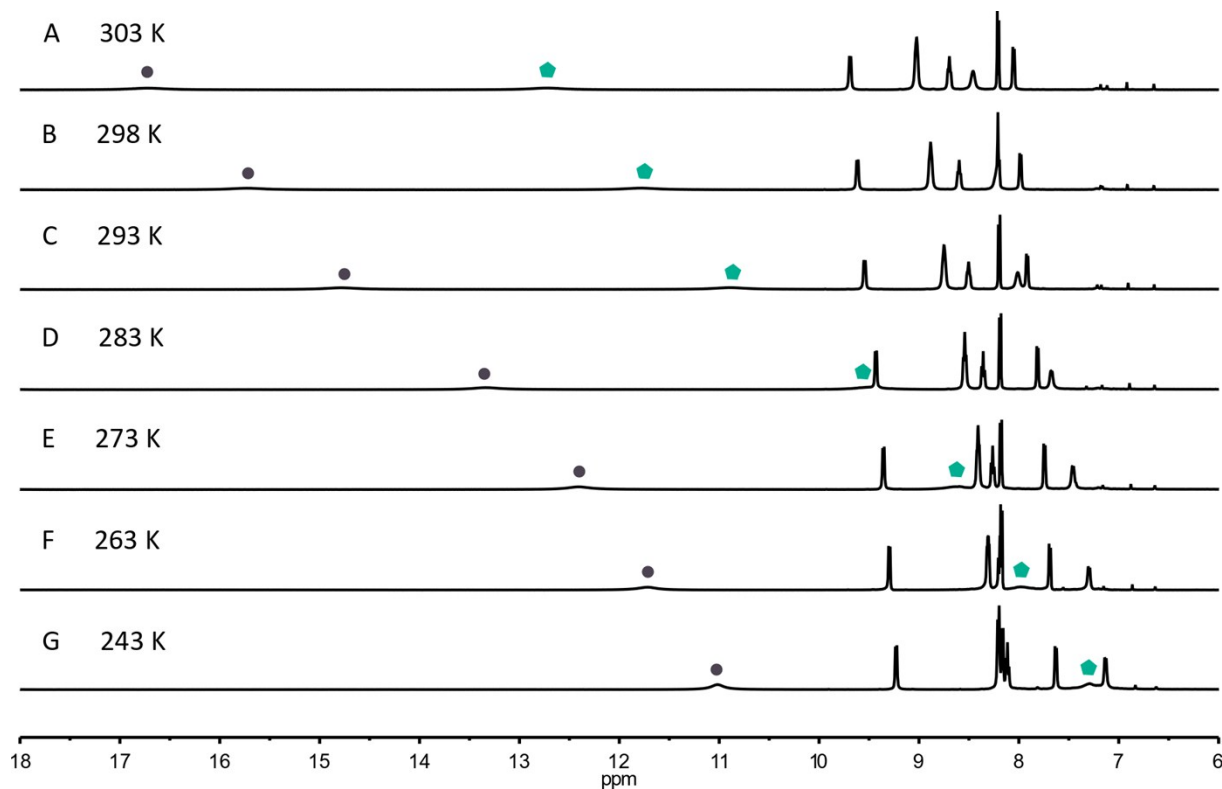


Figure S31. Partial ^1H NMR spectra (500 MHz, CD_3CN) of the Fe^{II} complex $[\text{Fe}(\mathbf{3},\mathbf{9})_2](\text{BF}_4)_2$ at variable temperature from 303 K to 243 K. VT-NMR was performed from high to low temperature, starting from 303 K. The position of the peak of H^7 is highlighted by grey circles and the position of the peak of H^6 is highlighted by green pentagons.

2.2.15 Synthesis of Ag^{I} complex $[\text{Ag}(\mathbf{7},\mathbf{8})_2](\text{BF}_4)$



$[\text{Ag}(\mathbf{7},\mathbf{8})_2](\text{BF}_4)_2$ was synthesized using the general procedure described in section 2.2.1.

^1H -NMR (500 MHz, CD_3CN): δ (ppm) 8.86 (s, 2H, H^{10}), 8.09 (t, $J = 7.8$ Hz, 2H, H^7), 7.79 (d, $J = 7.9$ Hz, 2H, H^6), 7.78 (d, $J = 7.6$ Hz, 2H, H^8), 7.56 (d, $J = 7.3$ Hz, 4H, H^3), 7.48 (d, $J = 8.9$ Hz, 4H, H^{12}), 7.20 (t, $J = 7.4$ Hz, 2H, H^1), 7.09 (t, $J = 7.6$ Hz, 4H, H^2), 6.95 (d, $J = 8.9$ Hz, 4H, H^{13}), 3.80 (s, 6H, H^{15}).

^{13}C -NMR (125.8 MHz, CD_3CN): δ (ppm) 161.34 (C^{14}), 159.67 (C^5), 157.49 (C^{10}), 150.70 (C^9), 141.16 (C^{11}), 140.78 (C^4), 140.66 (C^7), 130.53 (C^1), 129.34 (C^2), 128.10 (C^{3+8}), 127.18 (C^6), 125.18 (C^{12}), 115.70 (C^{13}), 56.34 (C^{15}).

HRMS (ESI+): m/z calcd. for $[\text{Ag}(\mathbf{7},\mathbf{8})_2]^+$ 683.1571 found 683.1572.

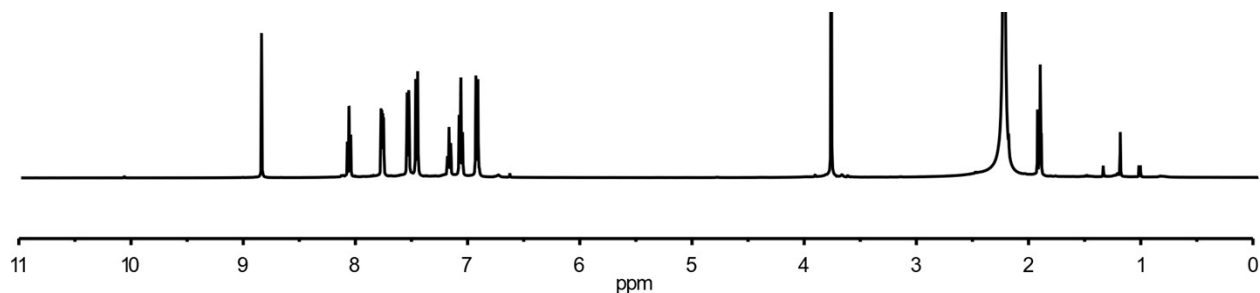


Figure S32. ^1H NMR (500 MHz, 297 K, CD_3CN) of Ag^{I} complex $[\text{Ag}(\mathbf{7},\mathbf{8})_2](\text{BF}_4)$.

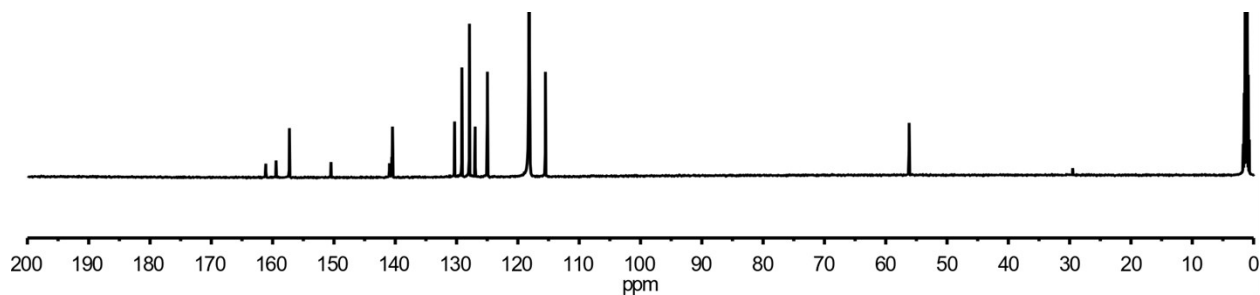
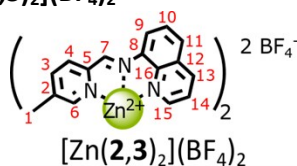


Figure S33. ^{13}C NMR (125 MHz, 297 K, CD_3CN) of Ag^{I} complex $[\text{Ag}(\mathbf{7},\mathbf{8})_2](\text{BF}_4)$.

2.2.16 Synthesis of Zn^{II} complex [Zn(2,3)₂](BF₄)₂



[Zn(2,3)₂](BF₄)₂ was synthesized using the general procedure described in section 2.2.1.

¹H-NMR (500 MHz, CD₃CN): δ (ppm) 9.84 (s, 2H, H⁷), 8.68 (d, *J* = 7.7 Hz, 2H, H⁹), 8.54 (d, *J* = 8.3 Hz, 2H, H¹³), 8.30 (d, *J* = 4.6 Hz, 2H, H¹⁵), 8.24 (d, *J* = 8.3 Hz, 2H, H¹¹), 8.13 (d, *J* = 8.3 Hz, 2H, H⁴), 8.05 (t, *J* = 8.0 Hz, 2H, H¹⁰), 7.97 (s, 2H, H⁶), 7.96 (d, *J* = 7.4 Hz, 2H, H³), 7.45 (dd, *J* = 8.3, 4.6 Hz, 2H, H¹⁴), 2.18 (s, 6H, H¹).

¹³C-NMR (125.8 MHz, CD₃CN): δ (ppm) 158.22 (C⁷), 150.69 (C⁶⁺¹⁵), 145.36 (C⁵), 142.41 (C²), 142.14 (C³), 141.29 (C¹⁶), 140.98 (C¹³), 136.19 (C⁸), 131.80 (C¹¹), 130.57 (C¹²), 130.21 (C⁴), 129.16 (C¹⁰), 124.34 (C¹⁴), 120.24 (C⁹), 18.59 (C¹).

HRMS (ESI+): *m/z* calcd. for [Zn(2,3)₂]²⁺ 279.0750 found 279.0750.

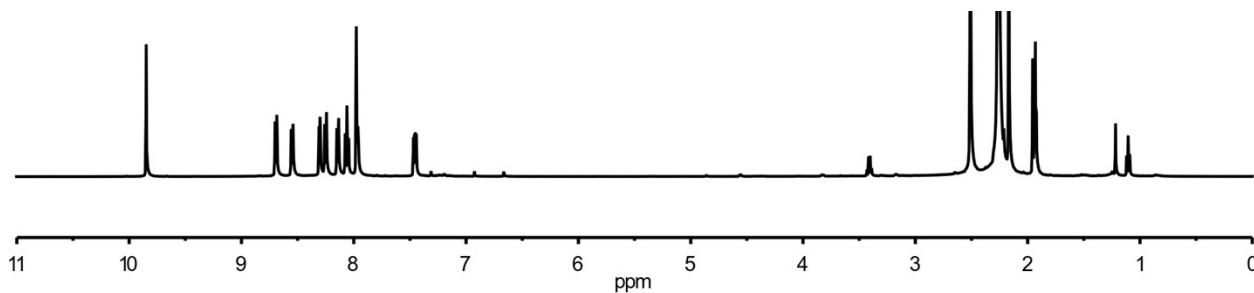


Figure S34. ¹H NMR (500 MHz, 297 K, CD₃CN) of Zn^{II} complex [Zn(2,3)₂](BF₄)₂.

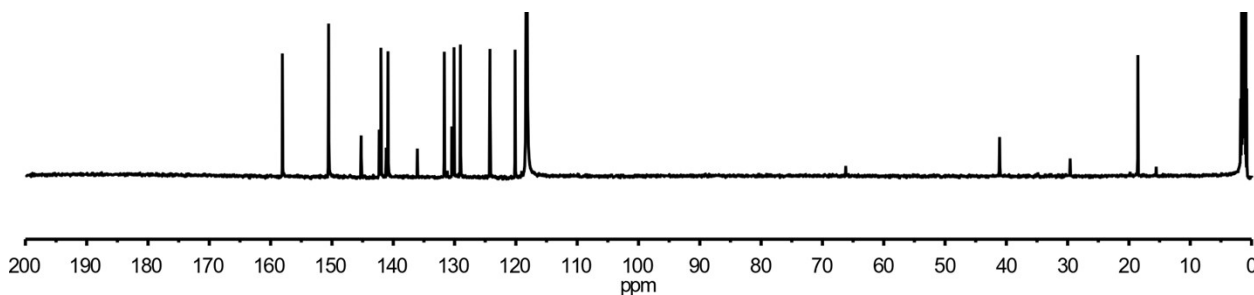


Figure S35. ¹³C NMR (125 MHz, 297 K, CD₃CN) of Zn^{II} complex [Zn(2,3)₂](BF₄)₂.

2.2.17 Synthesis of Zn^{II} complex [Zn(2,7)₂](BF₄)₂



[Zn(2,7)₂](BF₄)₂ was synthesized using the general procedure described in section 2.2.1.

¹H-NMR (500 MHz, CD₃CN): δ (ppm) 9.07 (s, 2H, H¹⁰), 8.48 (dd, *J* = 8.4, 1.4 Hz, 2H, H¹⁶), 8.33 (dd, *J* = 7.8, 1.1 Hz, 2H, H¹²), 8.30 (dd, *J* = 4.7, 1.5 Hz, 2H, H¹⁸), 8.23 (t, *J* = 7.7 Hz, 2H, H⁷), 8.20 (dd, *J* = 8.4, 1 Hz, 2H,

H¹⁴), 7.97 (t, *J* = 8.0 Hz, 2H, H¹³), 7.97 (dd, *J* = 7.6, 1.1 Hz, 2H, H⁸), 7.57 (dd, *J* = 7.8, 1.1 Hz, 2H, H⁶), 7.42 (dd, *J* = 8.2, 4.7 Hz, 2H, H¹⁷), 7.39 (tt, *J* = 7.6, 1.2 Hz, 2H, H¹⁷), 6.79 (t, *J* = 7.8 Hz, 4H, H²), 6.39 (dd, *J* = 8.1, 1.2 Hz, 4H, H³).

¹³C-NMR (125.8 MHz, CD₃CN): δ (ppm) 162.13 (C⁵), 156.91 (C¹⁰), 150.43 (C¹⁸), 148.08 (C⁹), 142.28 (C⁷), 140.98 (C¹⁶), 140.40 (C¹⁹), 139.29 (C⁴), 135.49 (C¹¹), 132.07 (C¹⁴), 131.28 (C⁶), 130.76 (C¹), 130.44 (C¹⁵), 130.34 (C⁸), 129.38 (C²), 129.03 (C¹³), 128.58 (C³), 124.34 (C¹⁷), 120.58 (C¹²).

HRMS (ESI+): *m/z* calcd. for [Zn(2,7)₂]²⁺ 341.0906 found 341.0903.

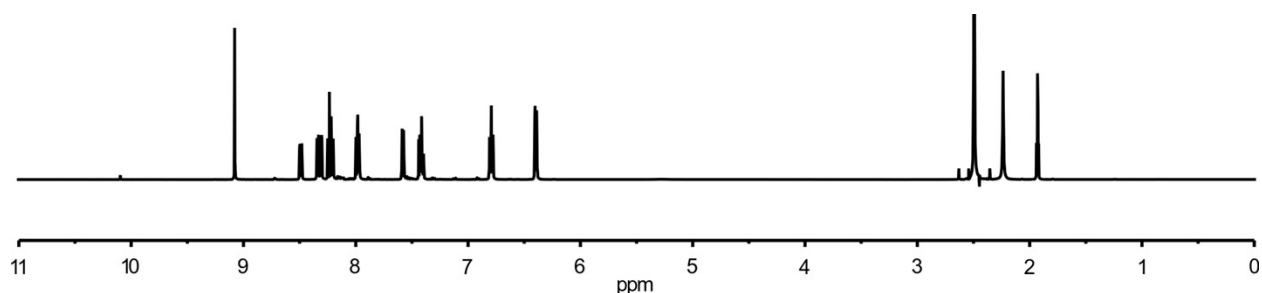


Figure S36. ¹H NMR (500 MHz, 297 K, CD₃CN) of Zn^{II} complex [Zn(2,7)₂](BF₄)₂.

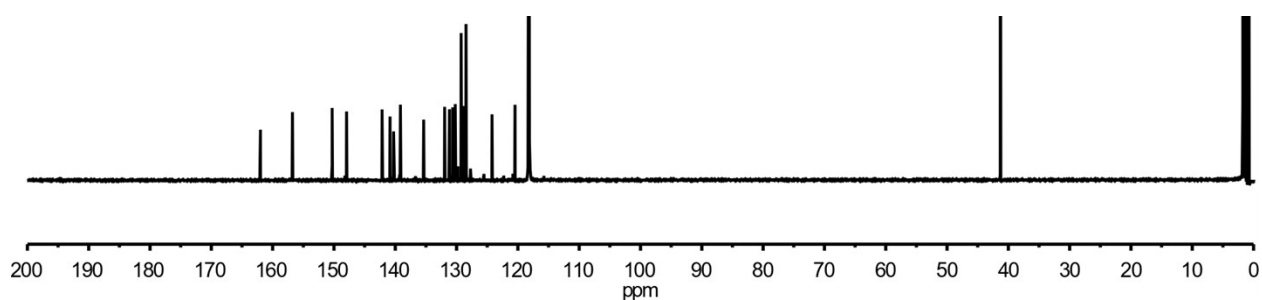
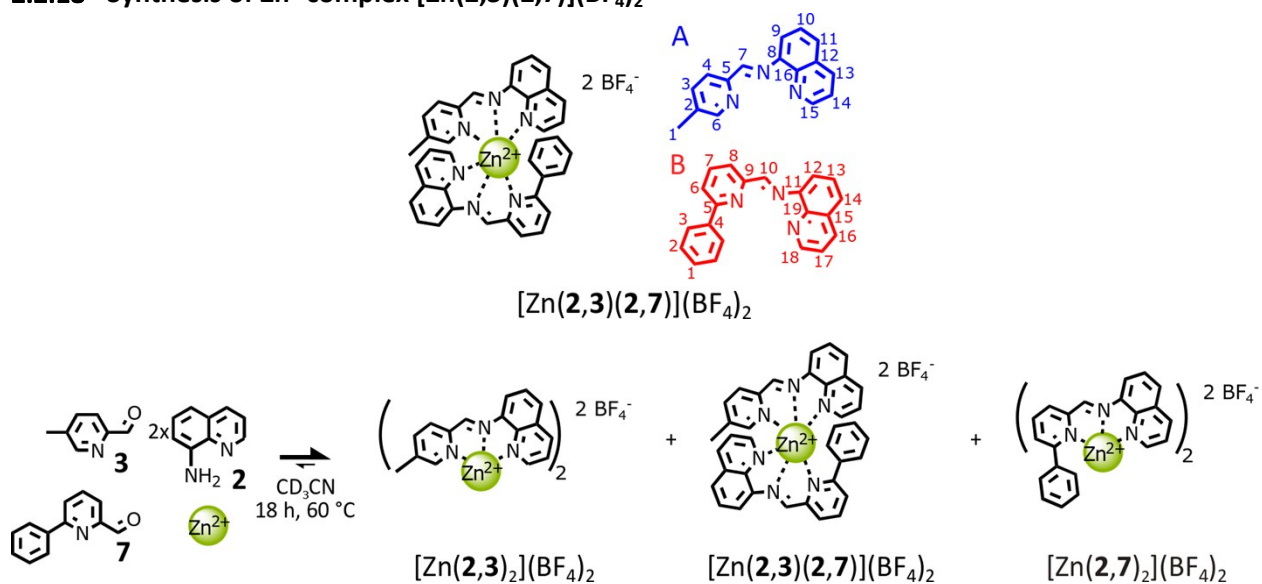


Figure S37. ¹³C NMR (125 MHz, 297 K, CD₃CN) of Zn^{II} complex [Zn(2,7)₂](BF₄)₂.

2.2.18 Synthesis of Zn^{II} complex [Zn(2,3)(2,7)](BF₄)₂



Scheme S4. Synthesis of the heteroleptic complex [Zn(2,3)(2,7)]²⁺.

CD₃CN solutions of the 2-formylpyridines **3** (50 μL of 320 mM, 16 μmol, 1 eq.) and **7** (50 μL of 320 mM, 16 μmol, 1 eq.) and a CD₃CN solution of amine **2** (100 μL of 320 mM, 32 μmol, 2 eq.) were combined. The resulting mixture was treated with a CD₃CN solution of [Zn(C₂H₆OS)₆](BF₄)₂ (100 μL of 160 mM, 16 μmol, 1 eq.) and was heated at 60 °C for 18 h. The complexes were not isolated, all the following experiments and analysis were done on the crude reaction mixture.

The heteroleptic complex [Zn(**2,3**)(**2,7**)]²⁺ could not be isolated. However, its ¹H and ¹³C NMR data could be determined by comparing the HMBC, HSQC, ROESY and COSY spectra of complexes [Zn(**2,3**)₂](BF₄)₂ and [Zn(**2,7**)₂](BF₄)₂ prepared in isolation with the spectra of the reaction mixture described above. Due to overlapping signals in the ¹H NMR spectrum, the multiplicity of some of the peaks could not be determined with precision.

¹H-NMR (500 MHz, CD₃CN): δ (ppm) 10.02 (s, 1H, H^{7A}), 9.06 (s, 1H, H^{10B}), 8.71 (d, *J* = 6.8 Hz, 1H, H^{9A}), 8.55 (dd, *J* = 6.1, 1.7 Hz, 2H, H^{13A}), 8.42 (dd, *J* = 6.0, 1.4 Hz, 1H, H^{16B}), 8.40 (2H, H^{4A+15A}), 8.30 (t, *J* = 8.4 Hz, 1H, H^{3A+7B}), 8.22 (d, *J* = 6.8 Hz, 1H, H^{12B}), 8.16 (d, *J* = 8.4 Hz, 1H, H^{11A}), 8.03 (d, *J* = 4.7, 1.4 Hz, 1H, H^{18B}), 8.02 (s, 1H, H^{6A}), 8.00 (d, *J* = 7.8 Hz, 1H, H^{10A}), 7.95 (d, *J* = 9.0 Hz, 1H, H^{14B}), 7.94 (d, *J* = 7.9 Hz, 1H, H^{8B}), 7.55 (dd, *J* = 7.8, 1.1 Hz, 1H, H^{6B}), 7.50 (dd, *J* = 8.3, 4.7 Hz, 1H, H^{14A}), 7.40 (d, *J* = 7.4 Hz, 1H, H^{13B}), 7.32 (dd, *J* = 8.3, 4.7 Hz, 1H, H^{17B}), 7.24 (tt, *J* = 7.4, 1.2 Hz, 1H, H¹⁸), 6.68 (t, *J* = 7.8 Hz, 2H, H^{2B}), 6.24 (dd, *J* = 8.0, 1.1 Hz, 2H, H^{3B}), 2.22 (s, 3H, H^{1A}).

¹³C-NMR (125.8 MHz, CD₃CN): δ (ppm) 162.44 (C^{5B}), 160.08 (C^{7A}), 155.15 (C^{10B}), 150.65 (C^{15A}), 150.63 (C^{6A}), 150.07 (C^{18B}), 148.34 (C^{5A}), 145.04 (C^{9B}), 144.97 (C^{2A}), 142.29 (C^{3A+7B}), 141.14 (C^{13A}), 141.04 (C^{16A}), 140.97 (C^{19B}), 140.67 (C^{16B}), 139.34 (C^{4B}), 136.44 (C^{8A}), 135.35 (C^{11B}), 131.94 (C^{11A}), 131.26 (C^{6B}), 130.54 (C^{12A}), 130.40 (C^{1B}), 130.26 (C^{15B}), 130.18 (C^{4A}), 130.17 (C^{14B}), 129.10 (C^{13B}), 129.00 (C^{8B}), 128.99 (C^{2B}), 128.98 (C^{10A}), 128.19 (C^{3B}), 124.33 (C^{14A}), 124.17 (C^{17B}), 120.38 (C^{12B}), 120.29 (C^{9A}) 18.04 (C^{1A}).

HRMS (ESI+): *m/z* calcd. for [Zn(**2,3**)(**2,7**)]²⁺ 310.5843 found 310.5833.

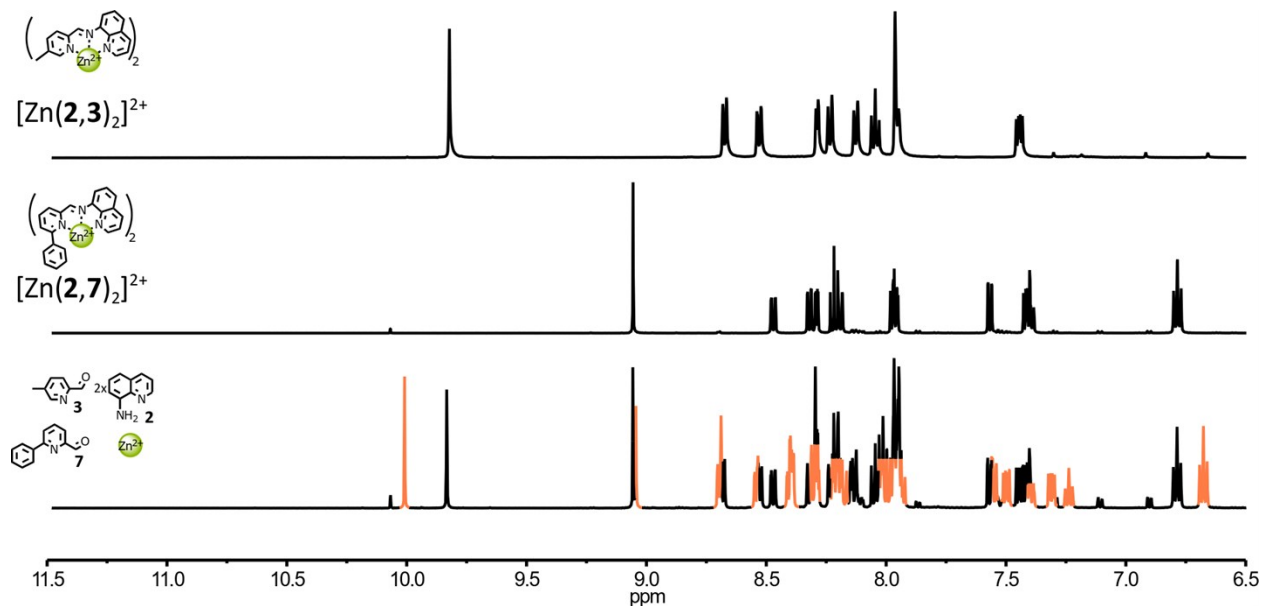


Figure S38. Partial ¹H NMR spectra (500 MHz, CD₃CN, 297 K) of: (top) complex [Zn(**2,3**)₂]²⁺, (middle) complex [Zn(**2,7**)₂]²⁺, (bottom) the crude reaction mixture obtained by mixing **2**, **3**, **7** and Zn(BF₄)₂ in the

molar ratio 2:1:1:1 at 60 °C for 18 h. The diagnostic signals of the heteroleptic complex $[\text{Zn}(\mathbf{2},\mathbf{3})(\mathbf{2},\mathbf{7})]^{2+}$ are colored in orange.

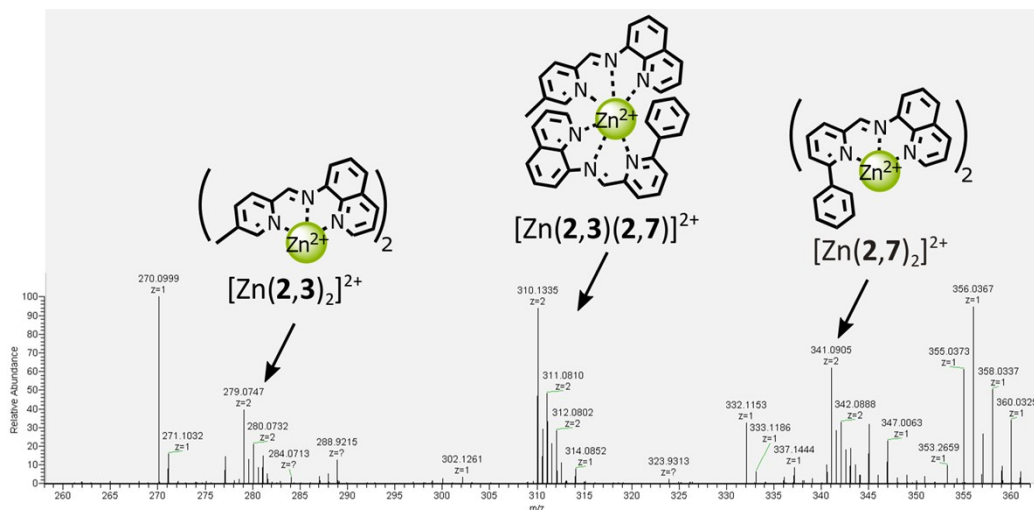


Figure S39. Partial HRESI-MS spectra of the reaction mixture obtained by mixing **2**, **3**, **7** and $\text{Zn}(\text{BF}_4)_2$ in the molar ratio 2:1:1:1 at 60 °C for 18 h.

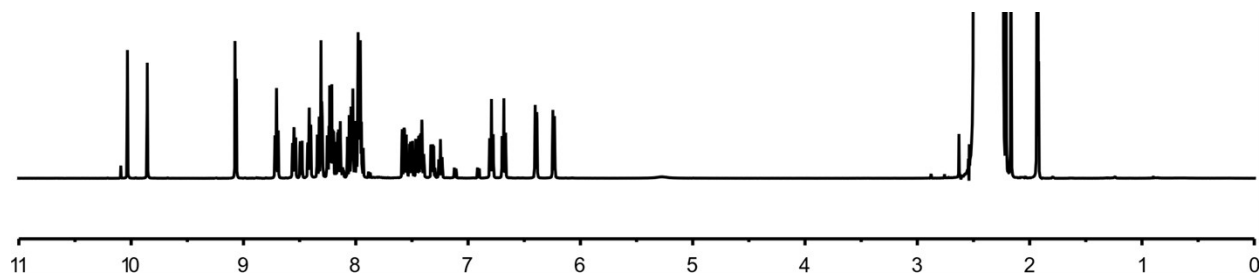


Figure S40. ^1H NMR (500 MHz, 297 K, CD_3CN) of the reaction mixture obtained by mixing **2**, **3**, **7** and $\text{Zn}(\text{BF}_4)_2$ in the molar ratio 2:1:1:1 at 60 °C for 18 h.

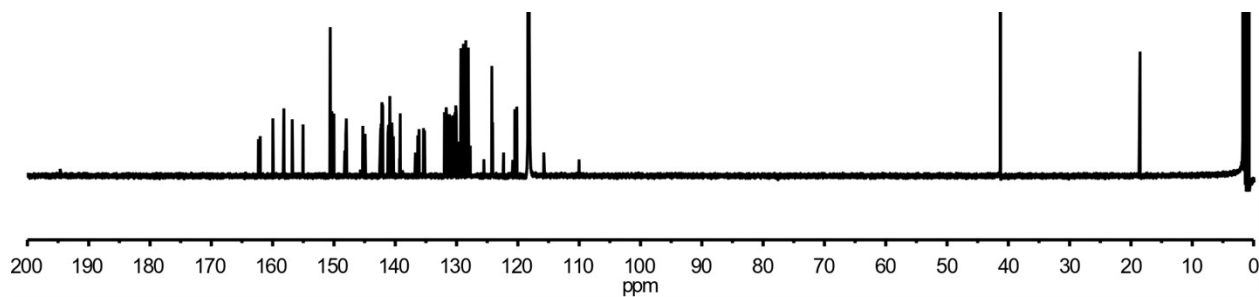
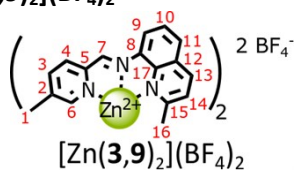


Figure S41. ^{13}C NMR (125 MHz, 297 K, CD_3CN) of the reaction mixture obtained by mixing **2**, **3**, **7** and $\text{Zn}(\text{BF}_4)_2$ in the molar ratio 2:1:1:1 at 60 °C for 18 h.

2.2.19 Synthesis of Zn^{II} complex [Zn(3,9)₂](BF₄)₂



[Zn(3,9)₂](BF₄)₂ was synthesized using the general procedure described in section 2.2.1.

¹H-NMR (500 MHz, CD₃CN): δ (ppm) 9.73 (s, 2H, H⁷), 8.69 (d, $J = 7.8$ Hz, 2H, H⁹), 8.52 (d, $J = 8.4$ Hz, 2H, H¹³), 8.29 (d, $J = 8.2$ Hz, 2H, H¹¹), 8.09 – 7.99 (m, 4H, H⁴⁺¹⁰), 7.87 (d, $J = 7.8$ Hz, 2H, H³), 7.65 (s, 2H, H⁶), 7.47 (d, $J = 8.4$ Hz, 2H, H¹⁴), 2.12 (s, 6H, H¹), 2.07 (s, 6H, H¹⁶).

¹³C-NMR (125.8 MHz, CD₃CN): δ (ppm) 163.18 (C¹⁵), 157.61 (C⁷), 150.24 (C⁶), 144.96 (C⁵), 142.45 (C²), 141.91 (C³), 141.23 (C¹³⁺¹⁷), 134.96 (C⁸), 132.21 (C¹¹), 130.41 (C⁴), 129.27 (C¹²), 128.36 (C¹⁰), 126.34 (C¹⁴), 120.73 (C⁹), 24.76 (C¹⁶), 18.72 (C¹).

HRMS (ESI+): m/z calcd. for [[Zn(3,9)₂](BF₄)⁺ 673.1853 found 673.1821.

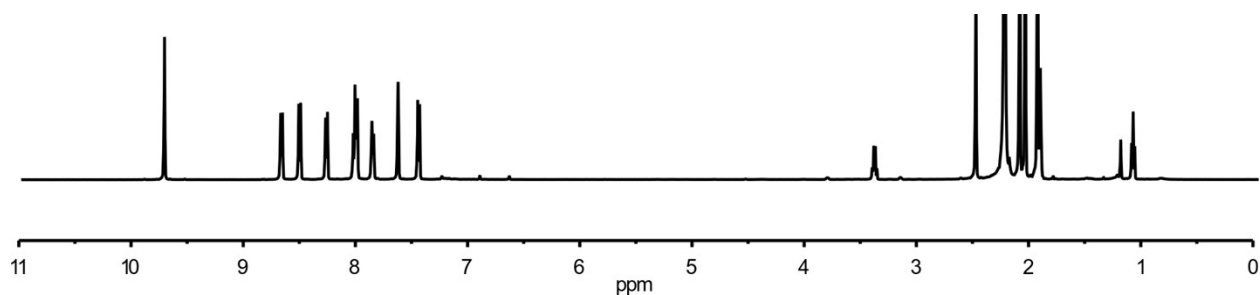


Figure S42. ¹H NMR (500 MHz, 297 K, CD₃CN) of Zn^{II} complex [Zn(3,9)₂](BF₄)₂.

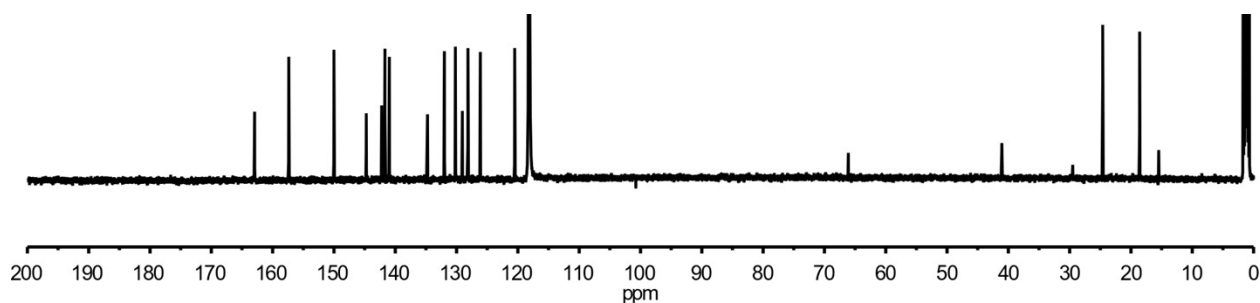
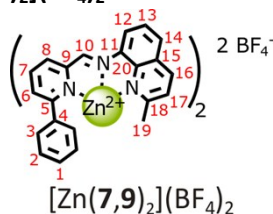


Figure S43. ¹³C NMR (125 MHz, 297 K, CD₃CN) of Zn^{II} complex [Zn(3,9)₂](BF₄)₂.

2.2.20 Synthesis of Zn^{II} complex [Zn(7,9)₂](BF₄)₂



[Zn(7,9)₂](BF₄)₂ was synthesized using the general procedure described in section 2.2.1.

$^1\text{H-NMR}$ (500 MHz, CD_3CN): δ (ppm) 8.77 (s, 2H, H^{10}), 8.52 (d, $J = 8.4$ Hz, 2H, H^{16}), 8.21 (dd, $J = 8.4, 1.2$ Hz, 2H, H^{14}), 8.05 (t, $J = 7.7$ Hz, 2H, H^7), 7.98 (dd, $J = 7.6, 1.2$ Hz, 2H, H^8), 7.91 (dd, $J = 7.8, 1.2$ Hz, 2H, H^{12}), 7.77 (t, $J = 8.0$ Hz, 2H, H^{13}), 7.54 (dd, $J = 7.8, 1.2$ Hz, 2H, H^6), 7.49 (d, $J = 8.4$ Hz, 2H, H^{17}), 6.97 (tt, $J = 7.5, 1.3$ Hz, 2H, H^1), 6.78 (dt, $J = 6.9, 1.3$ Hz, 4H, H^3), 6.62 (t, $J = 7.4$ Hz, 4H, H^2), 2.10 (s, 6H, H^{19}).

$^{13}\text{C-NMR}$ (125.8 MHz, CD_3CN): δ (ppm) 163.30 (C^{18}), 162.13 (C^5), 161.02 (C^{10}), 148.48 (C^9), 141.49 (C^7 or 16), 141.46 (C^7 or 16), 141.07 (C^{20}), 138.42 (C^4), 136.41 (C^{11}), 131.98 (C^{14}), 131.06 (C^6), 130.56 (C^1), 130.30 (C^8), 129.03 (C^2), 128.76 (C^{15}), 128.57 (C^3), 128.17 (C^{13}), 126.62 (C^{17}), 120.73 (C^{12}), 24.80 (C^{19}).

HRMS (ESI+): m/z calcd. for $[\text{Zn}(\mathbf{7},\mathbf{9})_2]^{2+}$ 355.1063 found 355.1059.

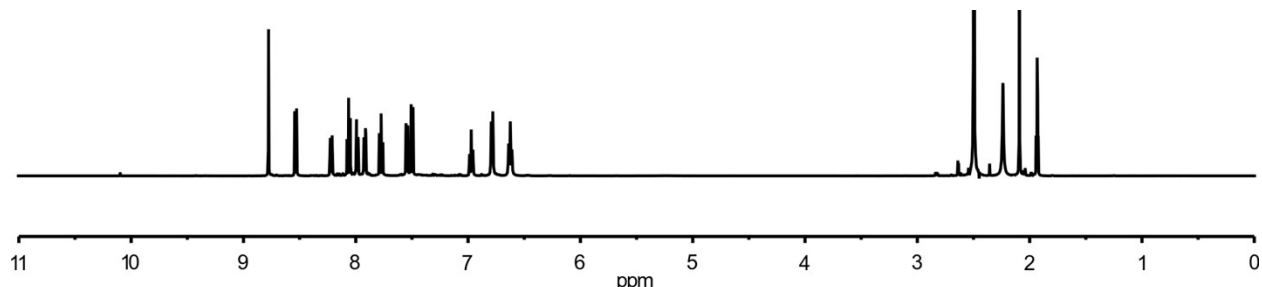


Figure S44. ^1H NMR (500 MHz, 297 K, CD_3CN) of Zn^{II} complex $[\text{Zn}(\mathbf{7},\mathbf{9})_2](\text{BF}_4)_2$.

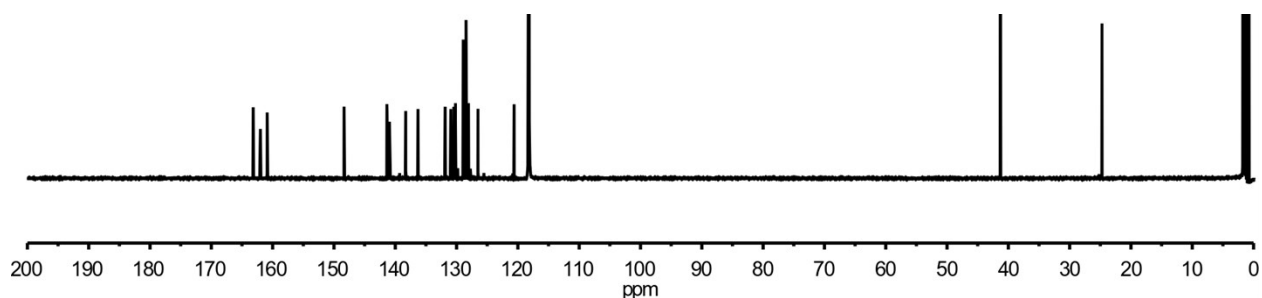
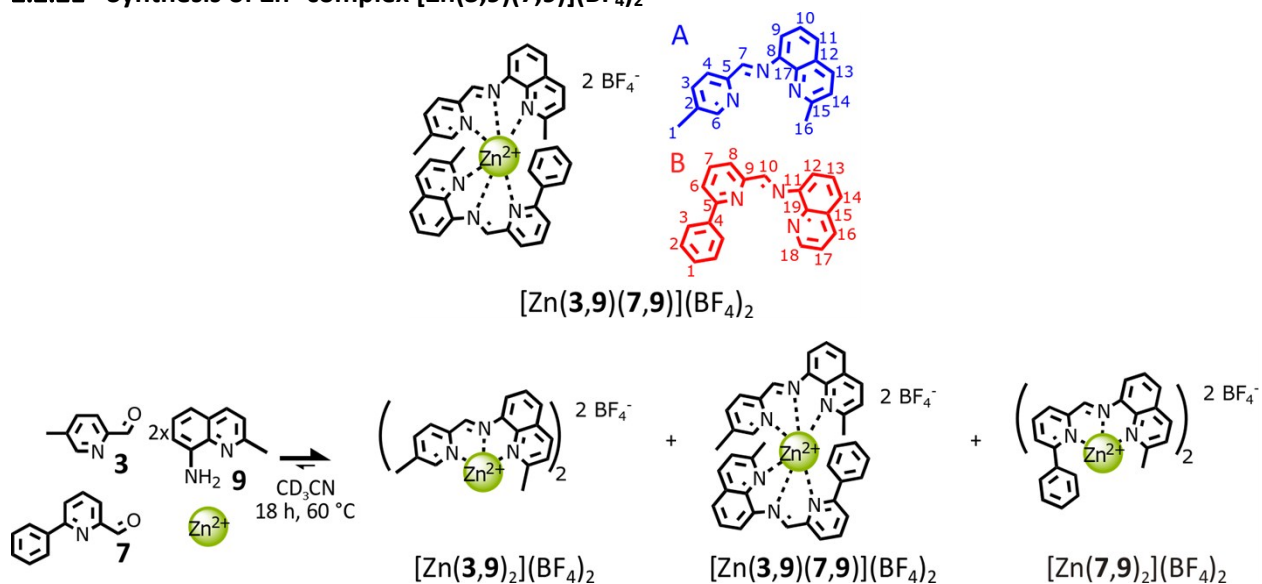


Figure S45. ^{13}C NMR (125 MHz, 297 K, CD_3CN) of Zn^{II} complex $[\text{Zn}(\mathbf{7},\mathbf{9})_2](\text{BF}_4)_2$.

2.2.21 Synthesis of Zn^{II} complex $[\text{Zn}(\mathbf{3},\mathbf{9})(\mathbf{7},\mathbf{9})](\text{BF}_4)_2$



Scheme S5. Synthesis of the heteroleptic complex $[\text{Zn}(\mathbf{3},\mathbf{9})(\mathbf{7},\mathbf{9})]^{2+}$.

CD_3CN solutions of the 2-formylpyridines **3** (50 μL of 320 mM, 16 μmol , 1 eq.) and **7** (50 μL of 320 mM, 16 μmol , 1 eq.) and a CD_3CN solution of amine **9** (100 μL of 320 mM, 32 μmol , 2 eq.) were combined. The resulting mixture was treated with a CD_3CN solution of $[\text{Zn}(\text{C}_2\text{H}_6\text{OS})_6](\text{BF}_4)_2$ (100 μL of 160 mM, 16 μmol , 1 eq.) and was heated at 60 $^\circ\text{C}$ for 18 h. The complexes were not isolated, all the following experiments and analysis were done on the crude reaction mixture.

The heteroleptic complex $[\text{Zn}(\mathbf{3},\mathbf{9})(\mathbf{7},\mathbf{9})]^{2+}$ could not be isolated. However, its ^1H and ^{13}C NMR data could be determined by comparing the HMBC, HSQC, ROESY and COSY spectra of complexes $[\text{Zn}(\mathbf{3},\mathbf{9})_2](\text{BF}_4)_2$ and $[\text{Zn}(\mathbf{7},\mathbf{9})_2](\text{BF}_4)_2$ prepared in isolation with the spectra of the reaction mixture described above. Due to overlapping signals in the ^1H NMR spectrum, the multiplicity of some of the peaks could not be determined with precision.

^1H -NMR (500 MHz, CD_3CN): δ (ppm) 9.91 (s, 1H, $\text{H}^{7\text{A}}$), 9.03 (s, 1H, $\text{H}^{10\text{B}}$), 8.72 (dd, $J = 7.9, 1.2$ Hz, 1H, $\text{H}^{9\text{A}}$), 8.50 (d, $J = 8.4$ Hz, 1H, $\text{H}^{16\text{B}}$), 8.44 (d, $J = 8.4$ Hz, 1H, $\text{H}^{13\text{B}}$), 8.25 (dd, $J = 8.4, 1.2$ Hz, 1H, $\text{H}^{11\text{A}}$), 8.21 (d, $J = 7.4$ Hz, 1H, $\text{H}^{4\text{A}}$), 8.16 (dd, $J = 8.4, 1.1$ Hz, 1H, $\text{H}^{14\text{B}}$), 8.11 (t, $J = 7.7$ Hz, 1H, $\text{H}^{17\text{B}}$), 8.02 (1H, $\text{H}^{10\text{A}}$), 7.97 (d, $J = 8.0$ Hz, 1H, $\text{H}^{8\text{B}}$), 7.91 (d, $J = 7.7$ Hz, 1H, $\text{H}^{12\text{B}}$), 7.90 (ddd, $J = 7.8, 2.0, 0.9$ Hz, 1H, $\text{H}^{3\text{A}}$), 7.82 (dd, $J = 1.9, 0.7$ Hz, 1H, $\text{H}^{6\text{A}}$), 7.72 (t, $J = 8.0$ Hz, 1H, $\text{H}^{13\text{B}}$), 7.51 (d, $J = 8.3$ Hz, 1H, $\text{H}^{17\text{B}}$), 7.43 (dd, $J = 7.8, 1.1$ Hz, 1H, $\text{H}^{6\text{B}}$), 7.35 (d, $J = 8.4$ Hz, 1H, $\text{H}^{14\text{A}}$), 7.02 (tt, $J = 7.6, 1.3$ Hz, 1H, $\text{H}^{1\text{B}}$), 6.70 (t, $J = 7.8$ Hz, 2H, $\text{H}^{2\text{B}}$), 6.48 (dd, $J = 8.2, 1.3$ Hz, 2H, $\text{H}^{3\text{B}}$), 2.23 (s, 3H, $\text{H}^{19\text{B}}$), 2.19 (s, 3H, $\text{H}^{1\text{A}}$), 1.80 (s, 3H, $\text{H}^{16\text{A}}$).

^{13}C -NMR (125.8 MHz, CD_3CN): δ (ppm) 163.37 ($\text{C}^{15\text{A}}$), 163.15 ($\text{C}^{18\text{B}}$), 162.86 ($\text{C}^{5\text{B}}$), 161.11 ($\text{C}^{7\text{A}}$), 157.11 ($\text{C}^{10\text{B}}$), 121.09 ($\text{C}^{9\text{A}}$), 149.96 ($\text{C}^{6\text{A}}$), 148.55 ($\text{C}^{9\text{B}+5\text{A}}$), 144.64 ($\text{C}^{2\text{A}}$), 142.00 ($\text{C}^{3\text{A}}$), 141.37 ($\text{C}^{16\text{B}}$), 141.32 ($\text{C}^{17\text{A}}$), 141.30 ($\text{C}^{20\text{B}}$), 141.27 ($\text{C}^{7\text{B}}$), 141.02 ($\text{C}^{13\text{A}}$), 138.71 ($\text{C}^{4\text{B}}$), 136.25 ($\text{C}^{8\text{A}}$), 134.55 ($\text{C}^{11\text{B}}$), 132.29 ($\text{C}^{11\text{A}}$), 131.85 ($\text{C}^{14\text{B}}$), 131.70 ($\text{C}^{6\text{B}}$), 130.60 ($\text{C}^{1\text{B}}$), 130.57 ($\text{C}^{12\text{B}}$), 130.48 ($\text{C}^{4\text{A}}$), 130.30 ($\text{C}^{8\text{B}}$), 129.13 ($\text{C}^{12\text{A}}$), 128.69 ($\text{C}^{15\text{B}}$), 128.62 ($\text{C}^{2\text{B}}$), 128.31 ($\text{C}^{10\text{A}}$), 128.17 ($\text{C}^{3\text{B}}$), 127.99 ($\text{C}^{13\text{B}}$), 126.50 ($\text{C}^{14\text{A}}$), 126.33 ($\text{C}^{17\text{B}}$), 24.94 ($\text{C}^{19\text{B}}$), 24.50 ($\text{C}^{16\text{A}}$), 18.78 ($\text{C}^{1\text{A}}$).

HRMS (ESI+): m/z calcd. for $[\text{Zn}(\mathbf{3},\mathbf{9})(\mathbf{7},\mathbf{9})]^{2+}$ 324.0984 found 324.0976.

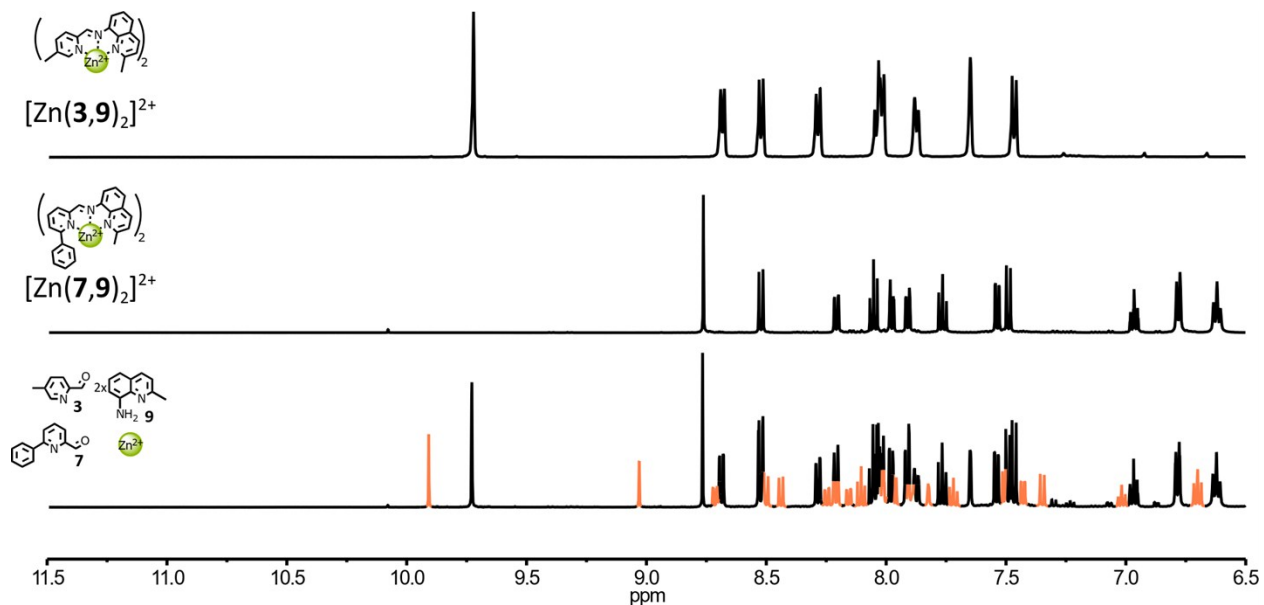


Figure S46. Partial ^1H NMR spectra (500 MHz, CD_3CN , 297 K) of: (top) complex $[\text{Zn}(\mathbf{2},\mathbf{3})_2]^{2+}$, (middle) complex $[\text{Zn}(\mathbf{2},\mathbf{7})_2]^{2+}$, (bottom) the crude reaction mixture obtained by mixing $\mathbf{3}$, $\mathbf{7}$, $\mathbf{9}$ and $\text{Zn}(\text{BF}_4)_2$ in the molar ratio 2:1:1:1 at 60 °C for 18 h. The diagnostic signals of the heteroleptic complex $[\text{Zn}(\mathbf{2},\mathbf{3})(\mathbf{2},\mathbf{7})]^{2+}$ are colored in orange.

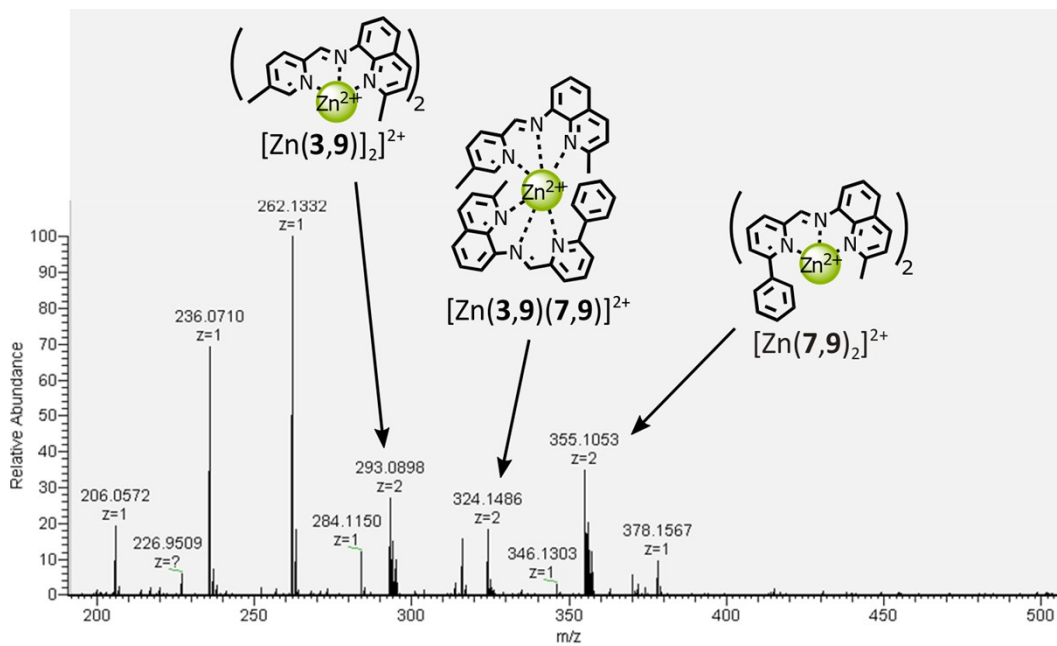


Figure S47. Partial HRESI-MS spectra of the reaction mixture obtained by mixing $\mathbf{3}$, $\mathbf{7}$, $\mathbf{9}$ and $\text{Zn}(\text{BF}_4)_2$ in the molar ratio 2:1:1:1 at 60 °C for 18 h.

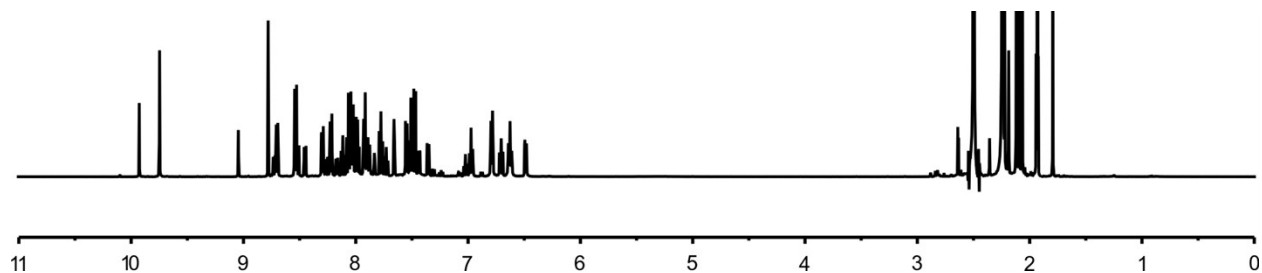


Figure S48. ^1H NMR (500 MHz, 297 K, CD_3CN) of the reaction mixture obtained by mixing **3**, **7**, **9** and $\text{Zn}(\text{BF}_4)_2$ in the molar ratio 2:1:1:1 at 60 °C for 18 h.

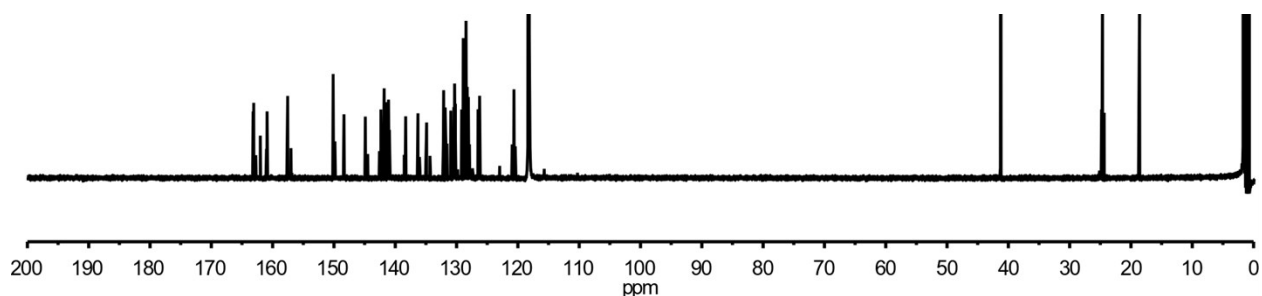
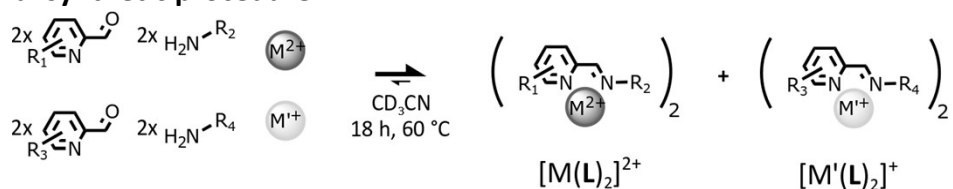


Figure S49. ^{13}C NMR (125 MHz, 297 K, CD_3CN) of the reaction mixture obtained by mixing **3**, **7**, **9** and $\text{Zn}(\text{BF}_4)_2$ in the molar ratio 2:1:1:1 at 60 °C for 18 h.

3. Self-sorting reactions

3.1 General synthetic procedure



Scheme S6. Synthesis of mononuclear complexes $[\text{M}(\text{L})_2]^{n+}$ and $[\text{M}'(\text{L})_2]^{n+}$ through the self-sorting of their initial reactants.

General synthetic procedure: CD_3CN solutions of each of the 2-formylpyridine containing components (100 μL of 32 mM, 3.2 μmol , 2 eq.) and of each of the amine containing components (100 μL of 32 mM, 3.2 μmol , 2 eq.) were combined. The resulting mixture was treated with CD_3CN solutions of each of the metal salts (100 μL of 16 mM, 1.6 μmol , 1 eq.) and heated at 60 °C for 18 h. The complexes were never isolated, all the present experiments and analysis were done on the crude reaction mixture.

3.2 Self-sorting of complexes $[\text{Cu}(\mathbf{1},\mathbf{4})_2]^+$ and $[\text{Fe}(\mathbf{2},\mathbf{3})_2]^{2+}$

3.2.1 Simultaneous generation of complexes $[\text{Cu}(\mathbf{1},\mathbf{4})_2]^+$ and $[\text{Fe}(\mathbf{2},\mathbf{3})_2]^{2+}$ at 2.7 mM

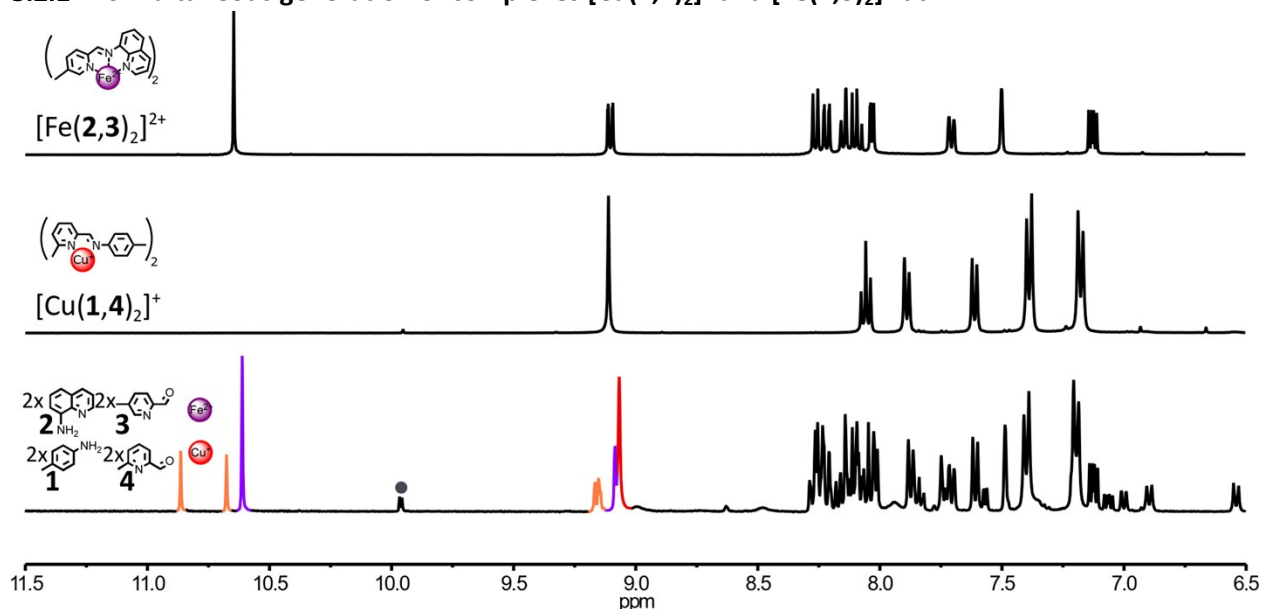


Figure S50. Partial ^1H NMR spectra (400 MHz, CD_3CN , 297 K) of: (top) complex $[\text{Fe}(\mathbf{2},\mathbf{3})_2]^{2+}$, (middle) complex $[\text{Cu}(\mathbf{1},\mathbf{4})_2]^+$, (bottom) the crude reaction mixture of the attempted Simultaneous generation of complexes $[\text{Cu}(\mathbf{1},\mathbf{4})_2]^+$ and $[\text{Fe}(\mathbf{2},\mathbf{3})_2]^{2+}$ through the self-sorting of their initial reactants (2.7 mM). Reaction conditions: $\mathbf{1}:\mathbf{2}:\mathbf{3}:\mathbf{4}:\text{Cu}(\text{BF}_4):\text{Fe}(\text{BF}_4)_2$ (2:2:2:2:1:1), CD_3CN , 60 °C, 18 h. Diagnostic signals of the complexes are colour coded, $[\text{Cu}(\mathbf{1},\mathbf{4})_2]^+$ in red, $[\text{Fe}(\mathbf{2},\mathbf{3})_2]^{2+}$ in purple and $[\text{Fe}(\mathbf{2},\mathbf{3})(\mathbf{2},\mathbf{4})]^{2+}$ in orange, one of the diagnostic signals of the free aldehydes $\mathbf{3}$ and $\mathbf{4}$ are highlighted by a grey circle.

3.2.2 Effect of concentration on the self-sorting of complexes $[\text{Cu}(\mathbf{1},\mathbf{4})_2]^+$ and $[\text{Fe}(\mathbf{2},\mathbf{3})_2]^{2+}$

3.2.2.1 Simultaneous generation of complexes $[\text{Cu}(\mathbf{1},\mathbf{4})_2]^+$ and $[\text{Fe}(\mathbf{2},\mathbf{3})_2]^{2+}$ at 3.6 mM

CD_3CN solutions of the 2-formylpyridine containing components $\mathbf{3}$ (10 μL of 320 mM, 3.2 μmol , 2 eq.) and $\mathbf{4}$ (10 μL of 320 mM, 3.2 μmol , 2 eq.) and of the amine containing components $\mathbf{1}$ (10 μL of 320 mM, 3.2 μmol , 2 eq.) and $\mathbf{2}$ (10 μL of 320 mM, 3.2 μmol , 2 eq.) were combined. The resulting mixture was treated with CD_3CN solutions of CuBF_4 (20 μL of 80 mM, 1.6 μmol , 1 eq.) and $\text{Fe}(\text{BF}_4)_2$ (20 μL of 80 mM, 1.6 μmol , 1 eq.) before being diluted with 360 μL of CD_3CN and heated at 60 °C for up to 20 days. The complexes were never isolated, all the present experiments and analysis were done on the crude reaction mixture.

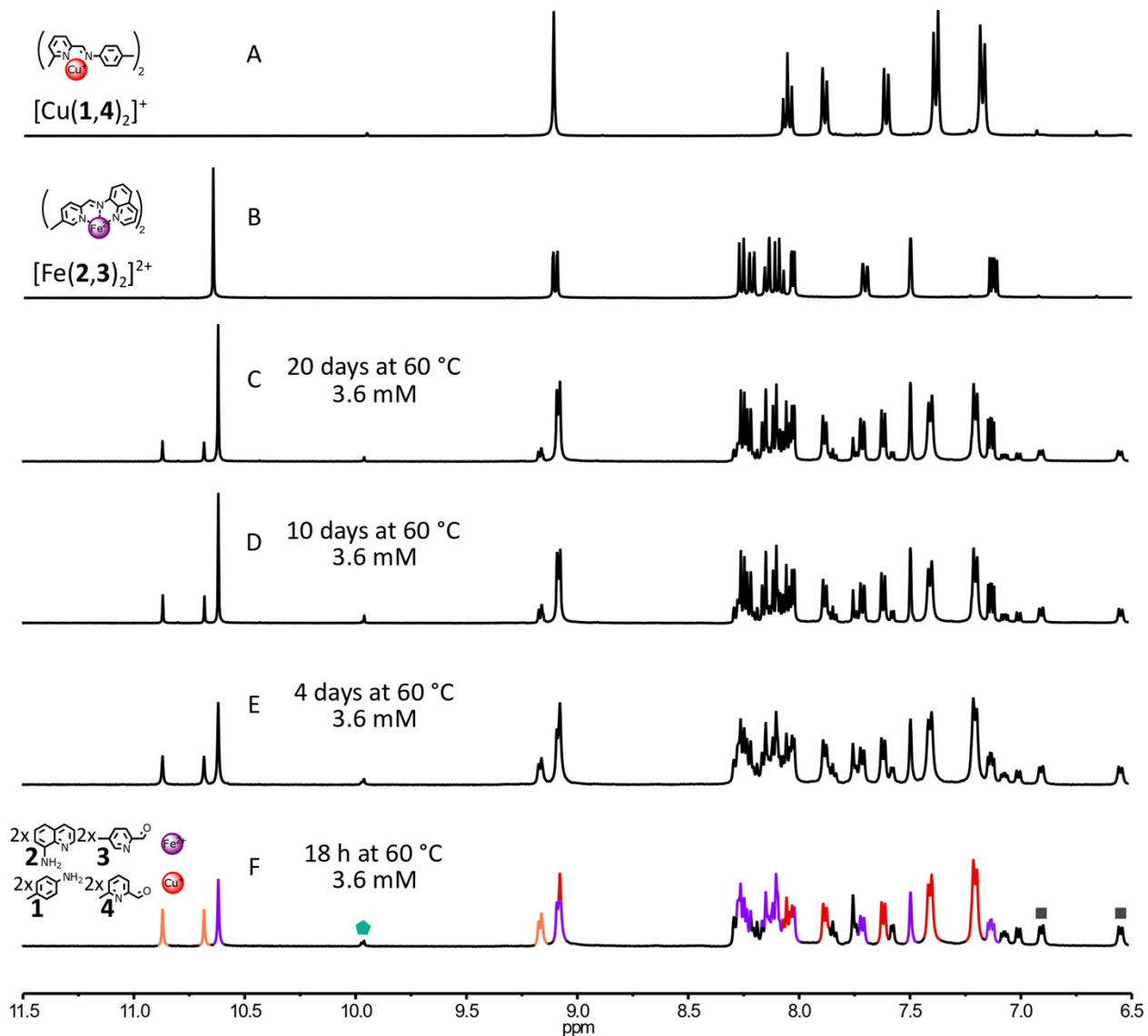


Figure S51. Partial ^1H NMR spectra (500 MHz, CD_3CN , 297 K) of: (A) complex $[\text{Cu}(\mathbf{1},\mathbf{4})_2]^+$, (B) complex $[\text{Fe}(\mathbf{2},\mathbf{3})_2]^{2+}$, the crude reaction mixture obtained by reacting components $\mathbf{1}$, $\mathbf{2}$, $\mathbf{3}$ and $\mathbf{4}$ with $\text{Cu}(\text{BF}_4)$ and $\text{Fe}(\text{BF}_4)_2$ in the molar ratio 2:2:2:2:1:1 (3.6 mM) at 60 °C for 18 h (C), 4 days (D), 10 days (E) and 20 days (F). Diagnostic signals of the complexes are colour coded, $[\text{Cu}(\mathbf{1},\mathbf{4})_2]^+$ in red, $[\text{Fe}(\mathbf{2},\mathbf{3})_2]^{2+}$ in purple. Three of the diagnostic signals of $[\text{Fe}(\mathbf{2},\mathbf{3})(\mathbf{2},\mathbf{4})]^{2+}$ are colour coded in orange. One of the diagnostic signals of the free aldehyde $\mathbf{4}$ is highlighted by a green pentagon and two of the diagnostic signals of the free amine $\mathbf{1}$ are highlighted by grey squares.

3.2.2.2 Probing the selectivity of the self-assembly of $[\text{Cu}(\mathbf{5},\mathbf{7})_2]^+$ and $[\text{Fe}(\mathbf{2},\mathbf{3})_2]^{2+}$ from a mixture of components **1**, **2**, **3** and **7** at 3.6 mM

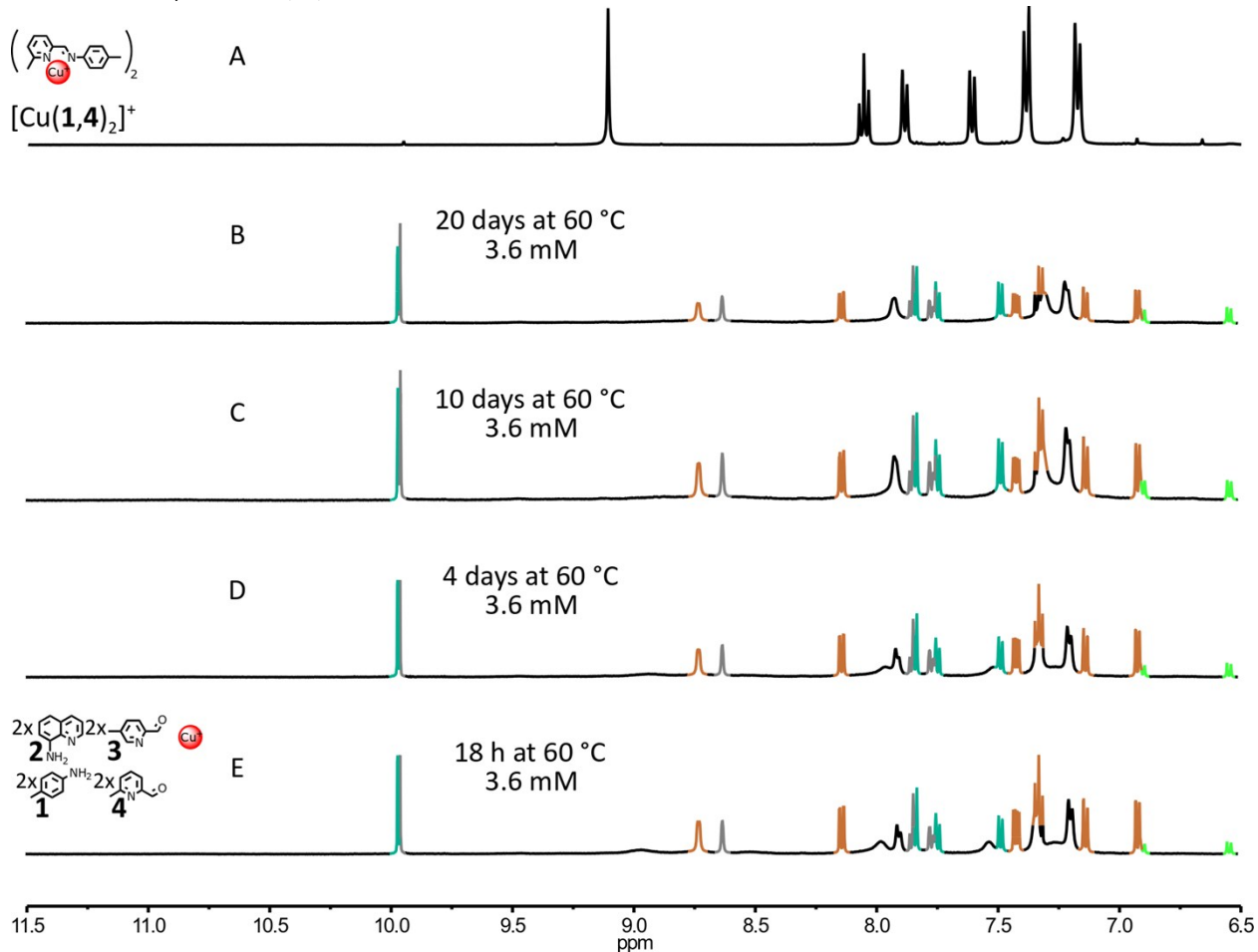


Figure S52. Partial ^1H NMR spectra (500 MHz, CD_3CN , 297 K) of: (A) complex $[\text{Cu}(\mathbf{1},\mathbf{4})_2]^+$, the crude reaction mixture obtained by reacting components **1**, **2**, **3** and **4** with $\text{Cu}(\text{BF}_4)$ in the molar ration 2:2:2:1 (3.6 mM) at 60 °C for 18 h (B), 4 days (C), 10 days (D) and 20 days (E). The diagnostic signals of the free aldehyde **3**, free aldehyde **4**, the free amine **2** and free amine **1** are respectively highlighted in grey, turquoise, brown and light green.

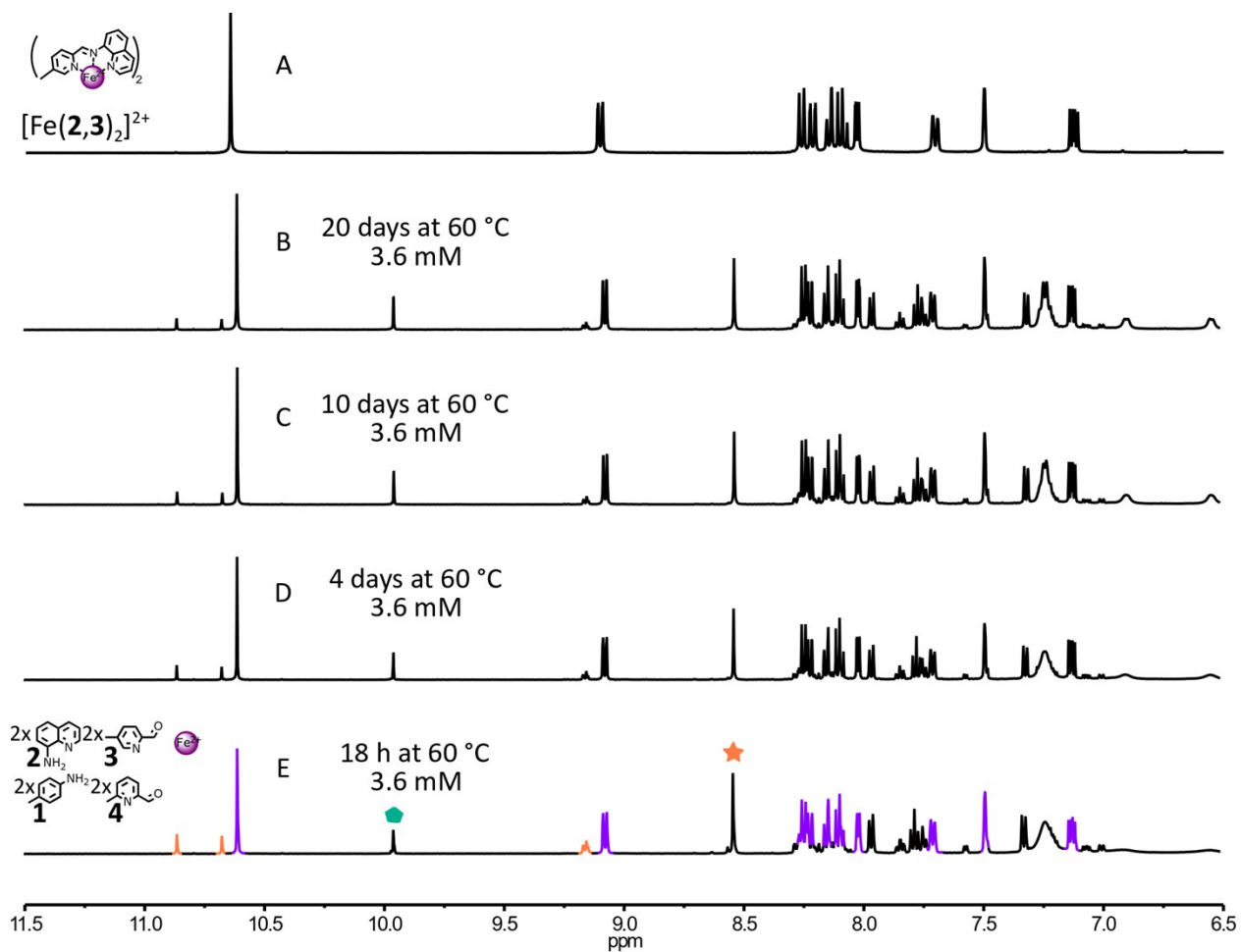


Figure S53. Partial ^1H NMR spectra (500 MHz, CD_3CN , 297 K) of: (A) complex $[\text{Fe}(\mathbf{2},\mathbf{3})_2]^{2+}$, the crude reaction mixture obtained by reacting components $\mathbf{1}$, $\mathbf{2}$, $\mathbf{3}$ and $\mathbf{4}$ with $\text{Fe}(\text{BF}_4)_2$ in the molar ration 2:2:2:1 (3.6 mM) at 60°C for 18 h (B), 4 days (C), 10 days (D) and 20 days (E). Diagnostic signals of the complex $[\text{Fe}(\mathbf{2},\mathbf{3})_2]^{2+}$ are colour coded in purple. Three of the diagnostic signals of $[\text{Fe}(\mathbf{2},\mathbf{3})(\mathbf{2},\mathbf{4})]^{2+}$ are colour coded in orange. One of the diagnostic signals of the free aldehyde $\mathbf{4}$ is highlighted by a green pentagon and one of the diagnostic signals of the imine constituent $(\mathbf{1},\mathbf{4})$ is highlighted by an orange star.

3.2.2.3 Simultaneous generation of complexes $[\text{Cu}(\mathbf{1},\mathbf{4})_2]^+$ and $[\text{Fe}(\mathbf{2},\mathbf{3})_2]^{2+}$ at 20 mM

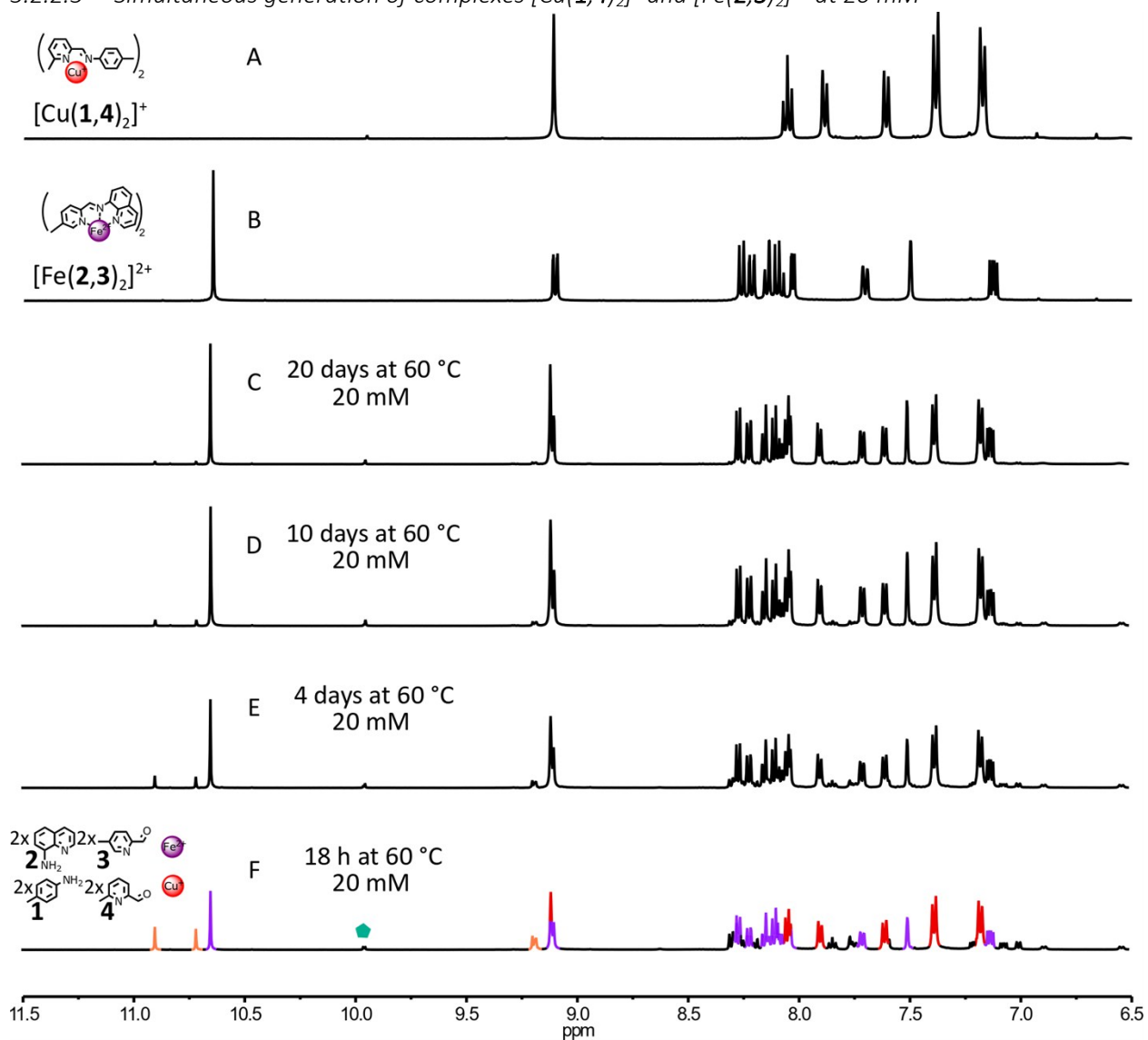


Figure S54. Partial ^1H NMR spectra (500 MHz, CD_3CN , 297 K) of: (A) complex $[\text{Cu}(\mathbf{1},\mathbf{4})_2]^+$, (B) complex $[\text{Fe}(\mathbf{2},\mathbf{3})_2]^{2+}$, the crude reaction mixture obtained by reacting components **1**, **2**, **3** and **4** with $\text{Cu}(\text{BF}_4)$ and $\text{Fe}(\text{BF}_4)_2$ in the molar ratio 2:2:2:2:1:1 (20 mM) at 60°C for 18 h (C), 4 days (D), 10 days (E) and 20 days (F). Diagnostic signals of the complexes are colour coded, $[\text{Cu}(\mathbf{1},\mathbf{4})_2]^+$ in red, $[\text{Fe}(\mathbf{2},\mathbf{3})_2]^{2+}$ in purple. Three of the diagnostic signals of $[\text{Fe}(\mathbf{2},\mathbf{3})(\mathbf{2},\mathbf{4})]^{2+}$ are colour coded in orange. One of the diagnostic signals of the free aldehyde **4** is highlighted by a green pentagon.

3.2.2.4 Probing the selectivity of the self-assembly of $[\text{Cu}(\mathbf{5},\mathbf{7})_2]^+$ and $[\text{Fe}(\mathbf{2},\mathbf{3})_2]^{2+}$ from a mixture of components **1**, **2**, **3** and **4** at 20 mM

CD_3CN solutions of the 2-formylpyridine containing components **3** (100 μL of 320 mM, 32 μmol , 2 eq.) and **4** (100 μL of 320 mM, 32 μmol , 2 eq.) and of the amine containing components **1** (100 μL of 320 mM, 32 μmol , 2 eq.) and **2** (10 μL of 320 mM, 32 μmol , 2 eq.) were combined. The resulting mixture was treated with CD_3CN solutions of CuBF_4 (200 μL of 80 mM, 16 μmol , 1 eq.) and $\text{Fe}(\text{BF}_4)_2$ (200 μL of 80 mM, 16 μmol , 1 eq.) and heated at 60 $^\circ\text{C}$ for up to 20 days. The complexes were never isolated, all the present experiments and analysis were done on the crude reaction mixture.

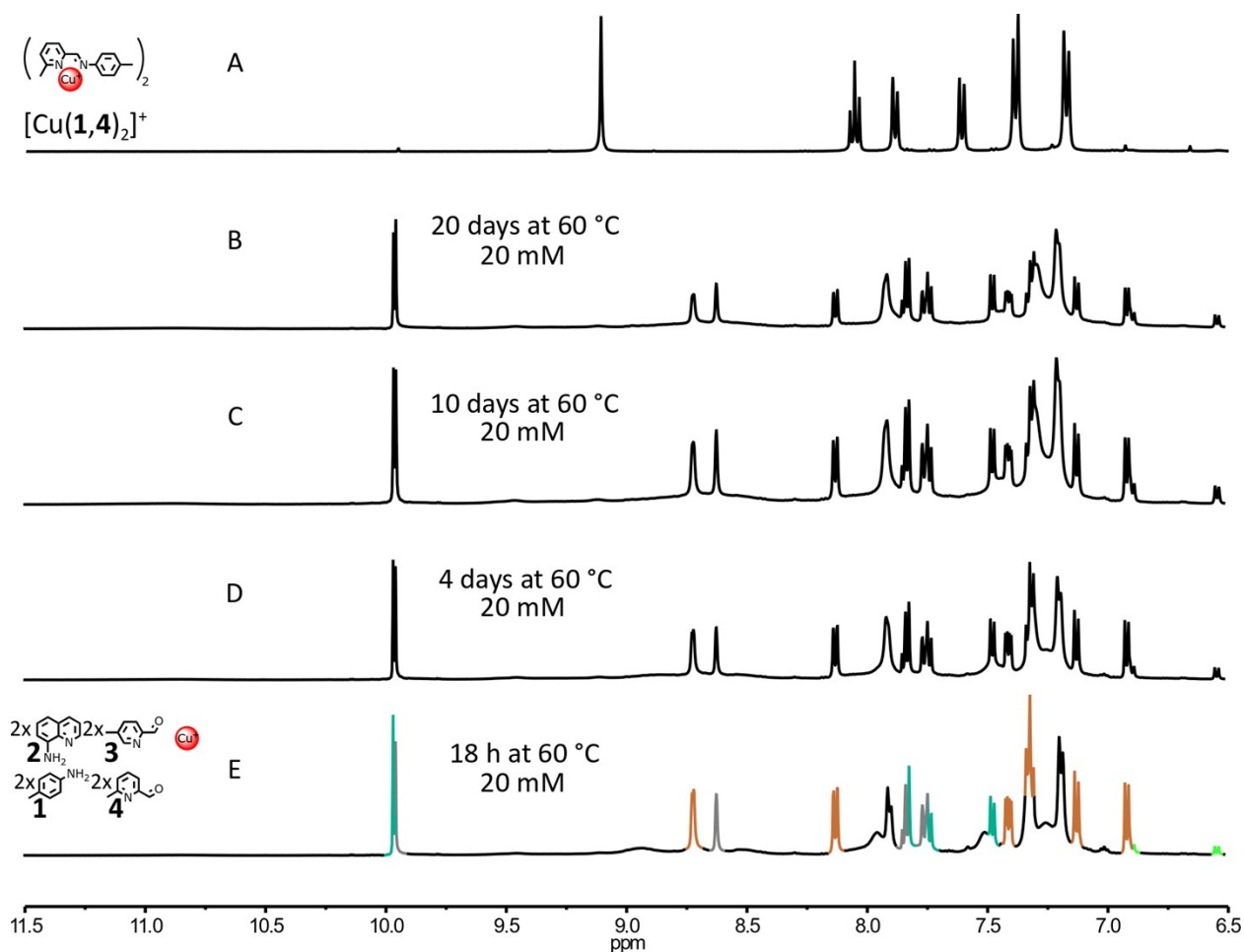


Figure S55. Partial ^1H NMR spectra (500 MHz, CD_3CN , 297 K) of: (A) complex $[\text{Cu}(\mathbf{1},\mathbf{4})_2]^+$, the crude reaction mixture obtained by reacting components **1**, **2**, **3** and **4** with $\text{Cu}(\text{BF}_4)$ in the molar ratio 2:2:2:1 (20 mM) at 60 $^\circ\text{C}$ for 18 h (B), 4 days (C), 10 days (D) and 20 days (E). The diagnostic signals of the free aldehyde **3**, free aldehyde **4**, the free amine **2** and free amine **1** are respectively highlighted in grey, turquoise, brown and light green.

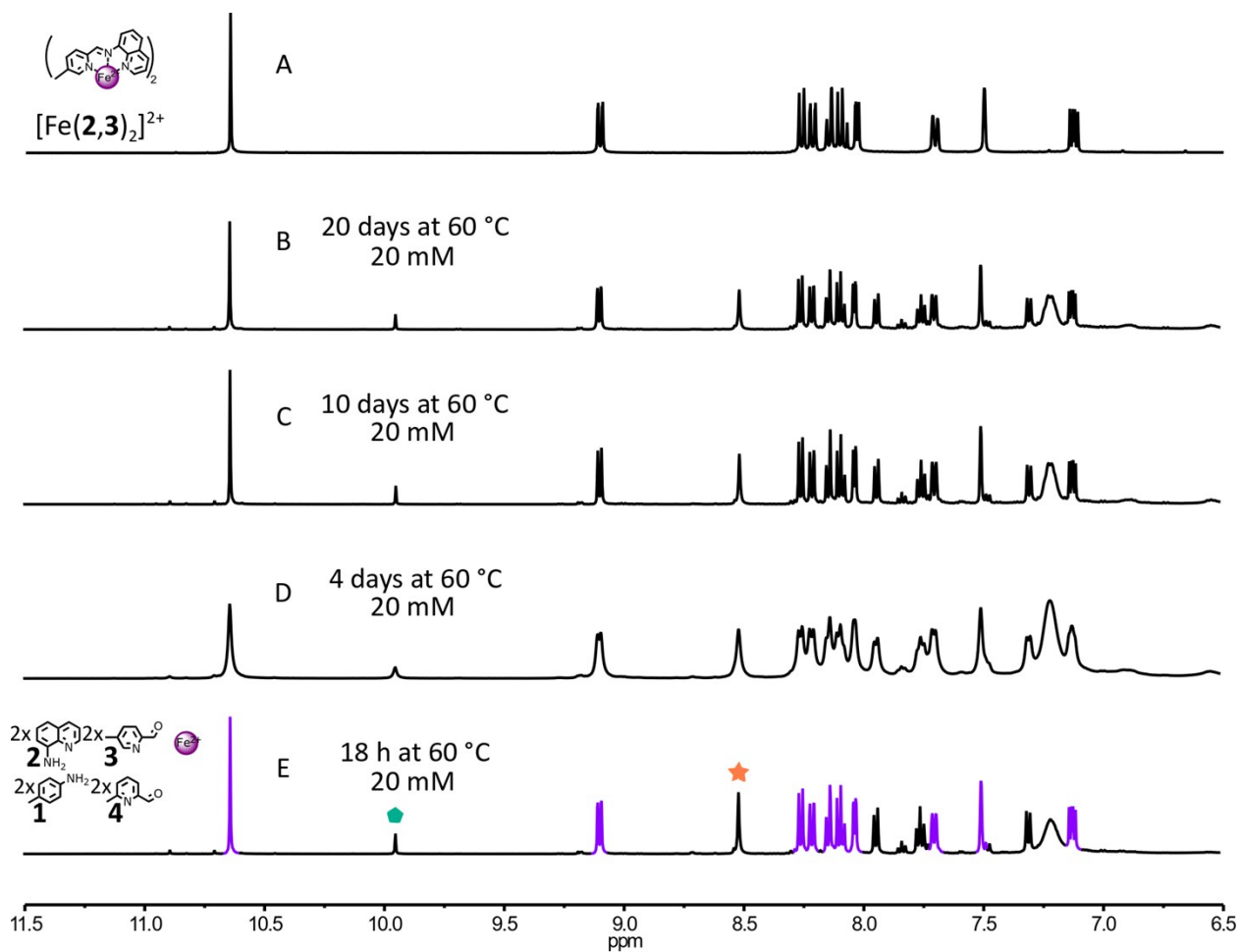


Figure S56. Partial ^1H NMR spectra (500 MHz, CD_3CN , 297 K) of: (A) complex $[\text{Fe}(\mathbf{2},\mathbf{3})_2]^{2+}$, the crude reaction mixture obtained by reacting components **1**, **2**, **3** and **4** with $\text{Fe}(\text{BF}_4)_2$ in the molar ration 2:2:2:1 (20 mM) at 60 °C for 18 h (B), 4 days (C), 10 days (D) and 20 days (E). Diagnostic signals of the complex $[\text{Fe}(\mathbf{2},\mathbf{3})_2]^{2+}$ are colour coded in purple. One of the diagnostic signals of the free aldehyde **4** is highlighted by a green pentagon, one of the diagnostic signals of the imine constituent (**1,4**) is highlighted by an orange star.

3.3 Self-sorting of complexes $[\text{Cu}(4,5)_2]^+$ and $[\text{Fe}(2,3)_2]^{2+}$

3.3.1 Simultaneous generation of complexes $[\text{Cu}(4,5)_2]^+$ and $[\text{Fe}(2,3)_2]^{2+}$

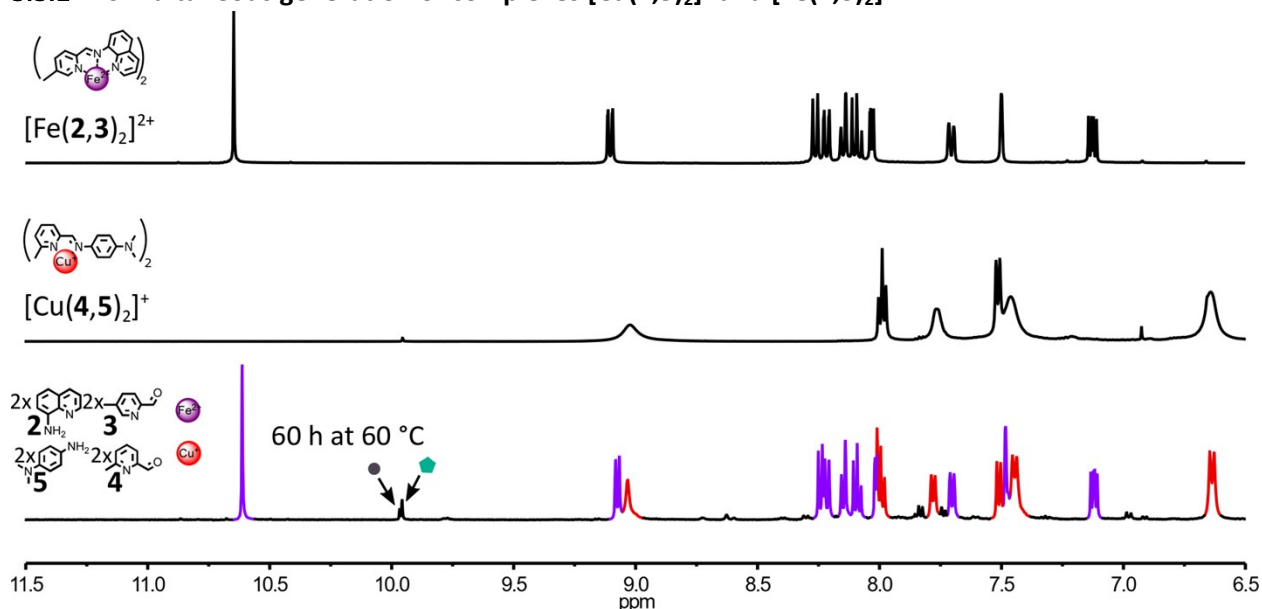


Figure S57. Partial ^1H NMR spectra (500 MHz, CD_3CN , 297 K) of: (top) complex $[\text{Fe}(2,3)_2]^{2+}$, (middle) complex $[\text{Cu}(4,5)_2]^+$, (bottom) the crude reaction mixture of the simultaneous generation of complexes $[\text{Cu}(4,5)_2]^+$ and $[\text{Fe}(2,3)_2]^{2+}$ through the self-sorting of their initial reactants. Reaction conditions: **2**:**3**:**4**:**5**: $\text{Cu}(\text{BF}_4)$: $\text{Fe}(\text{BF}_4)_2$ (2:2:2:2:1:1), CD_3CN , 60 °C, 60 h. Diagnostic signals of the complexes are colour coded, $[\text{Cu}(4,5)_2]^+$ in red, $[\text{Fe}(2,3)_2]^{2+}$ in purple, one of the diagnostic signals of the free aldehyde **3** is highlighted by a grey circle and one of the diagnostic signals of the free aldehyde **4** is highlighted by a green pentagon.

3.3.2 Monitoring of the formation of complexes $[\text{Cu}(4,5)_2]^+$ and $[\text{Fe}(2,3)_2]^{2+}$

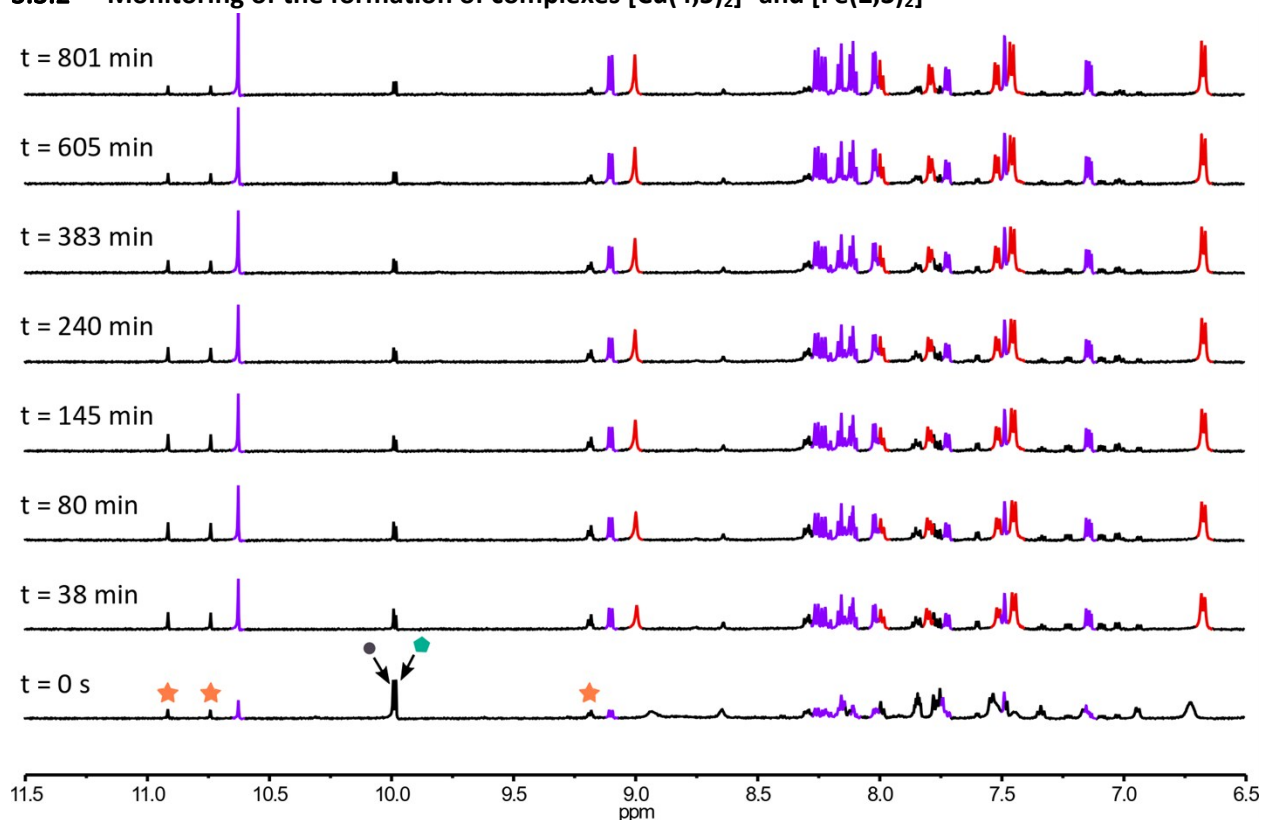


Figure S58. Formation of complexes $[\text{Cu}(4,5)_2]^+$ and $[\text{Fe}(2,3)_2]^{2+}$ from their initial reactants monitored by ^1H NMR (600 MHz, CD_3CN , 333 K), aromatic region of the spectrum shown. The sample was maintained at 60 °C and spectra of the crude reaction mixture were recorded at increasing time increments (up to a final total time of 801 min). Reaction conditions: **2**:**3**:**4**:**5**: $\text{Cu}(\text{BF}_4)$: $\text{Fe}(\text{BF}_4)_2$ (2:2:2:2:1:1), CD_3CN , 60 °C. Diagnostic signals of the complexes are colour coded, $[\text{Cu}(4,5)_2]^+$ in red, $[\text{Fe}(2,3)_2]^{2+}$ in purple. Three of the diagnostic signals of the heteroleptic complex $[\text{Fe}(2,3)(2,5)]^{2+}$ are highlighted by orange stars. One of the diagnostic signals of the free aldehyde **3** is highlighted by a grey circle, one of the diagnostic signals of the free aldehyde **4** is highlighted by a green pentagon.

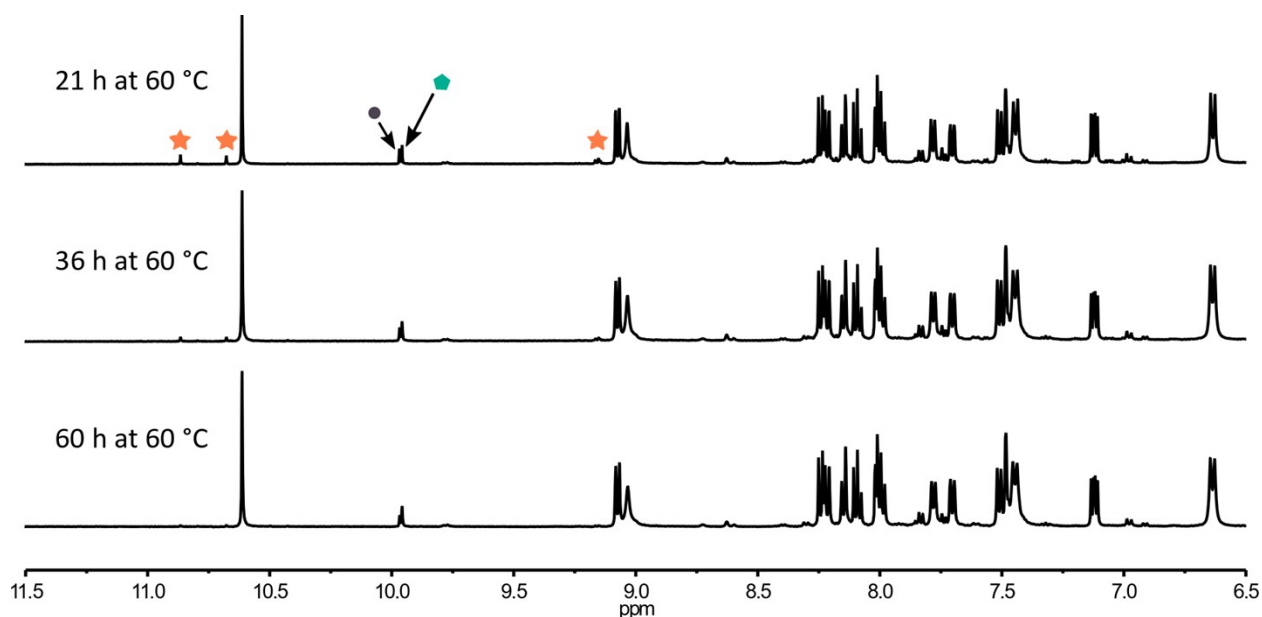


Figure S59. Formation of complexes $[\text{Cu}(\mathbf{4},\mathbf{5})_2]^+$ and $[\text{Fe}(\mathbf{2},\mathbf{3})_2]^{2+}$ from their initial reactants monitored by ^1H NMR (500 MHz, CD_3CN , 297 K), aromatic region of the spectrum shown. Spectra of the crude reaction mixture were collected after 21 h (top), 36 h (middle) and 60 h (bottom). Reaction conditions: $\mathbf{2}:\mathbf{3}:\mathbf{4}:\mathbf{5}:\text{Cu}(\text{BF}_4):\text{Fe}(\text{BF}_4)_2$ (2:2:2:2:1:1), CD_3CN , 60 °C. Three of the diagnostic signals of the complex $[\text{Fe}(\mathbf{2},\mathbf{3})(\mathbf{2},\mathbf{4})]^{2+}$ are highlighted by orange stars, one of the diagnostic signals of the free aldehyde $\mathbf{3}$ is highlighted by a grey circle and one of the diagnostic signals of the free aldehyde $\mathbf{4}$ is highlighted by a green pentagon.

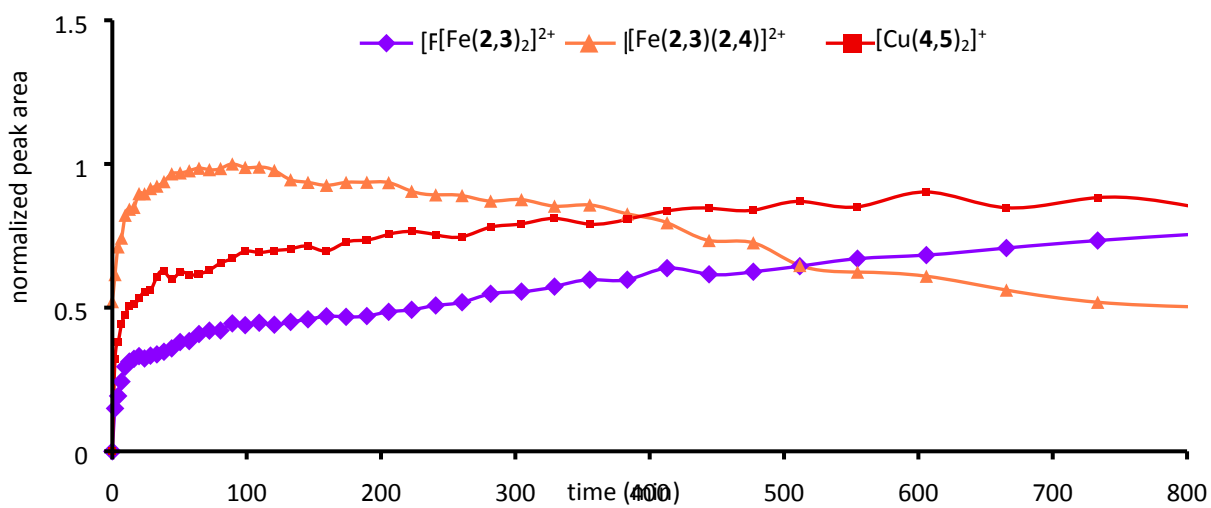


Figure S60. Formation as a function of time of the thermodynamic products $[\text{Cu}(\mathbf{4},\mathbf{5})_2]^+$ (red squares) and $[\text{Fe}(\mathbf{2},\mathbf{3})_2]^{2+}$ (purple diamonds) and disappearance as a function of time of the kinetic product $[\text{Fe}(\mathbf{2},\mathbf{3})(\mathbf{2},\mathbf{4})]^{2+}$ (orange triangles). Graph plotting of the area of the imine peaks of the different complexes normalized to the area of the same peaks at the final time-point (after 60h).

3.4 Self-sorting of complexes $[\text{Cu}(\mathbf{1},\mathbf{6})_2]^+$ and $[\text{Fe}(\mathbf{2},\mathbf{3})_2]^{2+}$

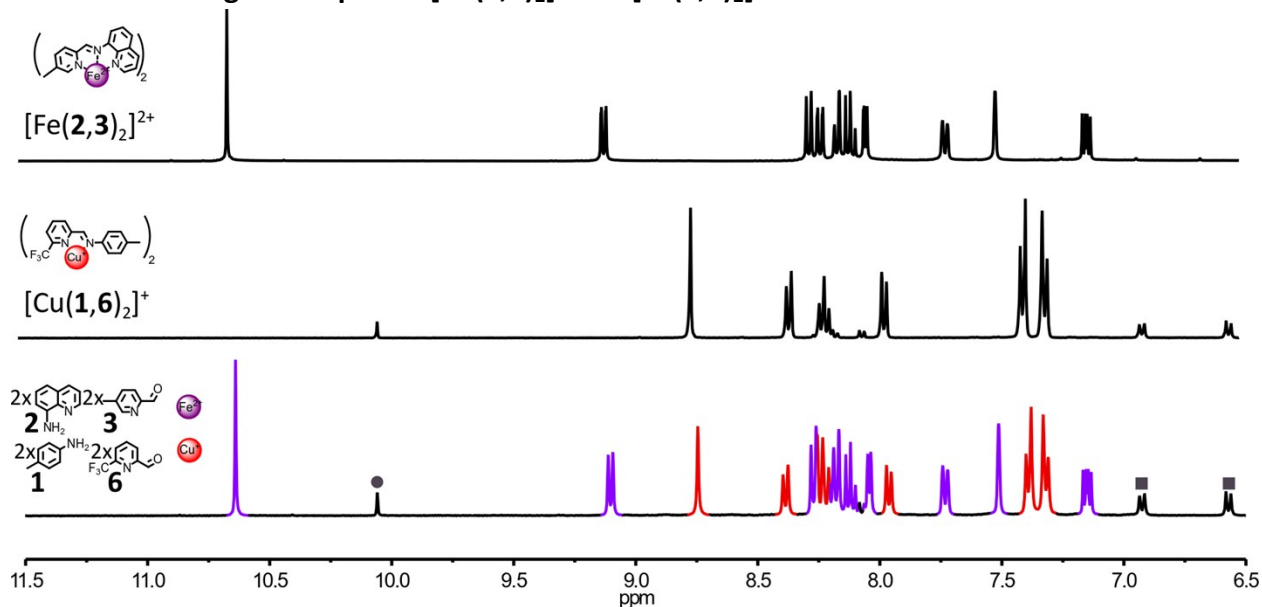


Figure S61. Partial ^1H NMR spectra (400 MHz, CD_3CN , 297 K) of: (top) complex $[\text{Fe}(\mathbf{2},\mathbf{3})_2]^{2+}$, (middle) complex $[\text{Cu}(\mathbf{1},\mathbf{6})_2]^+$, (bottom) the crude reaction mixture of the simultaneous generation of complexes $[\text{Cu}(\mathbf{1},\mathbf{6})_2]^+$ and $[\text{Fe}(\mathbf{2},\mathbf{3})_2]^{2+}$ through the self-sorting of their initial reactants. Reaction conditions: $\mathbf{1}:\mathbf{2}:\mathbf{3}:\mathbf{6}:\text{Cu}(\text{BF}_4):\text{Fe}(\text{BF}_4)_2$ (2:2:2:2:1:1), CD_3CN , 60 °C, 18 h. Diagnostic signals of the complexes are colour coded, $[\text{Cu}(\mathbf{1},\mathbf{6})_2]^+$ in red, $[\text{Fe}(\mathbf{2},\mathbf{3})_2]^{2+}$ in purple. One of the diagnostic signals of the free aldehyde $\mathbf{6}$ is highlighted by a grey circle and two of the diagnostic signals of the free aniline $\mathbf{1}$ are highlighted by grey squares.

3.5 Self-sorting of complexes $[\text{Cu}(\mathbf{1},\mathbf{7})_2]^+$ and $[\text{Fe}(\mathbf{2},\mathbf{3})_2]^{2+}$

3.5.1 Simultaneous generation of complexes $[\text{Cu}(\mathbf{1},\mathbf{7})_2]^+$ and $[\text{Fe}(\mathbf{2},\mathbf{3})_2]^{2+}$

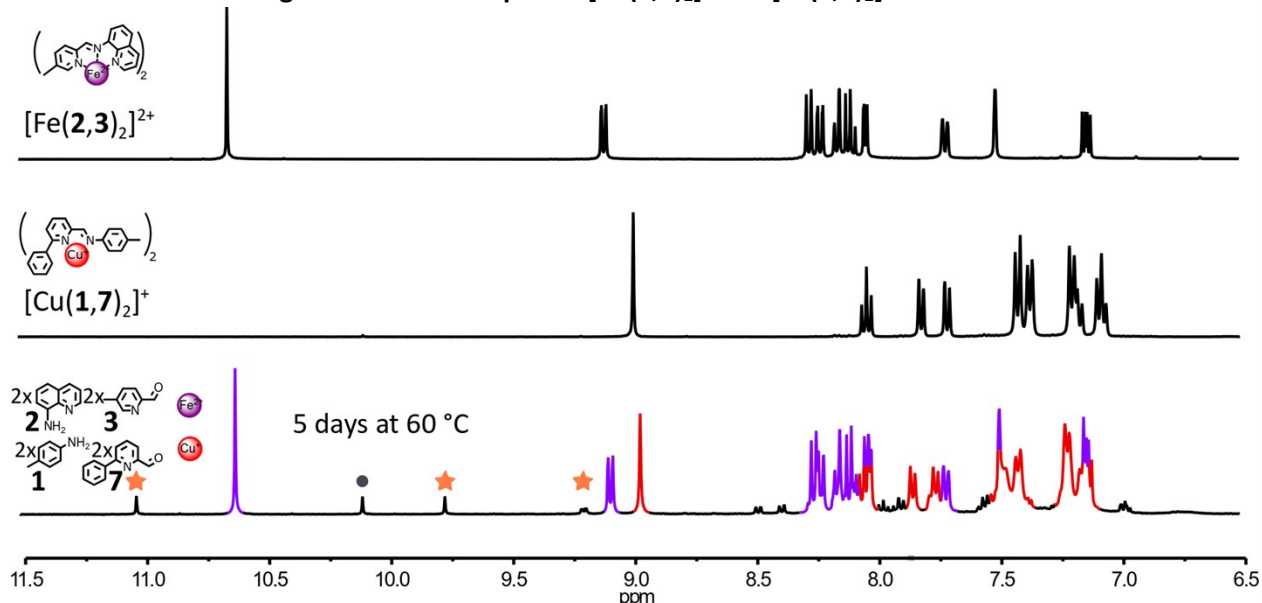


Figure S62. Partial ^1H NMR spectra (400 MHz, CD_3CN , 297 K) of: (top) complex $[\text{Fe}(\mathbf{2},\mathbf{3})_2]^{2+}$, (middle) complex $[\text{Cu}(\mathbf{1},\mathbf{7})_2]^+$, (bottom) the crude reaction mixture of the simultaneous generation of complexes $[\text{Cu}(\mathbf{1},\mathbf{7})_2]^+$ and $[\text{Fe}(\mathbf{2},\mathbf{3})_2]^{2+}$ through the self-sorting of their initial reactants. Reaction conditions: $\mathbf{1}:\mathbf{2}:\mathbf{3}:\mathbf{7}:\text{Cu}(\text{BF}_4):\text{Fe}(\text{BF}_4)_2$ (2:2:2:2:1:1), CD_3CN , 60 °C, 5 days. Diagnostic signals of the complexes are colour coded, $[\text{Cu}(\mathbf{1},\mathbf{7})_2]^+$ in red, $[\text{Fe}(\mathbf{2},\mathbf{3})_2]^{2+}$ in purple. One of the diagnostic signals of the free aldehyde $\mathbf{6}$ is highlighted by a grey circle and two of the diagnostic signals of the free aniline $\mathbf{1}$ are highlighted by grey squares.

$[\text{Cu}(\mathbf{1},\mathbf{7})_2]^+$ and $[\text{Fe}(\mathbf{2},\mathbf{3})_2]^{2+}$ through the self-sorting of their initial reactants. Reaction conditions: $\mathbf{1}:\mathbf{2}:\mathbf{3}:\mathbf{7}:\text{Cu}(\text{BF}_4):\text{Fe}(\text{BF}_4)_2$ (2:2:2:2:1:1), CD_3CN , 60 °C, 5 days. Diagnostic signals of the complexes are colour coded, $[\text{Cu}(\mathbf{1},\mathbf{7})_2]^+$ in red, $[\text{Fe}(\mathbf{2},\mathbf{3})_2]^{2+}$ in purple and three of the diagnostic signals of the heteroleptic complex $[\text{Fe}(\mathbf{2},\mathbf{3})(\mathbf{2},\mathbf{7})]^{2+}$ are highlighted by orange stars and one of the diagnostic signals of the free aldehyde $\mathbf{7}$ is highlighted by a grey circle.

3.5.2 Monitoring of the formation of complexes $[\text{Cu}(\mathbf{1},\mathbf{7})_2]^+$ and $[\text{Fe}(\mathbf{2},\mathbf{3})_2]^{2+}$

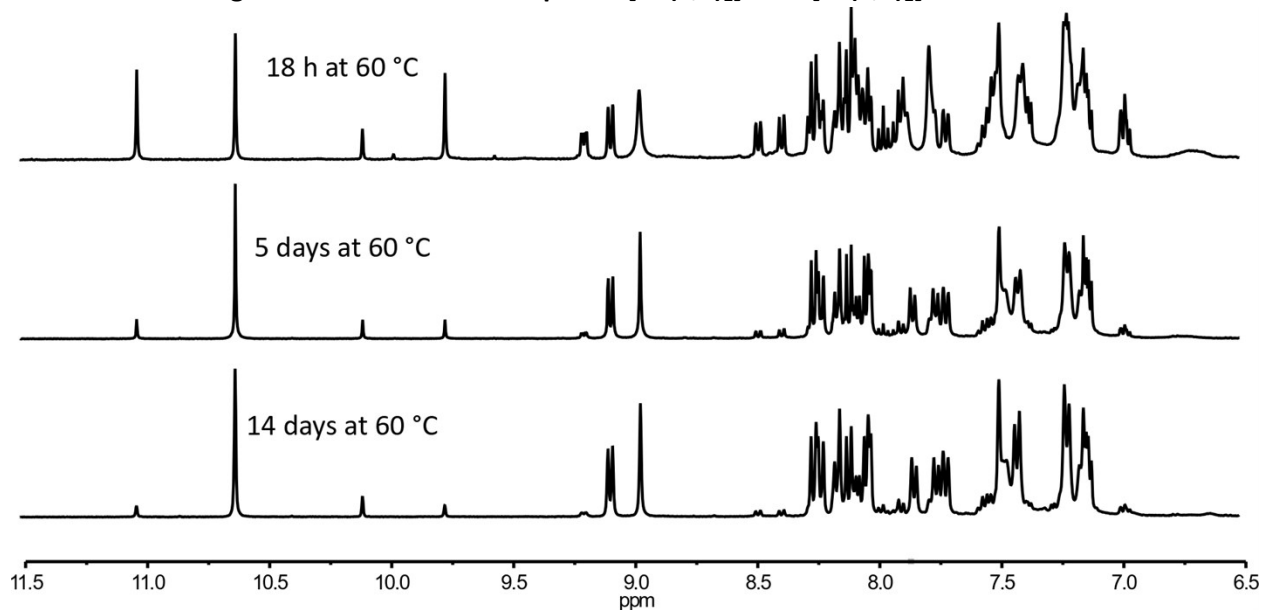


Figure S63. Formation of complexes $[\text{Cu}(\mathbf{1},\mathbf{7})_2]^+$ and $[\text{Fe}(\mathbf{2},\mathbf{3})_2]^{2+}$ from their initial reactants monitored by ^1H NMR (400 MHz, CD_3CN , 297 K), aromatic region of the spectrum shown. Spectra of the crude reaction mixture were collected after 18 h (top), 5 days (middle) and 14 days (bottom). Reaction conditions: $\mathbf{1}:\mathbf{2}:\mathbf{3}:\mathbf{7}:\text{Cu}(\text{BF}_4):\text{Fe}(\text{BF}_4)_2$ (2:2:2:2:1:1), CD_3CN , 60 °C.

3.6 Self-sorting of complexes $[\text{Cu}(\mathbf{5},\mathbf{7})_2]^+$ and $[\text{Fe}(\mathbf{2},\mathbf{3})_2]^{2+}$

3.6.1 Simultaneous generation of complexes $[\text{Cu}(\mathbf{5},\mathbf{7})_2]^+$ and $[\text{Fe}(\mathbf{2},\mathbf{3})_2]^{2+}$

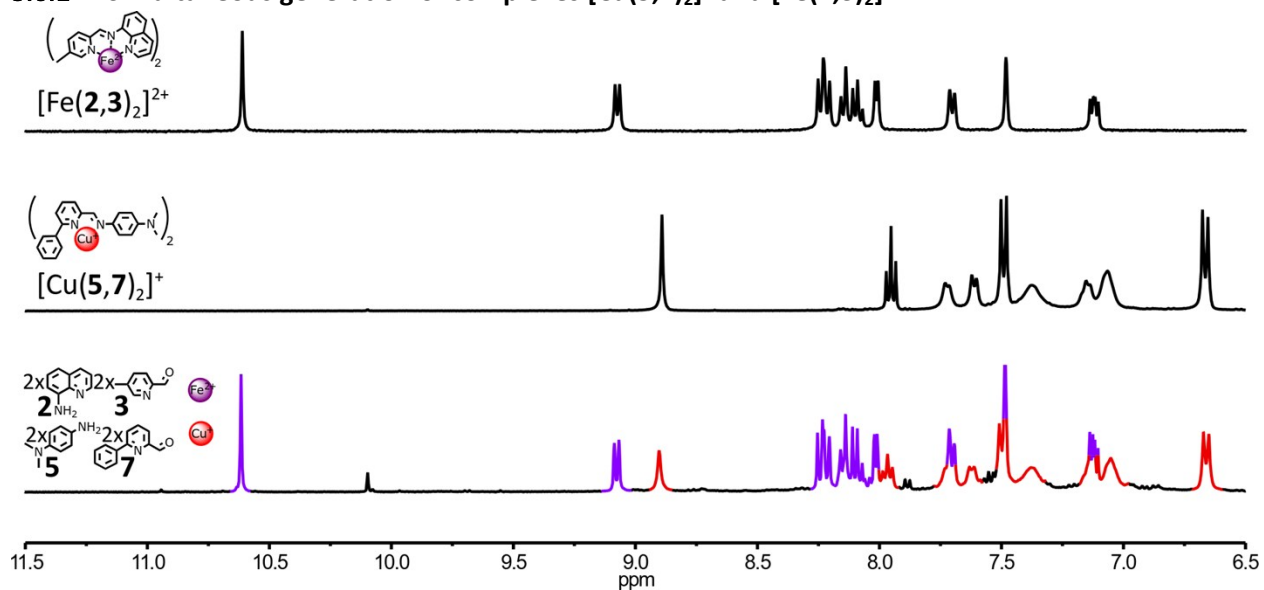


Figure S64. Partial ^1H NMR spectra (400 MHz, CD_3CN , 297 K) of: (top) complex $[\text{Fe}(\mathbf{2},\mathbf{3})_2]^{2+}$, (middle) complex $[\text{Cu}(\mathbf{5},\mathbf{7})_2]^+$, (bottom) the crude reaction mixture of the simultaneous generation of complexes $[\text{Cu}(\mathbf{5},\mathbf{7})_2]^+$ and $[\text{Fe}(\mathbf{2},\mathbf{3})_2]^{2+}$ through the self-sorting of their initial reactants. Reaction conditions: $\mathbf{2}:\mathbf{3}:\mathbf{5}:\mathbf{7}:\text{Cu}(\text{BF}_4):\text{Fe}(\text{BF}_4)_2$ (2:2:2:2:1:1), CD_3CN , 60 °C, 18 h. Diagnostic signals of the complexes are colour coded, $[\text{Cu}(\mathbf{5},\mathbf{7})_2]^+$ in red, $[\text{Fe}(\mathbf{2},\mathbf{3})_2]^{2+}$ in purple.

3.6.2 Monitoring of the formation of complexes $[\text{Cu}(\mathbf{5},\mathbf{7})_2]^+$ and $[\text{Fe}(\mathbf{2},\mathbf{3})_2]^{2+}$

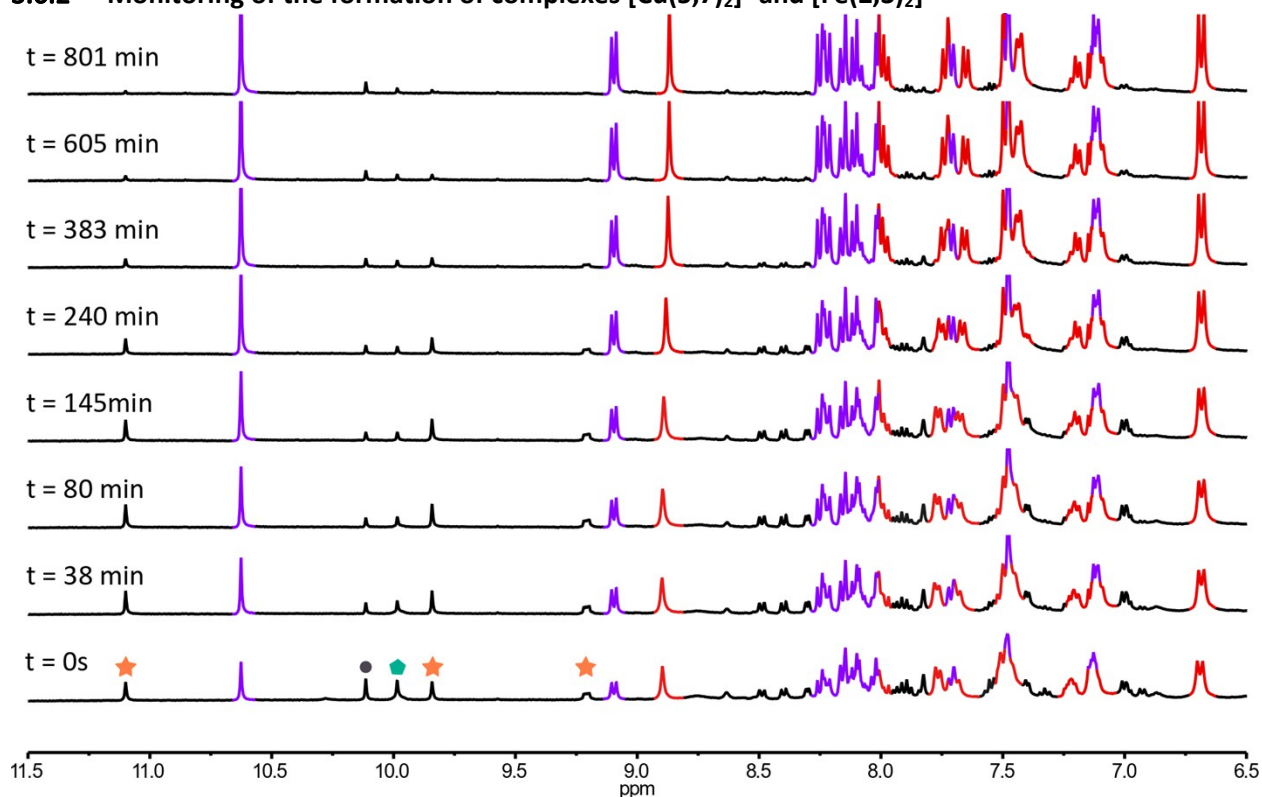


Figure S65. Formation of complexes $[\text{Cu}(\mathbf{5},\mathbf{7})_2]^+$ and $[\text{Fe}(\mathbf{2},\mathbf{3})_2]^{2+}$ from their initial reactants monitored by ^1H NMR (400 MHz, CD_3CN , 333 K), aromatic region of the spectrum shown. The sample was maintained at 60°C and spectra of the crude reaction mixture were recorded at increasing time increments (up to a final total time of 801 min). Reaction conditions: $\mathbf{2}:\mathbf{3}:\mathbf{5}:\mathbf{7}:\text{Cu}(\text{BF}_4):\text{Fe}(\text{BF}_4)_2$ (2:2:2:2:1:1), CD_3CN , 60°C .

Diagnostic signals of the complexes are colour coded, $[\text{Cu}(\mathbf{5},\mathbf{7})_2]^+$ in red, $[\text{Fe}(\mathbf{2},\mathbf{3})_2]^{2+}$ in purple. Diagnostic signals of the heteroleptic complex $[\text{Fe}(\mathbf{2},\mathbf{3})(\mathbf{2},\mathbf{7})]^{2+}$ are highlighted by orange stars. One of the diagnostic signals of the free aldehyde $\mathbf{7}$ is highlighted by a grey circle and one of the diagnostic signals of the free aldehyde $\mathbf{3}$ is highlighted by a green pentagon.

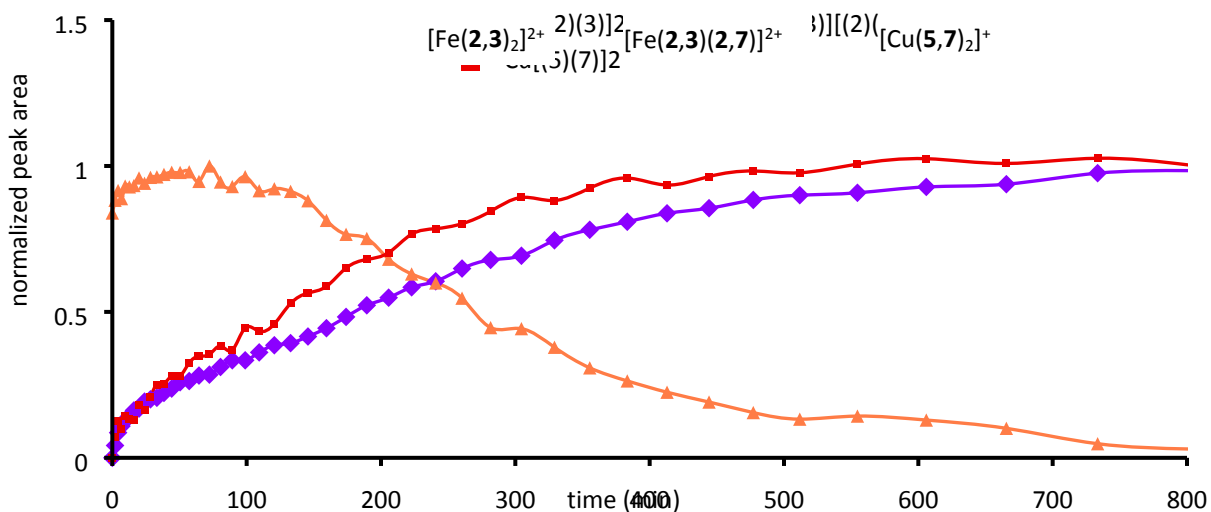


Figure S66. Formation as a function of time of thermodynamic products $[\text{Cu}(5,7)_2]^+$ (red squares) and $[\text{Fe}(2,3)_2]^{2+}$ (purple diamonds) and disappearance as a function of time of the kinetic product $[\text{Fe}(2,3)(2,7)]^{2+}$ (orange triangles). Graph plotting of the area of the imine peaks of the different complexes normalized to the area of the same peaks at the final time-point.

3.6.3 Probing of the selectivity of the self-assembly of $[\text{Cu}(5,7)_2]^+$ and $[\text{Fe}(2,3)_2]^{2+}$ from a mixture of components 1, 2, 3 and 7

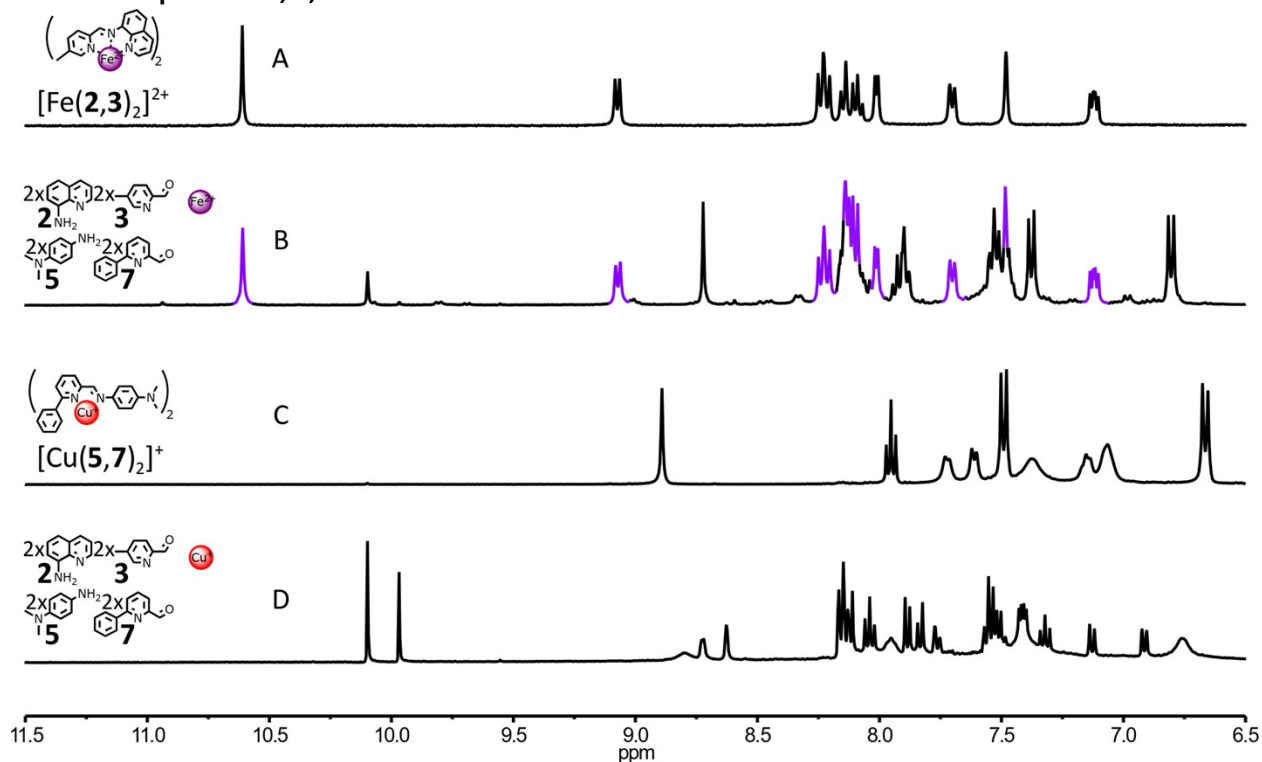


Figure S67. Partial ^1H NMR spectra (400 MHz, CD_3CN , 297 K) of: (A) complex $[\text{Fe}(2,3)_2]^{2+}$, (B) the crude reaction mixture obtained by mixing $2:3:5:7:\text{Fe}(\text{BF}_4)_2$ in the molar ratio 2:2:2:2:1 at 60 °C for 18 h, (C)

complex $[\text{Cu}(\mathbf{5},\mathbf{7})^+]$ and (D) the crude reaction mixture obtained by mixing $\mathbf{2}:\mathbf{3}:\mathbf{5}:\mathbf{7}:\text{Cu}(\text{BF}_4)$ in the molar ratio 2:2:2:2:1 at 60 °C for 18 h. The diagnostic signals of the complex $[\text{Fe}(\mathbf{2},\mathbf{3})_2]^{2+}$ are colour coded in purple.

3.7 Self-sorting of complexes $[\text{Cu}(\mathbf{7},\mathbf{8})_2]^+$ and $[\text{Fe}(\mathbf{2},\mathbf{3})_2]^{2+}$

3.7.1 Simultaneous generation of complexes $[\text{Cu}(\mathbf{7},\mathbf{8})_2]^+$ and $[\text{Fe}(\mathbf{2},\mathbf{3})_2]^{2+}$

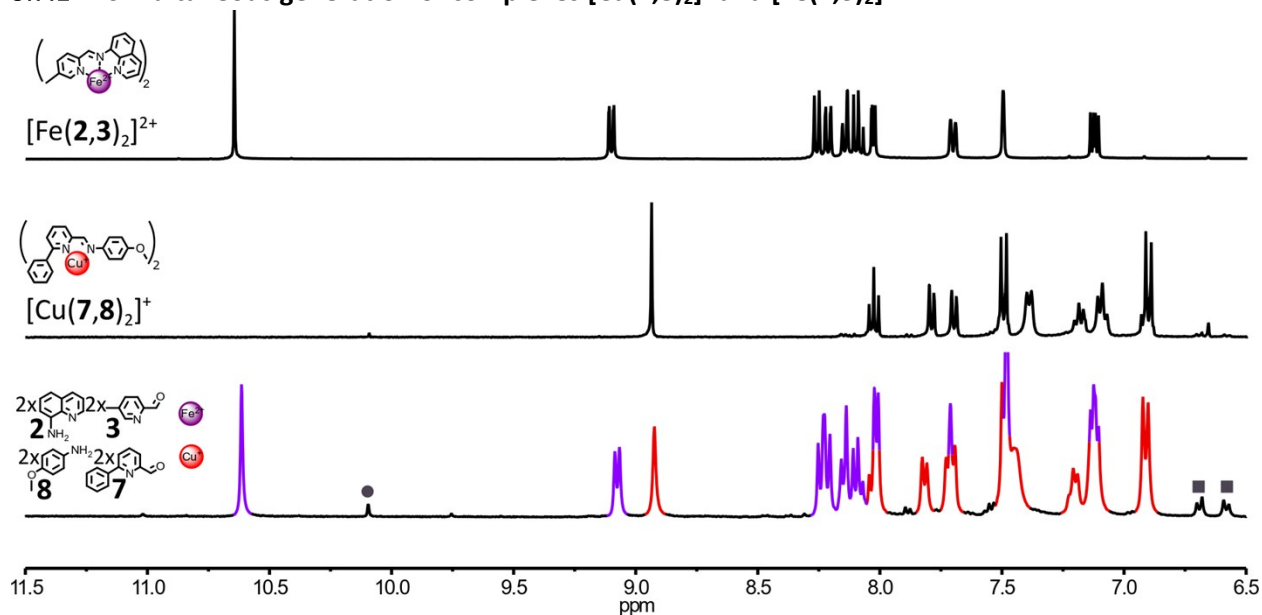


Figure S68. Partial ¹H NMR spectra (400 MHz, CD₃CN, 297 K) of: (top) complex $[\text{Fe}(\mathbf{2},\mathbf{3})_2]^{2+}$, (middle) complex $[\text{Cu}(\mathbf{7},\mathbf{8})_2]^+$, (bottom) the crude reaction mixture of the simultaneous generation of complexes $[\text{Cu}(\mathbf{7},\mathbf{8})_2]^+$ and $[\text{Fe}(\mathbf{2},\mathbf{3})_2]^{2+}$ through the self-sorting of their initial reactants. Reaction conditions: $\mathbf{2}:\mathbf{3}:\mathbf{7}:\mathbf{8}:\text{Cu}(\text{BF}_4):\text{Fe}(\text{BF}_4)_2$ (2:2:2:2:1:1), CD₃CN, 60 °C, 18 h. Diagnostic signals of the complexes are colour coded, $[\text{Cu}(\mathbf{7},\mathbf{8})_2]^+$ in red, $[\text{Fe}(\mathbf{2},\mathbf{3})_2]^{2+}$ in purple. One of the diagnostic signals of the free aldehyde **7** is highlighted by a grey circle and two of the diagnostic signals of the free aniline **8** are highlighted by grey squares.

3.7.2 Monitoring of the formation of complexes $[\text{Cu}(\mathbf{7},\mathbf{8})_2]^+$ and $[\text{Fe}(\mathbf{2},\mathbf{3})_2]^{2+}$

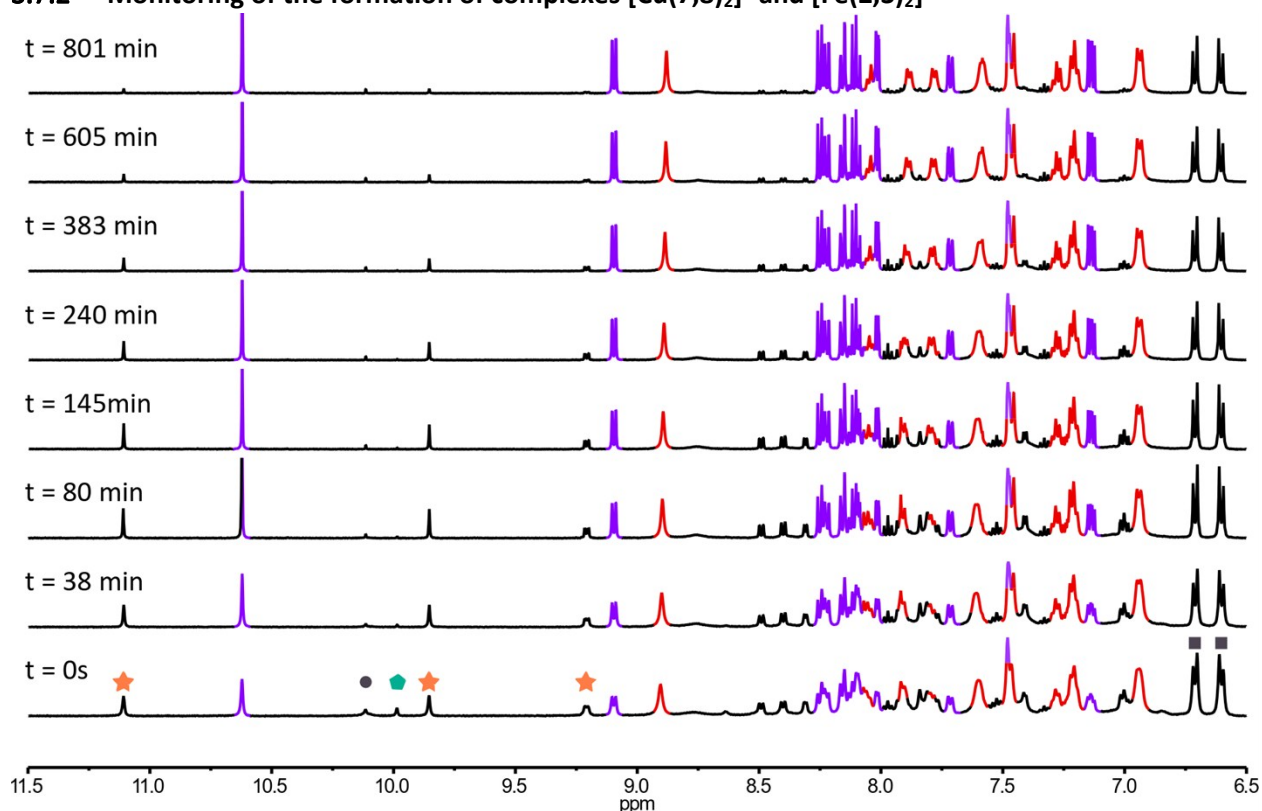


Figure S69. Formation of complexes $[\text{Cu}(\mathbf{7},\mathbf{8})_2]^+$ and $[\text{Fe}(\mathbf{2},\mathbf{3})_2]^{2+}$ from their initial reactants monitored by ^1H NMR (500 MHz, CD_3CN , 333 K), aromatic region of the spectrum shown. The sample was maintained at 60°C and spectra of the crude reaction mixture were recorded at increasing time increments (up to a final total time of 801 min). Reaction conditions: $\mathbf{2}:\mathbf{3}:\mathbf{7}:\mathbf{8}:\text{Cu}(\text{BF}_4):\text{Fe}(\text{BF}_4)_2$ (2:2:2:2:1:1), CD_3CN , 60°C .

Diagnostic signals of the complexes are colour coded, $[\text{Cu}(\mathbf{7},\mathbf{8})_2]^+$ in red, $[\text{Fe}(\mathbf{2},\mathbf{3})_2]^{2+}$ in purple. Diagnostic signals of the heteroleptic complex $[\text{Fe}(\mathbf{2},\mathbf{3})(\mathbf{2},\mathbf{7})]^{2+}$ are highlighted by orange stars. One of the diagnostic signals of the free aldehyde **7** is highlighted by a grey circle, one of the diagnostic signals of the free aldehyde **3** is highlighted by a green pentagon and two of the diagnostic signals of the free aniline **8** are highlighted by grey squares.

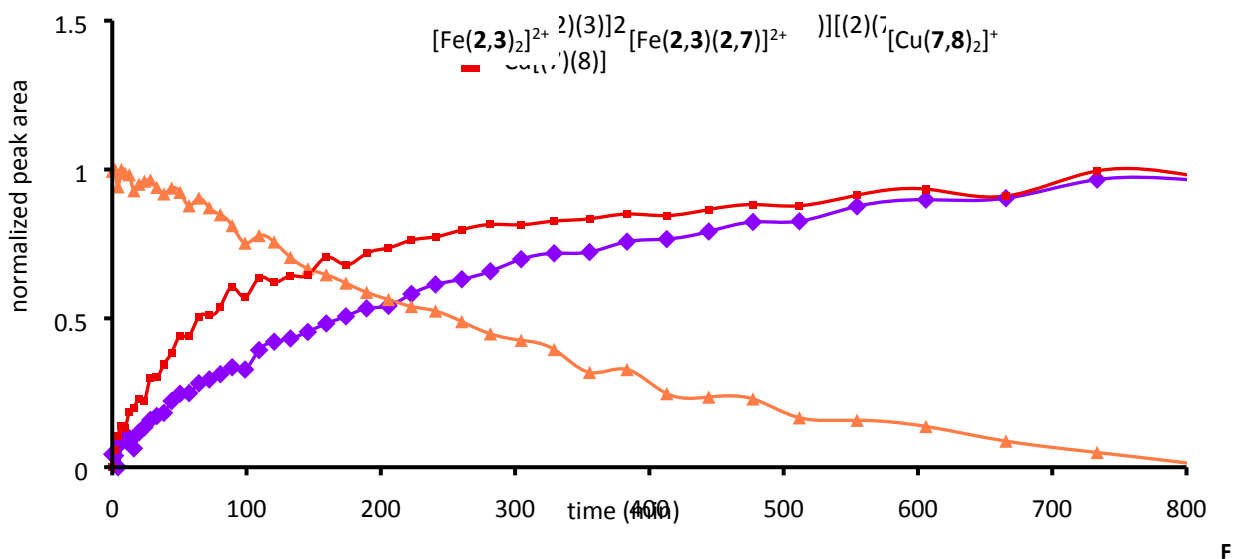


figure S70. Formation as a function of time of the thermodynamic products $[\text{Cu}(7,8)_2]^+$ (red squares) and $[\text{Fe}(2,3)_2]^{2+}$ (purple diamonds) and disappearance as a function of time of the kinetic product $[\text{Fe}(2,3)(2,7)]^{2+}$ (orange triangles). Graph plotting of the area of the imine peaks of the different complexes normalized to the area of the same peaks at the final time-point.

3.8 Self-sorting of complexes $[\text{Cu}(4,8)_2]^+$ and $[\text{Fe}(3,9)_2]^{2+}$

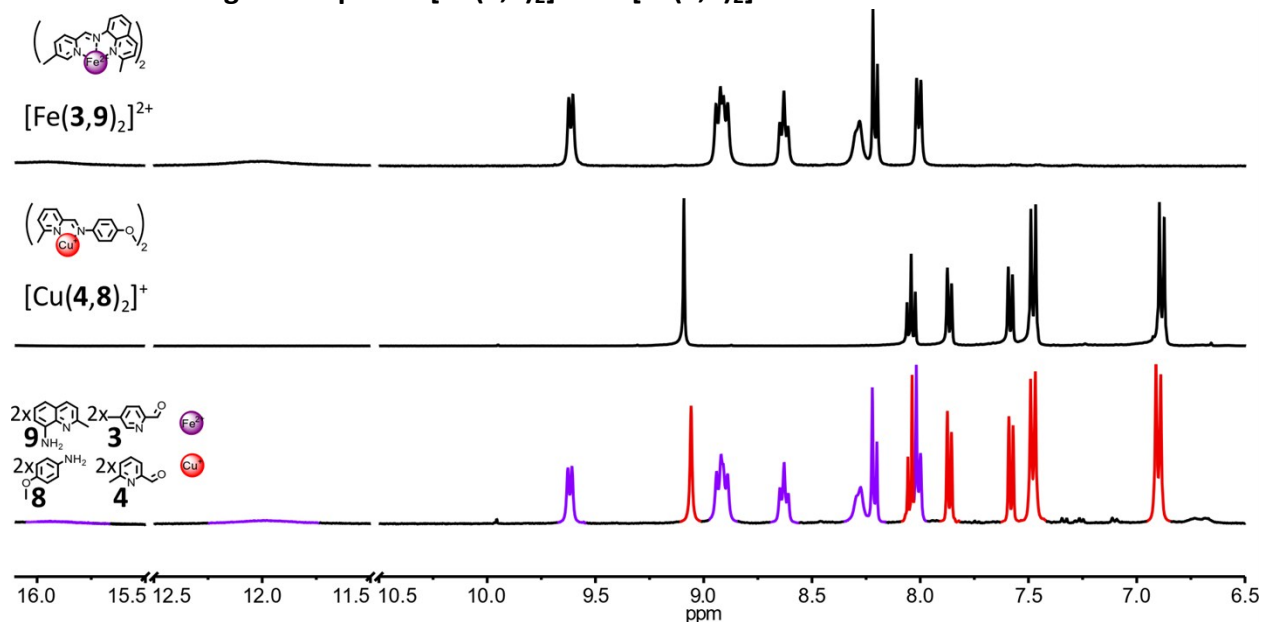


Figure S71. Partial ^1H NMR spectra (400 MHz, CD_3CN , 297 K) of: (top) complex $[\text{Fe}(3,9)_2]^{2+}$, (middle) complex $[\text{Cu}(4,8)_2]^+$, (bottom) the crude reaction mixture of the simultaneous generation of complexes $[\text{Cu}(4,8)_2]^+$ and $[\text{Fe}(3,9)_2]^{2+}$ through the self-sorting of their initial reactants. Reaction conditions: $3:4:8:9:\text{Cu}(\text{BF}_4):\text{Fe}(\text{BF}_4)_2$ (2:2:2:2:1:1), CD_3CN , 60 °C, 18 h. Diagnostic signals of the complexes are colour coded, $[\text{Cu}(4,8)_2]^+$ in red, $[\text{Fe}(3,9)_2]^{2+}$ in purple.

3.9 Self-sorting of complexes $[\text{Cu}(\mathbf{7},\mathbf{8})_2]^+$ and $[\text{Fe}(\mathbf{3},\mathbf{9})_2]^{2+}$

3.9.1 Simultaneous generation of complexes $[\text{Cu}(\mathbf{7},\mathbf{8})_2]^+$ and $[\text{Fe}(\mathbf{3},\mathbf{9})_2]^{2+}$

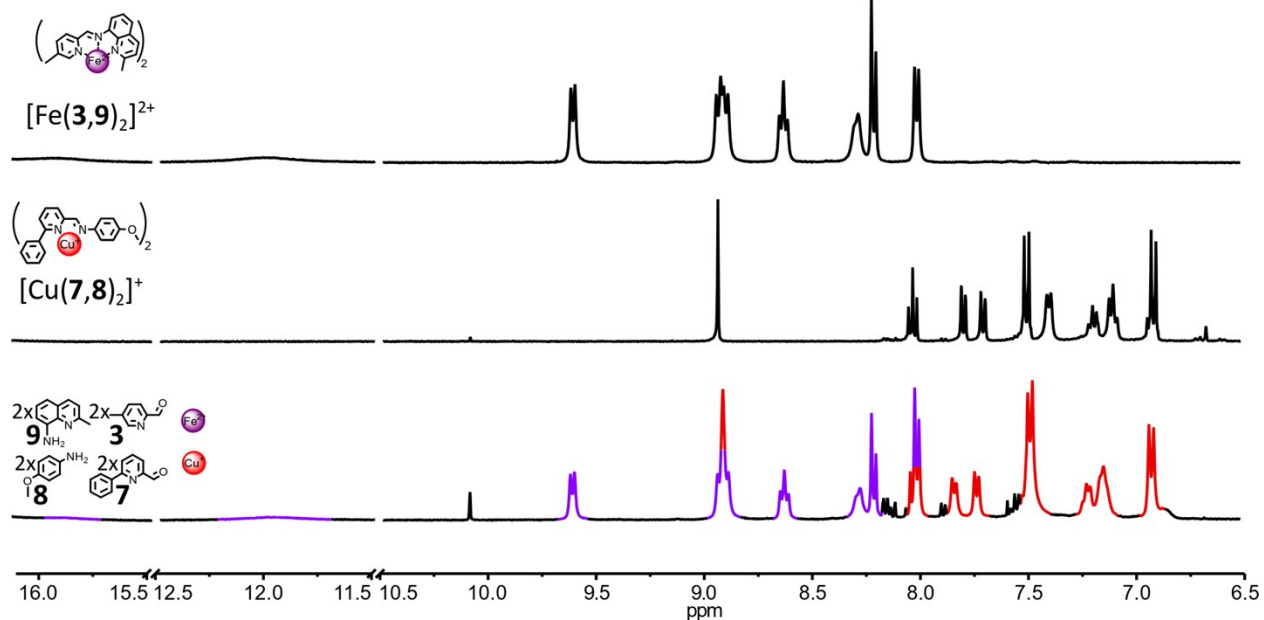


Figure S72. Partial ^1H NMR spectra (400 MHz, CD_3CN , 297 K) of: (top) complex $[\text{Fe}(\mathbf{3},\mathbf{9})_2]^{2+}$, (middle) complex $[\text{Cu}(\mathbf{7},\mathbf{8})_2]^+$, (bottom) the crude reaction mixture of the simultaneous generation of complexes $[\text{Cu}(\mathbf{7},\mathbf{8})_2]^+$ and $[\text{Fe}(\mathbf{3},\mathbf{9})_2]^{2+}$ through the self-sorting of their initial reactants. Reaction conditions: **3**:**7**:**8**:**9**: $\text{Cu}(\text{BF}_4)$: $\text{Fe}(\text{BF}_4)_2$ (2:2:2:2:1:1), CD_3CN , 60 °C, 18 h. Diagnostic signals of the complexes are colour coded, $[\text{Cu}(\mathbf{7},\mathbf{8})_2]^+$ in red, $[\text{Fe}(\mathbf{3},\mathbf{9})_2]^{2+}$ in purple.

3.9.2 Monitoring of the formation of complexes $[\text{Cu}(\mathbf{7},\mathbf{8})_2]^+$ and $[\text{Fe}(\mathbf{3},\mathbf{9})_2]^{2+}$

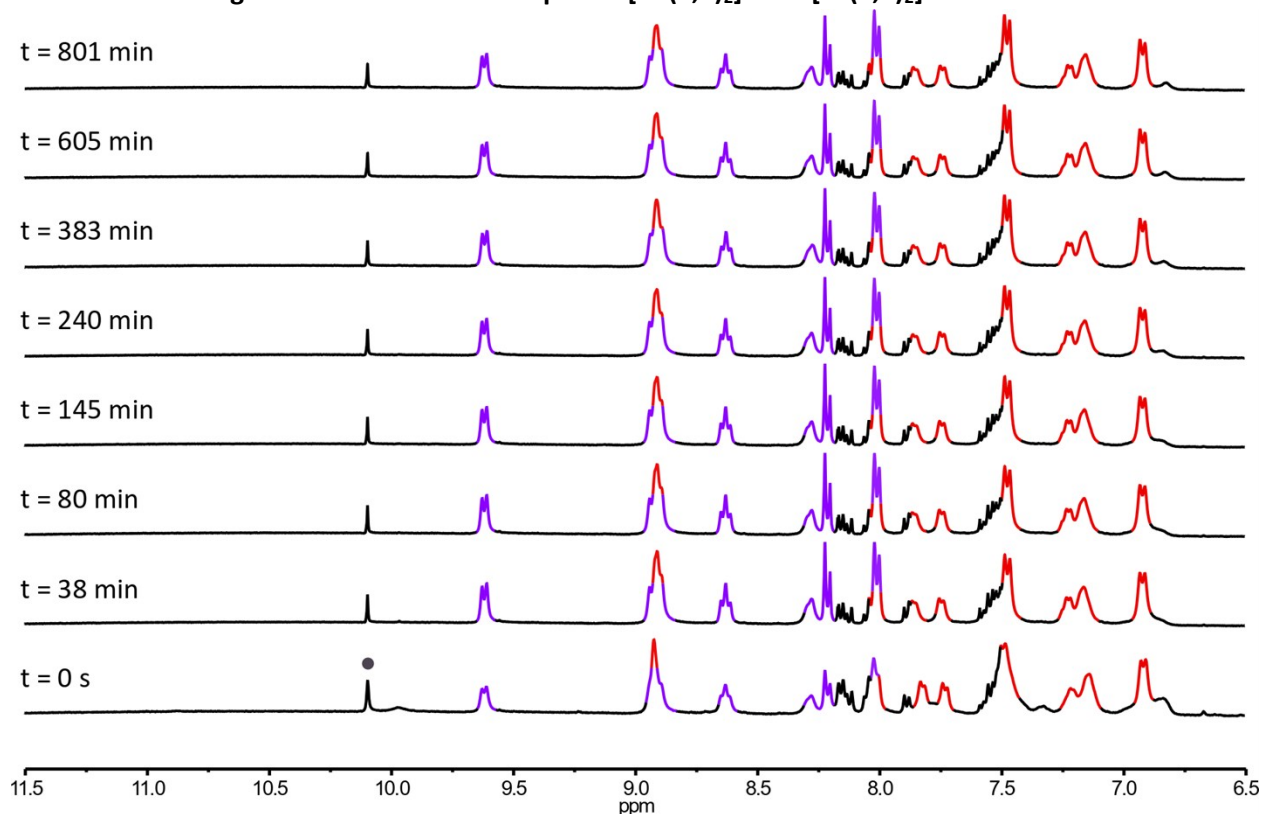
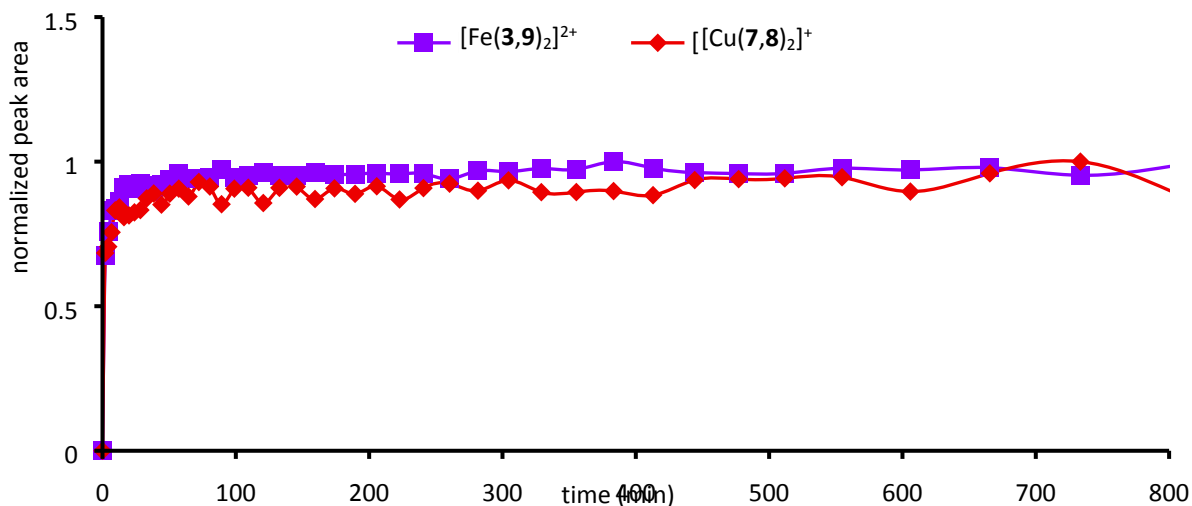


Figure S73. Formation of complexes $[\text{Cu}(\mathbf{7},\mathbf{8})_2]^+$ and $[\text{Fe}(\mathbf{3},\mathbf{9})_2]^{2+}$ from their initial reactants monitored by ^1H NMR (400 MHz, CD_3CN , 333 K), aromatic region of the spectrum shown. The sample was maintained at 60 °C and spectra of the crude reaction mixture were recorded at increasing time increments (up to a final total time of 801 min). Reaction conditions: **3**:**7**:**8**:**9**: $\text{Cu}(\text{BF}_4)$: $\text{Fe}(\text{BF}_4)_2$ (2:2:2:2:1:1), CD_3CN , 60 °C. Diagnostic signals of the complexes are colour coded, $[\text{Cu}(\mathbf{7},\mathbf{8})_2]^+$ in red, $[\text{Fe}(\mathbf{3},\mathbf{9})_2]^{2+}$ in purple. One of the diagnostic signals of the free aldehyde **7** is highlighted by a grey circle.



Fi

Figure S74. Formation as a function of time of the thermodynamic products $[\text{Cu}(7,8)_2]^+$ (red diamonds) and $[\text{Fe}(3,9)_2]^{2+}$ (purple squares). Graph plotting of the area of the imine peak of $[\text{Fe}(3,9)_2]^{2+}$ and of the proton H^7 of $[\text{Cu}(7,8)_2]^+$ normalized to the area of the same peaks at the final time-point.

3.10 Comparison of the rate of formation of bis-2,2':6'2''-terpyridine-like Fe^{II} complexes

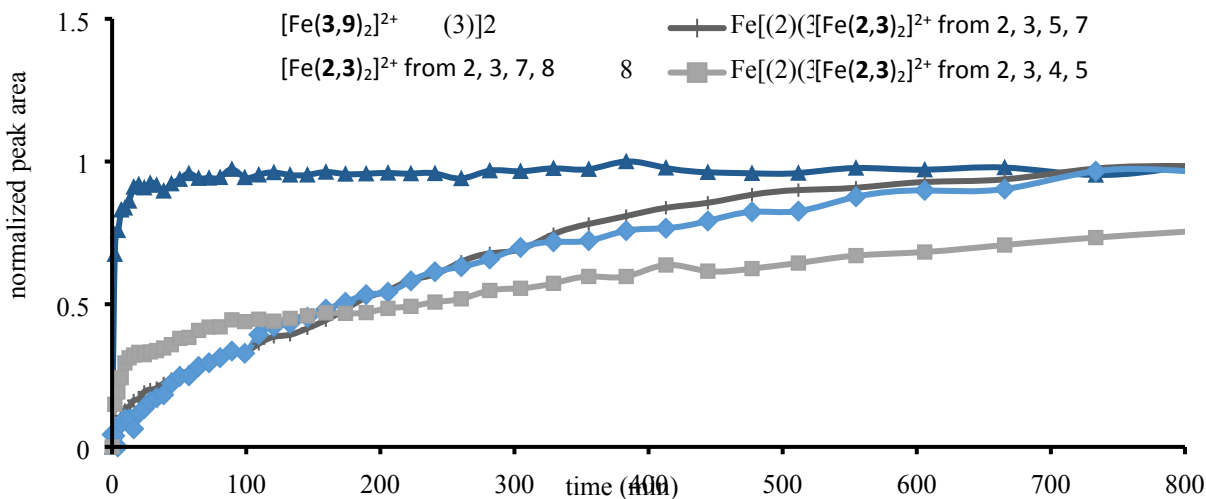


Figure S75. Formation as a function of time of bis-2,2':6'2''-terpyridine-like Fe^{II} complexes: $[\text{Fe}(3,10)_2]^{2+}$ from **3:7:8:10**: $\text{Cu}(\text{BF}_4)$: $\text{Fe}(\text{BF}_4)_2$ in the molar ratio 2:2:2:2:1:1 in CD_3CN at 60°C (dark blue triangles), $[\text{Fe}(2,3)_2]^{2+}$ from **2:3:5:7**: $\text{Cu}(\text{BF}_4)$: $\text{Fe}(\text{BF}_4)_2$ in the molar ratio 2:2:2:2:1:1 in CD_3CN at 60°C (dark grey lines), $[\text{Fe}(2,3)_2]^{2+}$ from **2:3:7:8**: $\text{Cu}(\text{BF}_4)$: $\text{Fe}(\text{BF}_4)_2$ in the molar ratio 2:2:2:2:1:1 in CD_3CN at 60°C (light blue diamonds) and **2:3:4:5**: $\text{Cu}(\text{BF}_4)$: $\text{Fe}(\text{BF}_4)_2$ in the molar ratio 2:2:2:2:1:1 in CD_3CN at 60°C (light grey squares). Graph plotting of the area of the imine peaks of the different complexes normalized to the area of the same peaks at the final time-point. See section 3.1.8, 3.1.6, 3.1.7 and 3.1.3, respectively, for more details on each individual reactions.

3.11 Self-sorting of complexes $[\text{Ag}(\mathbf{7},\mathbf{8})_2]^+$ and $[\text{Fe}(\mathbf{2},\mathbf{3})_2]^{2+}$

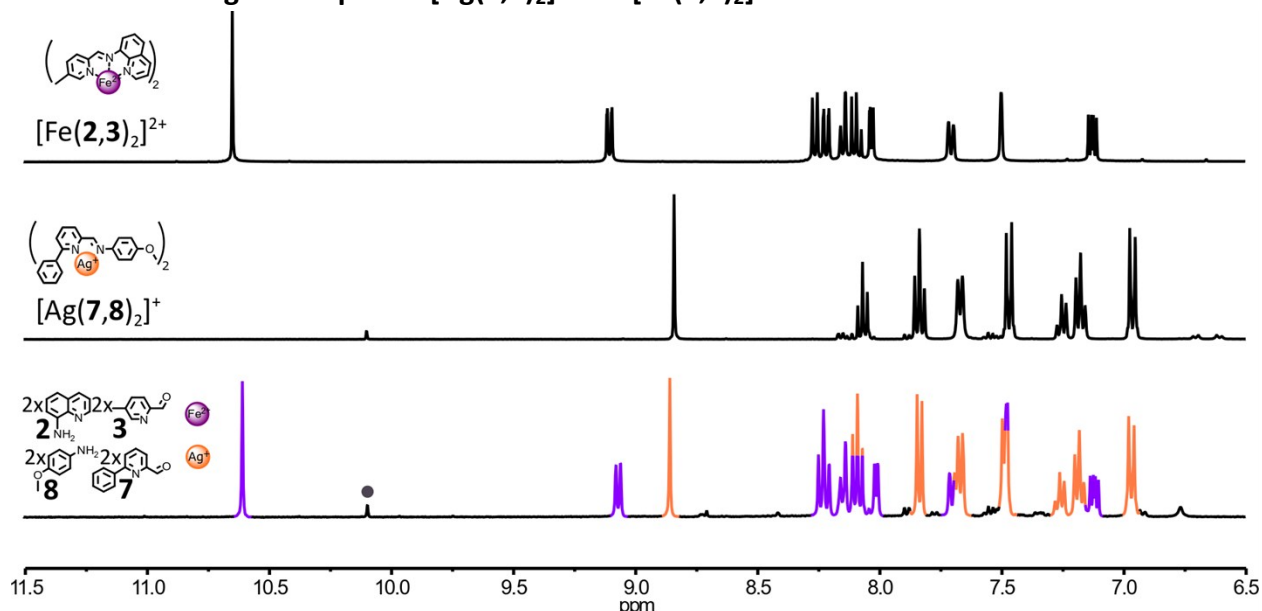


Figure S76. Partial ^1H NMR spectra (400 MHz, CD_3CN , 297 K) of: (top) complex $[\text{Fe}(\mathbf{2},\mathbf{3})_2]^{2+}$, (middle) complex $[\text{Ag}(\mathbf{7},\mathbf{8})_2]^+$, (bottom) the crude reaction mixture of the simultaneous generation of complexes $[\text{Ag}(\mathbf{7},\mathbf{8})_2]^+$ and $[\text{Fe}(\mathbf{2},\mathbf{3})_2]^{2+}$ through the self-sorting of their initial reactants. Reaction conditions: $\mathbf{2}:\mathbf{3}:\mathbf{7}:\mathbf{8}:\text{Ag}(\text{BF}_4):\text{Fe}(\text{BF}_4)_2$ (2:2:2:2:1:1), CD_3CN , 60 °C, 18 h. Diagnostic signals of the complexes are colour coded, $[\text{Ag}(\mathbf{7},\mathbf{8})_2]^+$ in orange, $[\text{Fe}(\mathbf{2},\mathbf{3})_2]^{2+}$ in purple. One of the diagnostic signals of the free aldehyde $\mathbf{7}$ is highlighted by a grey circle.

3.12 Self-sorting of complexes $[\text{Cu}(\mathbf{7},\mathbf{8})_2]^+$ and $[\text{Zn}(\mathbf{2},\mathbf{3})_2]^{2+}$

3.12.1 Simultaneous generation of complexes $[\text{Cu}(\mathbf{7},\mathbf{8})_2]^+$ and $[\text{Zn}(\mathbf{2},\mathbf{3})_2]^{2+}$

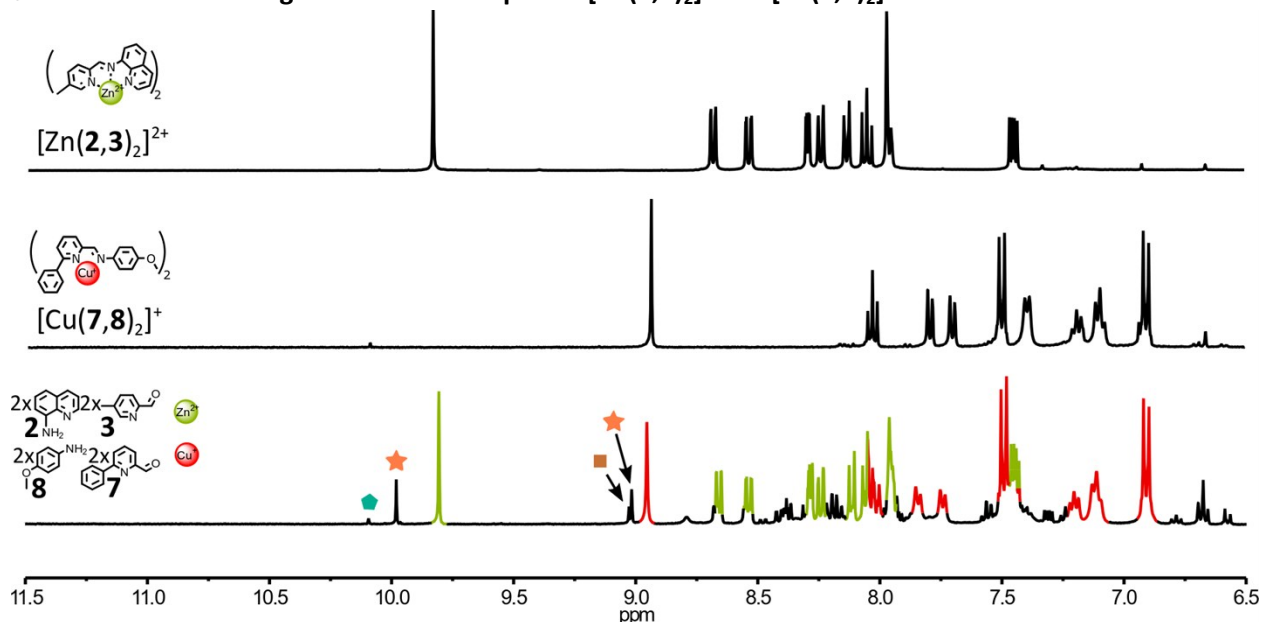


Figure S77. Partial ^1H NMR spectra (400 MHz, CD_3CN , 297 K) of: (top) complex $[\text{Zn}(\mathbf{2},\mathbf{3})_2]^{2+}$, (middle) complex $[\text{Cu}(\mathbf{7},\mathbf{8})_2]^+$, (bottom) the crude reaction mixture of the simultaneous generation of complexes

$[\text{Cu}(\mathbf{7},\mathbf{8})_2]^+$ and $[\text{Zn}(\mathbf{2},\mathbf{3})_2]^{2+}$ through the self-sorting of their initial reactants. Reaction conditions: $\mathbf{2}:\mathbf{3}:\mathbf{7}:\mathbf{8}:\text{Cu}(\text{BF}_4):\text{Zn}(\text{BF}_4)_2$ (2:2:2:2:1:1), CD_3CN , 60 °C, 18 h. Diagnostic signals of the complexes are colour coded, $[\text{Cu}(\mathbf{7},\mathbf{8})_2]^+$ in red, $[\text{Zn}(\mathbf{2},\mathbf{3})_2]^{2+}$ in green. . Two of the diagnostic signals of $[\text{Zn}(\mathbf{2},\mathbf{3})(\mathbf{2},\mathbf{7})]^{2+}$ are highlighted by orange stars, one of the diagnostic signals of $[\text{Zn}(\mathbf{2},\mathbf{7})_2]^{2+}$ is highlighted by a brown square and one of the diagnostic signals of the free aldehyde $\mathbf{7}$ is highlighted by a green pentagon.

3.12.2 Monitoring of the formation of complexes $[\text{Cu}(\mathbf{7},\mathbf{8})_2]^+$ and $[\text{Zn}(\mathbf{2},\mathbf{3})_2]^{2+}$

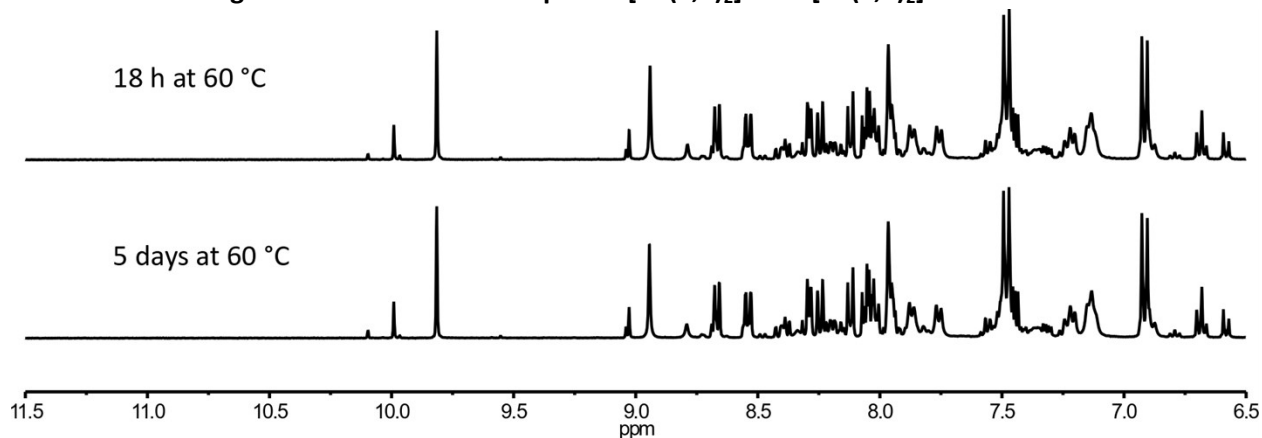
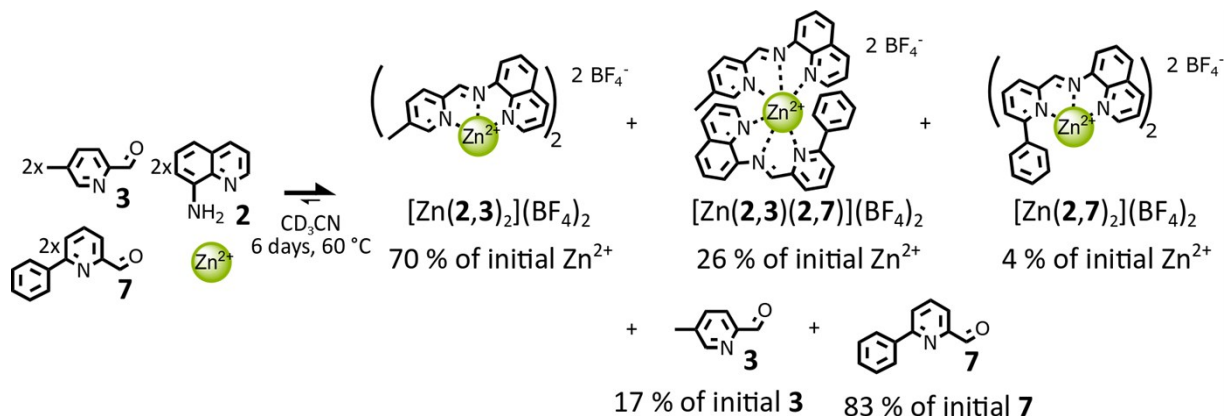


Figure S78. Formation of complexes $[\text{Cu}(\mathbf{7},\mathbf{8})_2]^+$ and $[\text{Zn}(\mathbf{2},\mathbf{3})_2]^{2+}$ from their initial reactants monitored by ^1H NMR (400 MHz, CD_3CN , 297 K), aromatic region of the spectrum shown. Spectra of the crude reaction mixture were collected after 18 h (upper) and 5 days (lower). Reaction conditions: $\mathbf{1}:\mathbf{2}:\mathbf{3}:\mathbf{7}:\text{Cu}(\text{BF}_4):\text{Fe}(\text{BF}_4)_2$ (2:2:2:2:1:1), CD_3CN , 60 °C.

3.12.2.1 Probing the selectivity of Zn^{II} cations for aldehyde $\mathbf{3}$ over aldehyde $\mathbf{7}$ in the presence of aminoquinoline $\mathbf{2}$

3.12.2.2 Procedure



Scheme S7. Probing the selectivity of Zn^{II} cations for aldehyde $\mathbf{3}$ over aldehyde $\mathbf{7}$ in the presence of aminoquinoline $\mathbf{2}$. Distribution of the products generated by mixing $\mathbf{2}$, $\mathbf{3}$, $\mathbf{7}$ and $\text{Zn}(\text{BF}_4)_2$ in the molar ratio 2:2:2:1 at 60 °C for 6 days. Error on % determination: $\pm 3\%$.

CD_3CN solutions of the 2-formylpyridine containing components $\mathbf{3}$ (50 μL of 32 mM, 1.6 μmol , 1 eq.) and $\mathbf{7}$ (50 μL of 32 mM, 3.2 μmol , 1 eq.) and of the aminoquinoline $\mathbf{2}$ (100 μL of 32 mM, 3.2 μmol , 2 eq.) were

combined. The resulting mixture was treated with CD_3CN solutions of $[\text{Zn}(\text{C}_2\text{H}_6\text{OS})_6](\text{BF}_4)_2$ (100 μL of 32 mM, 3.2 μmol , 2 eq.) and heated at 60 $^\circ\text{C}$ for up to 6 days. The complexes were never isolated, all the present experiments and analysis were done on the crude reaction mixture.

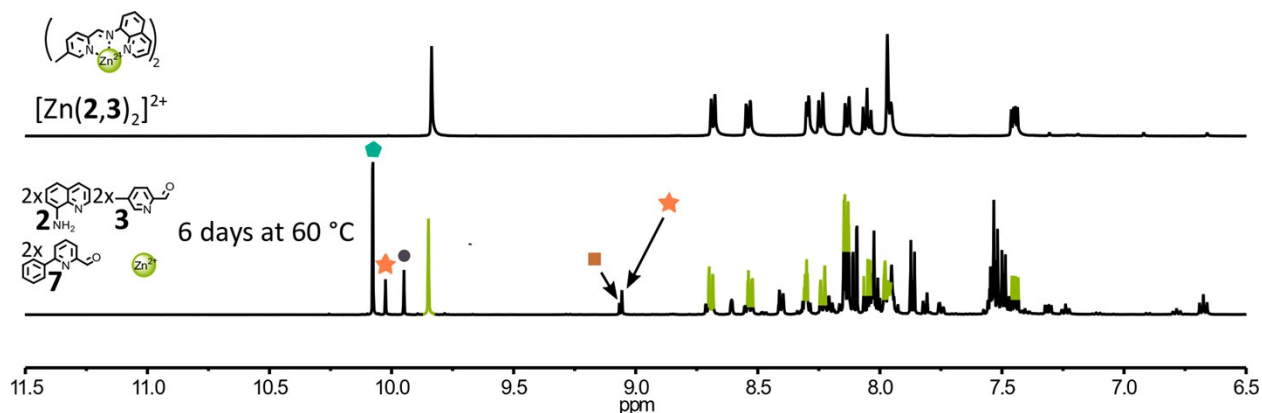


Figure S79. Partial ^1H NMR spectra (500 MHz, CD_3CN , 297 K) of: (upper) complex $[\text{Zn}(\mathbf{2},\mathbf{3})_2]^{2+}$ and (lower) the crude reaction mixture obtained by mixing $\mathbf{2}$, $\mathbf{3}$, $\mathbf{7}$ and $\text{Zn}(\text{BF}_4)_2$ in the molar ratio 2:2:2:1 at 60 $^\circ\text{C}$ for 6 days. Diagnostic signals of the complex $[\text{Zn}(\mathbf{2},\mathbf{3})_2]^{2+}$ are colour coded in green, two of the diagnostic signals of $[\text{Zn}(\mathbf{2},\mathbf{3})(\mathbf{2},\mathbf{7})]^{2+}$ are highlighted by orange stars, one of the diagnostic signals of $[\text{Zn}(\mathbf{2},\mathbf{7})_2]^{2+}$ is highlighted by a brown square, one of the diagnostic signals of the free aldehyde $\mathbf{3}$ is highlighted by a grey circle and one of the diagnostic signals of the free aldehyde $\mathbf{7}$ is highlighted by a green pentagon.

3.12.2.3 Monitoring of the formation of the complex $[\text{Zn}(\mathbf{2},\mathbf{3})_2]^{2+}$

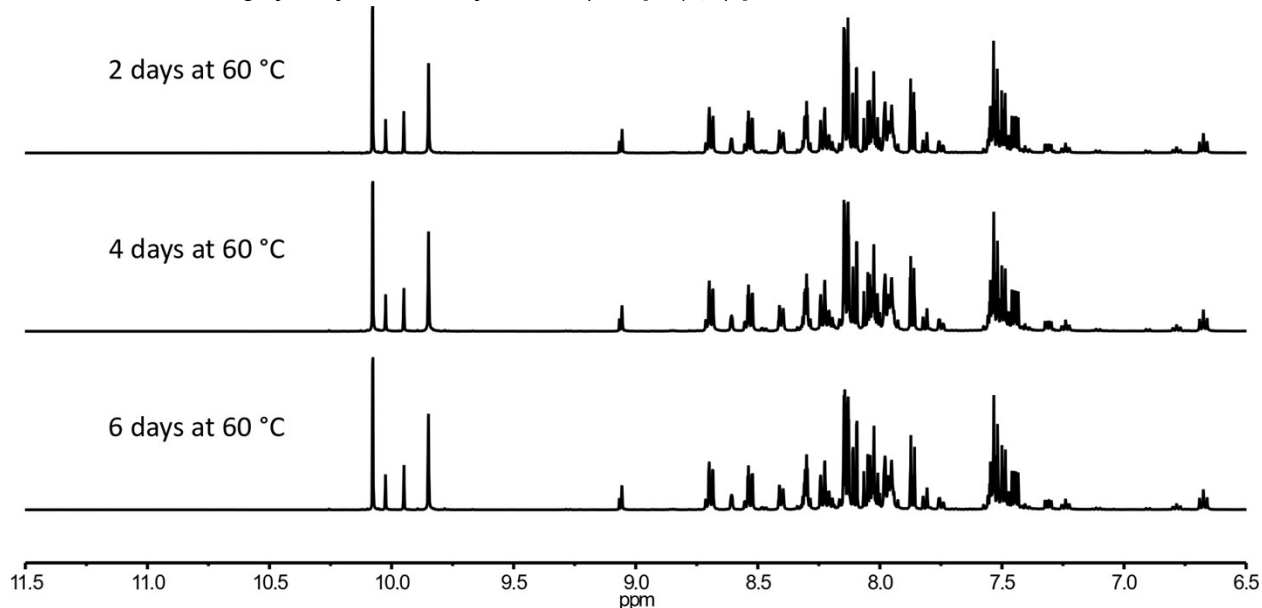


Figure S80. Formation of complex $[\text{Zn}(\mathbf{2},\mathbf{3})_2]^{2+}$ from a mixture of $\mathbf{2}$, $\mathbf{3}$, $\mathbf{7}$ and $\text{Zn}(\text{BF}_4)_2$ in the molar ratio 2:2:2:1 monitored by ^1H NMR (500 MHz, CD_3CN , 297 K), aromatic region of the spectrum shown. Spectra of the crude reaction mixture were collected after 2 days (top), 4 days (middle) and 6 days (bottom). Reaction conditions: $\mathbf{2}:\mathbf{3}:\mathbf{7}:\text{Zn}(\text{BF}_4)_2$ (2:2:2:1), CD_3CN , 60 $^\circ\text{C}$.

3.13 Self-sorting of complexes $[\text{Cu}(\mathbf{7},\mathbf{8})_2]^+$ and $[\text{Zn}(\mathbf{3},\mathbf{9})_2]^{2+}$

3.13.1 Simultaneous generation of complexes $[\text{Cu}(\mathbf{7},\mathbf{8})_2]^+$ and $[\text{Zn}(\mathbf{3},\mathbf{9})_2]^{2+}$

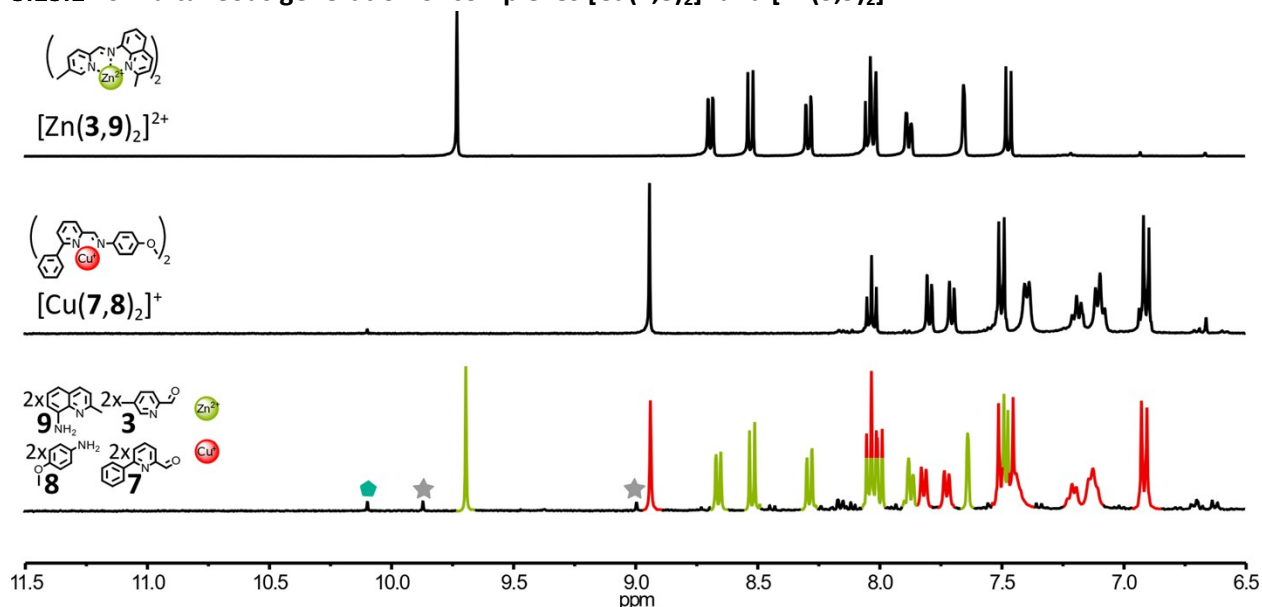
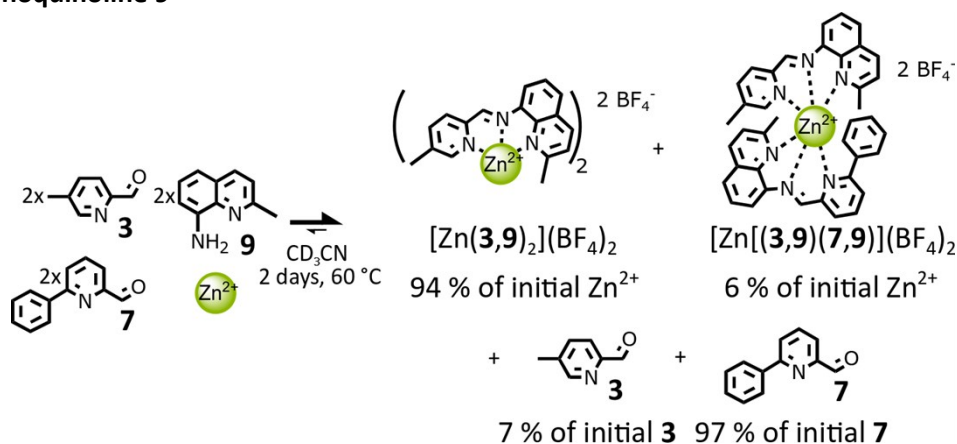


Figure S81. Partial ^1H NMR spectra (400 MHz, CD_3CN , 297 K) of: (top) complex $[\text{Zn}(\mathbf{3},\mathbf{9})_2]^{2+}$, (middle) complex $[\text{Cu}(\mathbf{7},\mathbf{8})_2]^+$, (bottom) the crude reaction mixture of the simultaneous generation of complexes $[\text{Cu}(\mathbf{7},\mathbf{8})_2]^+$ and $[\text{Zn}(\mathbf{3},\mathbf{9})_2]^{2+}$ through the self-sorting of their initial reactants. Reaction conditions: $\mathbf{3}:\mathbf{7}:\mathbf{8}:\mathbf{9}:\text{Cu}(\text{BF}_4)_2:\text{Zn}(\text{BF}_4)_2$ (2:2:2:2:1:1), CD_3CN , 60 °C, 18 h. Diagnostic signals of the complexes are colour coded, $[\text{Cu}(\mathbf{7},\mathbf{8})_2]^+$ in red, $[\text{Zn}(\mathbf{3},\mathbf{9})_2]^{2+}$ in green. Two of the diagnostic signals of $[\text{Zn}(\mathbf{3},\mathbf{9})(\mathbf{7},\mathbf{9})]^{2+}$ are highlighted by grey stars and one of the diagnostic signals of the free aldehyde $\mathbf{7}$ is highlighted by a green pentagon.

3.13.2 Probing the selectivity of Zn^{II} cations for aldehyde $\mathbf{3}$ over aldehyde $\mathbf{7}$ in the presence of aminoquinoline $\mathbf{9}$



Scheme S8. Probing the selectivity of Zn^{II} cations for aldehyde $\mathbf{3}$ over aldehyde $\mathbf{7}$ in the presence of aminoquinoline $\mathbf{9}$. Distribution of the products generated by mixing $\mathbf{2}:\mathbf{3}:\mathbf{9}:\text{Zn}(\text{BF}_4)_2$ in the molar ratio 2:2:2:1 at 60 °C for 2 days. Error on % determination: $\pm 3\%$.

CD₃CN solutions of 2-formylpyridine containing components **3** (50 μL of 32 mM, 1.6 μmol, 1 eq.) and **7** (50 μL of 32 mM, 3.2 μmol, 1 eq.) and of aminquinoline **9** (100 μL of 32 mM, 3.2 μmol, 2 eq.) were combined. The resulting mixture was treated with CD₃CN solutions of [Zn(C₂H₆OS)₆](BF₄)₂ (100 μL of 32 mM, 3.2 μmol, 2 eq.) and heated at 60 °C for up to 2 days. The complexes were never isolated, all the present experiments and analysis were done on the crude reaction mixture.

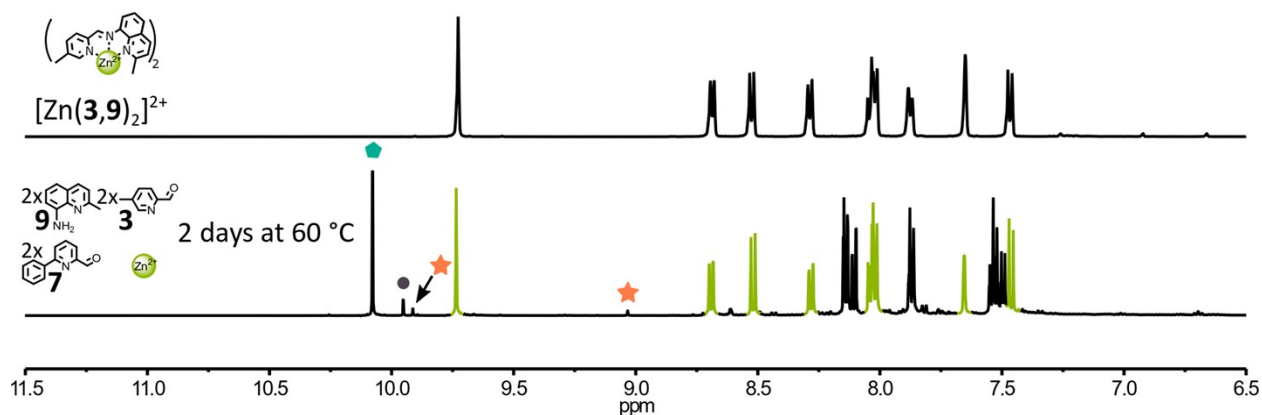


Figure S82. Partial ¹H NMR spectra (500 MHz, CD₃CN, 297 K) of: (upper) complex [Zn(**3,9**)₂]²⁺ and (lower) the crude reaction mixture obtained by mixing **2**, **3**, **9** and Zn(BF₄)₂ in the molar ratio 2:2:2:1 at 60 °C for 2 days. Diagnostic signals of the complex [Zn(**3,9**)₂]²⁺ are colour coded in green, two of the diagnostic signals of [Zn(**3,9**)(**7,9**)]²⁺ are highlighted by orange stars, one of the diagnostic signals of the free aldehyde **3** is highlighted by a grey circle and one of the diagnostic signals of the free aldehyde **7** is highlighted by a green pentagon.

4. References

- [S1] J. Holub, G. Vantomme, J.-M. Lehn, *J. Am. Chem. Soc.*, 2016, **138**, 11783–11791.
 [S2] G. A. Ardizzoia, S. Brenna, F. Castelli, S. Galli, *Inorg. Chim. Acta*, 2009, **362**, 3507–3512.
 [S3] G. Men, J.-M. Lehn, *J. Am. Chem. Soc.*, 2017, **139**, 2474–2483.